DESIGN AND ANALYSIS OF AMINO ACID SUPPLEMENTATION IN HEPATOCYTE CULTURE USING *IN VITRO* EXPERIMENT AND MATHEMATICAL MODELING

By

HONG YANG

A Dissertation submitted to the

Graduate School-New Brunswick

Rutgers, The State University of New Jersey

in partial fulfillment of the requirements

for the degree of

Doctor of Philosophy

Graduate Program in Chemical and Biochemical Engineering

written under the direction of

Dr. Marianthi G. Ierapetritou and Dr. Charles M. Roth

and approved by

_____

_____

_____

_____

_____

New Brunswick, New Jersey

[January, 2010]

ABSTRACT OF THE DISSERTATION

Design and Analysis of Amino Acid Supplementation in Hepatocyte Culture Using *in vitro* Experiment and Mathematical Modeling

By HONG YANG

Dissertation Directors:

Dr. Marianthi G. Ierapetritou, Ph.D.

Dr. Charles M. Roth, Ph.D.

Extracorporeal bioartificial liver (BAL) devices, involving primary hepatocytes, represent a promising option to provide temporary support for patients with liver failure. Current use of BAL is primary challenged by development of techniques for long-term culture of hepatocytes during plasma exposure, as occurs during clinical application. Previous *in vitro* studies and mathematical modeling analysis have shown that supplementation of amino acids to the plasma enhances liver-specific functions and reduces lipid accumulation. However, further improvement would be enhanced greatly by development of a rational strategy to design the profile of amino acid supplementation and by better understanding of the metabolic objectives of hepatocytes, and how they vary as a function of amino acid supplementation.

In order to address these issues, a rational design approach was first developed using flux balance analysis (FBA) to determine a profile of amino acid supplementation to achieve a specific cellular objective (urea production) in cultured hepatocytes exposed to plasma. Experiments based on the designed supplementation showed that both urea and albumin production were increased compared with previously reported (empirical) amino acid supplementation. However, the experimental values did not match our theoretical prediction mainly due to the insufficient constraints imposed to the modeling.

In an attempt to improve the model accuracy, we incorporated pathway energy balance (PEB) constraints, and amino acids transport constraints. It is found that both PEB and transport constraints significantly reduce the feasible region of the flux space. Moreover, metabolic objective prediction (MOP) model reveals that hepatocytes respond to variations in available amino acid supplementation by changing their metabolic objectives and pathway utilization. In particular, the analysis shows that fatty acid oxidation is vital to reduce the rate of lipid accumulation and to increase liver-specific functions with amino acid supplementation.

This study leads to a better understanding of amino acid supplementation effects on hepatocytes during plasma exposure based on the integration of *in vitro* experiments and mathematical modeling. The approach enables the metabolic manipulation of hepatocytes with rationally designed amino acid supplementation to improve the targeted liver cell functionality and improve the long-term technique of hepatocytes applied for BAL devices.

Acknowledgement and Dedication

I would like to express my sincere gratitude to my advisors, Prof. Marianthi Ierapetritou and Prof. Charles Roth for giving me the opportunity of being part of this project and their invaluable guidance and advices throughout my study. My research would not be as good as now without their helpful direction and continuous support. I learned a lot from them for their wide knowledge, logical way of thinking and wonderful balance between work and personal life. I feel really grateful and lucky to have both of them as my advisors. I specially thank Dr. Ierapetritou for her motivations in the hardest time.

I would like to thank my thesis proposal and defense committee members, Dr. Ioannis Androulakis, Dr. Yee Chiew, Dr. Francois Berthiaume and Dr. Martin Yarmush, for their contributing valuable suggestions to my study. I would like to express a special thanks to Dr. Chiew for his advises of successful life in the United State to me as a foreign student. I thank Dr. Henrik Pedersen for his kind help with acetonitrile supplies, and Dr. Kyongbum Lee (Associate Professor, Department of Chemical and Biological Engineering, Tufts University) for providing the standard Gibbs free energy data and his suggestions for pathway energy constraints.

Financial supports from NSF QSB program (BES-0456697), NSF Metabolic Engineering (BES-0519563), and USEPA-funded Environmental Bioinformatics and Computational Toxicology Center (GAD R 832721-010) are acknowledged.

I thank all of my past and present lab buddies. My special thanks to Dr. Vidya Iyer, who gave the thoughtful comments and suggestions on my work. I thank Dr. Partricia Portillo, Dr. Zhenya Jia and Stephen Guzikowski. It was a wonderful time to be with them. They helped me in many ways to make me strong in the fact of difficulties in research and personal life. I acknowledgement Dr. Sumati Sundaram, Dr. Li Kim Lee, and Dr. Nripen Sharma for training me in cell culture in the earlier of my research; Dr. Eddie Davis and Dr. Georgies Saharidis for their help in modeling; Carolyn Waite and Salaheldin Hamed for their advices about siRNA and PCR experiment. I sincerely thank to Stephen Guzikowski and Aina Andrianarijaona for their tough surgery work, and Dr. Vidya Iyer and Lavanya Peddada for ordering experimental supplies, and Dominik Naczynski for organizing and cleaning the lab. I thank the undergraduate student, Sarah Abdelsayed for her inputs to this project.

I would like to convert my special thanks to my husband, Zhi Qiao, for his unconditional love, great supports and faiths in my successes. Both of us learned about happiness through our personal growth and eternal supports from each other. Finally, I would like to dedicate this thesis to my grandpa, my parents and my brother for their unflagging love and unwavering support through my life. *I love you all dearly.*

Table of Contents

List of Tables

List of Illustrations

Chapter 1

INTRODUCTION

Abstract:

A large number of people suffer from liver disease in the United States due to the loss of important functions of the liver. Effective treatments of such liver failures using transplantation are limited by shortage of organ donors. Extracorporeal bioartificial liver devices, involving primary hepatocytes, become a promising option to provide temporary supports for patients with liver failure. *In vitro* hepatocyte cultures and stoichiometric modeling of hepatic metabolism are important tools for tackling the challenges of BAL, specifically to improve liver-specific functions during plasma exposure. Chapter 1 includes a brief summary of aspects of these issues and the organization of this thesis.

The liver is the largest and most complex internal organ in the human body, and is an organ present in vertebrates and some other animals. It is responsible for an astonishing number of functions including production of bile, regulation of carbohydrate, protein and fat metabolism, maintenance of nutrition levels in the blood including glucose and cholesterol, and storage of essential vitamins and minerals. Moreover, the liver plays a critical role for detoxification of internal toxins (endotoxins) and environmental toxins (exotoxins), such as drug, alcohol and foreign chemicals. Detoxification is achieved through a biotransformation process by conversion of toxic chemicals into hydrophilic substances that can be excreted into bile or urine and subsequently removed from the body (Hall et al. 1997).

The failure of liver regulatory and maintainable functions or the lack of liver detoxification leads to liver disease. Liver disease is an important cause of morbidity and mortality in the United States. The American Liver Foundation (www. liverfoundation.org) reported that 30 million people in the United States are suffering from liver disease with over 50,000 deaths per year. In the past 30 years, the number of deaths caused by liver cancer increased in the United States, among the eighth leading causes of cancer death with a clear tendency to increase further (Parkin et al. 2001). In 2009, U.S. National Cancer Institute (www.cancer.gov) reported that over 22,220 new cases were diagnosed and 18,160 people died from liver cancer.

Liver failure can be classified into three types: acute liver failure (ALF), acute-on-chronic liver failure (AoCLF), and chronic liver disease (CLD). ALF (also called fulminant hepatic failure) is characterized by rapid loss of hepatic cellular function in a patient without previous history of liver disease. Viral hepatic (worldwide) and drug-induced liver injury (in the Europe and North America) account for most of the cases of ALF (Lee 2008). AoCLF involves an acute pathophysiologic deterioration with progressive organ dysfunction in a patient with pre-existing cirrhosis, commonly caused by alcohol abuse (Jalan and Williams 2002; Shawcross and Wendon 2009). CLD is developed by progressive destruction of liver over a long period of time. Nonalcoholic fatty liver disease (NAFLD) is the most common cause of CLD. NAFLD is defined as the abnormal accumulation of fat in the liver of people who drink little or no alcohol. At the early stage of NAFLD, there may be no symptoms and complications (Adams and Angulo 2006), and people have chance to heal themselves at this stage. However, for some people, the

continuous accumulation of fat can cause liver inflammation and induce non-alcoholic steatohepatitis (NASH), representing the metabolic syndromes relative to obesity with insulin resistance, glucose metabolism disorder, and arterial hypertension (Hulek and Dresslerova 2009). NASH can slowly worsen, carry risk for cirrhosis, liver cancer and progress to liver-related death (Farrell and Larter 2006).

Liver can be regenerated with an early diagnosis and appropriate treatments for the patients with ALF and AoCLF. N-acetylcysteine (NAC) has been proved to be an effective treatment of acetaminophen overdose (Smilkstein et al. 1988) and recently it was also proved to be successfully used alone for treatment of patients with non-acetaminophen acute liver failure (Lee et al. 2009). However, ALF still carries a substantial mortality rate. With one-year survival rate above 80% compared with 30% in the 1970's, orthotopic liver transplantation (OLT) is dramatically developed and becomes the only effective life-saving treatment for patients with un-regenerative acute liver failure and chronic end-stage liver failure (Liou and Larson 2008; Neff et al. 2003). However, the number of transplants performed each year (5,000 in the U.S.) is far exceeded by its demands (about 18,000 in the U.S.) (Scientific Registry of Transplant Recipients, www.ustransplant.org). Almost 2,000 people die while waiting for a transplant in their first year. The liver transplantation has been hampered by the shortage of donor organs. Moreover, patients with AoCLF are unsuitable for the transplantation due to multi-organ failure. An effective extracorporeal liver support system would improve the chance of survival by temporarily supporting the patient during acute liver failure until its spontaneous regeneration or by providing a bridge for the patient with

chronic liver failure until donor organ is available (Chan et al. 2004). Extracorporeal liver devices can be divided into non-biological (cell-free technique) and bio-artificial (cell-based technique) devices. Non-biological devices aim at removal of toxins based on the principles of plasma exchange, albumin dialysis, filtration and sorbent-based devices (charcoal). However, the non-biological devices are limited to maintaining the required liver-specific functions (Rozga 2006). Extracorporeal bioartificial liver (BAL) devices, involving a biological component comprised of a mammalian liver tissue preparation and a synthetic membrane, have shown encouraging results in laboratory tests and clinical trails (Demetriou et al. 2004; Mundt et al. 2002). However, the significant challenges of BAL devices still remain to be (a) maximizing liver-specific functions in plasma; (b) potential sources of cells and minimum cell mass; and (c) minimal mass transfer hindrance (Chan et al. 2004; Gerlach 1997; Riordan and Williams 1997).

Liver research is hindered by the available patients, ethical reasons and animal rights (Lipscomb and Poet 2008). Using *in vitro* models in attempt to simulate *in vivo* liver architecture can avoid these limitations and help better understand the pathology and treatments for various liver failures and the application of liver-assist equipments. The other advantages of *in vitro* systems include a faster way to achieve data, lower research cost and reduction of the adverse effects for animals and humans. Although the liver is formed by different cell types (parenchymal cells (hepatocytes), liver endothelial cells, kupffer cells and stellate cells), hepatocytes occupy almost 80% the total liver volume, constitute 65% of the total liver cells, and perform the majority of liver functions (Weibel et al. 1969). In addition, results from hepatocyte studies can be further analyzed to

provide physiologically relative information regarding hepatic metabolism. *In vitro* hepatocyte models have attracted a lot of attention since a reproducible approach leading to high yield of cells was introduced in the 1970's (Seglen 1976), and came into widespread use in academic research and pharmaceutical industry in the earlier 1990's. Current and potential uses of isolated hepatocytes relate to study of drug discovery (McGinnity et al. 2004), drug-drug interactions (DDI) (Li and Jurima-Romet 1997), toxicological responses of drugs (Gebhardt et al. 2003; Nussler et al. 2001) and their use for artificial cell-based devices (Chan et al. 2003b; Flendrig et al. 1998; Wurm et al. 2009).

Hepatocytes are anchorage-dependent cells, and they rapidly lose liver-specific functions once they are removed from their host to culture in an artificial environment (Allen and Bhatia 2002). Therefore, current use of hepatocytes is primary challenged by development of long-term culture techniques. Collagen sandwich culture is one of promising techniques used to maintain their functions over a long period of time, where hepatocyte are fixed between two collagen layers (Dunn et al. 1989; Kern et al. 1997). The other encouraging culture techniques include gel immobilized hepatocytes (Guyomard et al. 1996), hepatocyte spheroid (Verma et al. 2007), and culturing hepatocytes on extracellular matrix (Page et al. 2007). Such three-dimensional (3D) approaches mimic the *in vivo* microenvironment of hepatocytes in the intact liver and exhibit stable liver-specific functions with higher cell viability compared to culture cells as a monolayer. Co-culturing hepatocytes with other types of cells such as 3T3 fibroblasts (Bhatia et al. 1997) or hepatic stellate cells (Krause et al. 2009) helps to maintain

hepatocyte differentiation *in vitro*. Use of hepatocytes is also limited by lack of fresh hepatocytes harvesting and inability to simulate hepatocyte proliferation *in vitro*. Therefore, cryopreserved hepatocytes become a variable option for *in vitro* analysis (Garcia et al. 2003; Park and Lee 2005), which can be stored indefinitely, transported to any site, and utilized when desired. It has been shown that cryopreserved hepatocytes successfully maintain over 90% of the fresh hepatocyte function for at least one year using a proper cryopreservation procedure (McGinnity et al. 2004). Additional factor identified to improve *in vitro* condition included an appropriate medium supply specially designed for BAL devices. Hepatocytes exposed to plasma *in vitro*, as occurs during clinical application, exhibit a progressive accumulation of lipid droplets and consequently a decrease in metabolic functions as accessed by urea synthesis and albumin production (Matthew et al. 1996a; Stefanovich et al. 1996). Supplementation of hormone and amino acids to the culture medium during plasma exposure provide the key metabolic functions which are either impaired or lost as result of severe liver failure including urea synthesis, albumin production, and cytochrome P450 activity (detoxification). Certain amino acids such as glycine and alanine have been used to protect cells from damage caused by energy insufficiency (Dickson et al., 1992; Maezono et al., 1996). Since hepatic functions are highly linked by intermediary metabolism and cellular energy, it is necessary to quantify the environmental effects on hepatic metabolism (Sharma et al. 2005).

Hepatic metabolism is the total sum of all the biochemical reactions taking place in the cell, which constitutes a complex and dynamic process with a large number of reactions and interaction of diverse pathways (Gombert and Nielsen 2000). Thus it is a challenge to

explain hepatic cellular behavior alone by observed measurement from *in vitro* experiments. Mathematical models need to be developed to help interpret, understand and eventually predict the cell behavior under different stimuli (Bailey 1998; De Maria et al. 2008). In mathematical modeling of hepatic metabolism, a comprehensive metabolic network, with interconnecting pathways consisting of a large number of reactions occurring in the cell, is established to mimic the actual hepatocyte phenomena (Chan et al. 2003a; Lee et al. 2000a). Three specific methodologies: metabolic flux analysis, flux balance analysis and network-based pathway analysis have steadily grown in scope leading to unravel the complexities of metabolic network (Llaneras and Pico 2008). Such stoichiometric models share common characteristics including the use of a metabolic network, the fact that they are based on pseudo-steady state assumption and do not use kinetic information.

Metabolic flux analysis (MFA) provides a comprehensive view of intracellular metabolism based on measurements of extracellular fluxes from *in vitro* experiments and application of mass balances around intracellular metabolites at a pseudo-steady state (Varma and Palsson 1994a). For hepatocyte culture, MFA has been utilized to explore the hepatic response to severe injury (Lee et al. 2000a) and to investigate insulin and amino acid effects on intracellular metabolic fluxes of primary rat hepatocyte (Chan et al. 2003b). MFA requires sufficient measurements from *in vitro* experiment which brings difficulties for its applications. Labeled substrate measurements either by nuclear magnetic resonance (NMR) or by gas chromatography/mass spectrometry (GC-MS) has been used to provide more observations to MFA model in addition to extracellular flux

measurements (Riascos et al. 2005; Szyperski 1998; Wiechert 2001). However, high cost and limited range of available substances restrict their applications. Flux balance analysis (FBA), an optimization framework, based on an extension of MFA by involving a specific objective and a set of constraints, can better compensate the issue of insufficient measurements (Lee et al. 2006). The new aspects of FBA focus on declaring appropriate objectives that cell strives to achieve (Gianchandani et al. 2008; Khannapho et al. 2008; Schuetz et al. 2007) and governing reasonable constraints leading to a space of feasible flux distribution (Bonarius et al. 1997). Since urea is a well-established marker of hepatocyte function and easy to measure with high accuracy, urea maximization has been chosen as an objective function for analysis of hepatocyte culture of BAL devices (Sharma et al. 2005), and for determination of amino acid supplementation in hepatocyte culture using a rational design approach (Yang et al. 2009). However, the metabolism of mammalian cells is robust and their cellular objectives may adapt to different environmental conditions. Recently, a modified FBA based on a bi-level optimization model called ObjFind (Burgard and Maranas 2003) has been developed to infer the metabolic objectives which are most consistent with experimental data. This approach has been applied to investigate the metabolic objectives of a hypermetabolic state of liver (Nolan et al. 2006) and cultured hepatocytes used for BAL devices (Nagrath et al. 2007; Uygun et al. 2007). The general constraints used to reduce the feasible region of an FBA problem include environmental (nutrients, physical factors etc.), physicochemical (mass balance, thermodynamic of internal reactions, maximum enzyme capacities), self-imposed regulatory and evolutionary constraints (Covert et al. 2003). However, these constraints are not sufficient to indentify a unique flux distribution in order to investigate

the cells behavior under various environmental conditions. Recently, thermodynamic constraints consistent with the second law of thermodynamics have been used including energy balance analysis (EBA) with reaction directionality (Beard and Qian 2005), pathway energy balance constraints (Nolan et al. 2006), network-embedded thermodynamic analysis (NET analysis) (Kummel et al. 2006; Zamboni et al. 2008). Such thermodynamic-based constraints significantly reduce the feasible region by elimination of infeasible solutions from FBA space. Beard and Lee groups very recently incorporated thermodynamic constraints to understand cellular regulation in hepatocytes (Beard and Qian 2005), to study drug-drug metabolic interactions between acetaminophen and ethanol (Yang and Beard 2006) and to investigate objectives of liver hepermetabolism (Nolan et al. 2006)

In contrast to flux analysis, network-based pathway analysis is used to identify metabolic pathway and their connections by separating the entire network into pathways (sub-network), which can be done without information of flux values or imposing any objective for cellular metabolism (Trinh et al. 2009). The most commonly used pathway analysis is the elementary flux modes (EFM), which identifies all pathways that consist of the minimum number of reactions that exist as a function unit (Schilling et al. 2000; Schuster et al. 1999). The majority of EFM applications for liver metabolism are related to the analysis of robustness of amino acid anabolism in human hepatocyte (Behre et al. 2008) and analysis of network flexibility of hepatic metabolism by incorporating pathway information (Nolan et al. 2006; Yoon and Lee 2007).

The potential applications of flux and pathway analysis in hepatic metabolism include (a) improvement of hepatocyte culture medium using an optimization algorithm in order to maintain liver-specific functions during plasma exposure; (b) development of mathematical frameworks with an appropriate objective function and sufficient constraints for application of drug detoxification and BAL devices; (c) identification of alternative pathways by performing small interfering RNA (siRNA)-aid inhibition of pathway; (d) regulation of drug metabolism which induces hepatotoxicity in cultured primary hepatocytes; and (e) integration of the gene expression data into metabolic flux levels of hepatic metabolism.

In this thesis, we focused on improvement of *in vitro* hepatocyte culture during plasma exposure using amino acid supplementation and development of optimization-based framework in order to: (i) improve cell functionality by manipulating the amino acid supplementation; and (ii) elucidate the behavior of hepatocytes under different amino acid supplementation.

This thesis is organized as follows. Chapter 2 presents the literature review of the mathematical modeling approaches for metabolic network analysis and their challenges. Chapter 3 describes a rational design approach for determination of an amino acid flux profile consistent with an achievement of enhanced performance of liver-specific functions of cultured hepatocytes during plasma exposure. Chapter 4 investigates the amino acid supplementation effects on hepatocyte culture by use of a number of metabolite measurements, a metabolic network flexibility analysis (MNFA) framework,

and a metabolic objective prediction (MOP) model. Chapter 5 makes use of transport constraints in addition to thermodynamic constraints to determine a more realistic amino acid profile that enhances two liver-specific functions i.e. urea production, and free fatty acid (FFA) oxidation (the key intracellular flux to reduce the lipid accumulation during the plasma exposure). Chapter 6 summarizes the main contributions of this thesis and presents ideas for future work including different *in vitro* experiment techniques and mathematical modeling approaches to identify alternative pathways and to investigate the drug-drug interaction by incorporating the drug metabolism into the hepatic network.

Chapter 2

MATHEMATICAL MODELING OF HEPATIC METABOLISM

Abstract:

In vitro experimental data on hepatic metabolism are collected and analyzed using mathematical modeling, in order to interpret the experimental results and predict the cell behavior under different perturbations. Mathematical modeling has been applied to cellular metabolism for more than three decades and can be distinctly classified into kinetic modeling and stoichiometric modeling. Chapter 2 briefly introduces the kinetic modeling approaches first and then presents stoichiometric modeling approaches including metabolic flux analysis, flux balance analysis, and pathway analysis in detail. Further their applications in hepatic metabolism and subsequent challenges have also been discussed.

2.1 Introduction

Mathematical models have been applied to cellular metabolism for more than three decades, which is a powerful tool not only for interpretation of cell phenotype and experimental results, but also for prediction and simulation of the cell behavior under different chemical and physical stimuli (Bailey 1998; De Maria et al. 2008). In mathematical modeling of cell metabolism, a comprehensive metabolic network, with interconnecting pathways consisting of a large number of reactions occurring in the cell, is established to mimic the actual cell phenomena. Such models can be classified into two groups, kinetic and stoichiometric modeling.

Kinetic modeling is based on time variant characteristics of metabolite concentrations and enzyme activities (Gombert and Nielsen 2000). A major challenge of kinetic modeling is availability of multiple parameters of the model. Stoichiometric modeling on the other hand is based on a pseudo-steady state assumption, which assumes the concentration of each intracellular metabolite to be constant. Recently, these mathematical models have been applied to cell's metabolism in order to analyze the flux distributions and identify the metabolic pathways under different environmental conditions, which provide effective guidance on the design of both *in vitro* and *in vivo* experiments.

2.2 Kinetic Modeling

The kinetic modeling is a dynamic model, which has been developed to investigate the cell's behavior under an unsteady state due to small perturbations from environmental changes or enzyme inhibitions. Two kinetic models, physiologically-based pharmacokinetic (PBPK) modeling and metabolic control analysis (MCA), are briefly summarized in this section.

2.2.1 Physiologically-based Pharmacokinetic (PBPK) Modeling

Physiologically-based pharmacokinetic (PBPK) modeling mathematically predicts the course of drug concentration (PK) in various organs, after intravenous infusion or oral drug administration, using a series of differential equations that are based on the anatomical and physiological structure of the body (PB). PBPK modeling was first developed in 1930's (Teorell 1937); however, only simple cases were studied due to the

limitations of computational methods and shortage of pharmaceutical datasets. Since 1990's, with significant improvements in computational techniques and the availability of *in vitro* and *in vivo* data of hepatic metabolism (Bartlett and Davis 2006; Lave et al. 1997) and tissue distribution (Poulin et al. 2001), PBPK modeling has been extensively used in drug discovery (Jones et al. 2009) and risk dose-response assessment (Andersen 1995).

PBPK modeling not only predicts the properties of a compound including absorption, distribution, metabolism and excretion (ADME), which reduce failure in clinical trails by rejection of the compounds with poor ADME, but also provides plasma and tissue concentration-profile which helps choose the suitable dose range for clinical trials.

2.2.2 Metabolic Control Analysis (MCA)

Metabolic control analysis (MCA) introduced in 1970's, has been developed as one of common approaches of kinetic modeling, to provide a way of analyzing the sensitivity of a metabolic network due to the perturbations and determining the control strategies to manipulate the metabolic pathways through individual enzymes (Fell 1992; Heinrich and Rapoport 1974; Moreno-Sanchez et al. 2008). In MCA, three types of coefficients are defined, including flux control coefficients (FCCs) expressing the enzyme concentration effect on the flux, elasticity coefficients (ECs) expressing the concentration change of single reaction on the particular reaction rate of individual enzyme, and concentration control coefficients (CCCs) measuring the control level managed by a particular enzyme on the constant concentration of a individual metabolite (Ehlde and Zacchi 1997; Fell 1992; Reder 1988).

In addition, there are two major theorems in MCA, the flux control connectivity theorem where the sum of FCC multiplied by relative EC is equal to 0 and the summation theorem where the sum of FCC in the metabolic network is equal to 1. At this point, MCA connects the local properties of the isolated flux, enzyme or metabolite (FCC, EC and CCC) with global properties of the metabolic network. Various modifications based on MCA coefficients and theorems have been developed, such as (log) linear kinetic modeling (Hatzimanikatis and Bailey 1997). In the hepatic metabolism, MCA has been used to simulate the substrate concentration in fed and fasted state of rat hepatocytes (Spurway et al. 1997), and to analyze the control temperature effect on respiratory chain network in isolated rat liver mitochondria (Dufour et al. 1996).

2.3 Stoichiometric Modeling

Kinetic modeling can be used to predict the dynamic behavior of the cell in response to external stimuli. However, the lack of complete kinetic information and high cost of manipulation of experiments in time series limit its applications. On the other hand, stoichiometric modeling has been widely used to unravel the complexities of metabolic based on the pseudo-steady state assumption (Llaneras and Pico 2008). A schematic of the different approaches of stoichiometric modeling is summarized in this section (see Figure 2.1), including metabolic flux analysis (MFA), flux balance analysis (FBA), and network-based pathway analysis (Lee et al. 2006; Raman and Chandra 2009; Sauer et al. 2007).

2.3.1 Hepatic Network

The first and most important step for stoichiometric modeling is to construct the metabolic network. The metabolic network is a scale-free network following a power law distribution, which consists of several highly connected functional modules that are connected by few intermodule links (Ravasz et al. 2002). This special structure makes it possible to simplify the complex metabolic network based on the relative functionalities.

A network of hepatic metabolism can be constructed based on the known stoichiometric relationships of the biochemical reactions occurring in the liver. The main hepatic metabolic network was originally developed for liver perfusion (Arai et al. 2001; Lee et al. 2000a) and modified for cultured hepatocytes with many simplifications (Chan et al. 2003a). The main simplification is that detoxification reactions are not involved into the basic hepatic network since their reaction rates are small enough to be ignored for carbon and nitrogen balance. The other simplifications are (a) reactions associated with protein degradation, nucleotide synthesis and energy-requiring pathways for amino acids biosynthesis are neglected; (b) mechanism of transport is not included; (c) distinct reactions/pathway in the different culture conditions, such as glycolysis/glyconeogenesis pathway, and fatty acid synthesis/fatty acid oxidation (Chan et al. 2003a).

With these simplifications, the basic hepatic network involves energy–related reactions: gluconeogenesis/glycolysis, glycogen storage, pentose phosphate pathway (PPP, as a lumped group), oxygen uptake and electron transport system, liver-specific functions such as urea cycle and albumin synthesis, free fatty acid (FFA) metabolism with

triglyceride (TG) and cholesterol ester oxidation, FFA synthesis/oxidation, ketone body synthesis and glycerol management, and other important reactions of tricarboxylic acid cycle (TCA), amino acid uptake/secretion and catabolism. It covers a majority of central carbon and nitrogen metabolism and has been used extensively for the analysis of hepatocyte metabolism *in vitro* (Chan et al. 2003a; Chan et al. 2003b; Chan et al. 2003c; Lee et al. 2003; Nagrath et al. 2007; Sharma et al. 2005; Uygun et al. 2007; Yang et al. 2009).

2.3.2 Metabolic Flux Analysis (MFA)

Metabolic flux analysis is a methodology used to calculate intracellular fluxes (i.e. conversion rates of metabolites through individual reactions) in a metabolic network using the stoichiometric relations of the major reactions and application of mass balance for intracellular metabolites. The mass balance equations are based on the pseudo-steady state assumption, where no accumulation or dissipation on intracellular metabolites is assumed (Stephanopoulos et al. 1998). This assumption is valid for the hepatic metabolism since the concentrations of intracellular metabolites are very small (~nmol/million cell) compared to their turnover (Marin et al. 2004).

Mass balances around intracellular metabolites at the pseudo-steady state are written as follows:

$$\sum_{j=1}^{N} S_{ij} v_j = 0 \qquad \forall i \in M \tag{2-1}$$

where S_{ij} is the stoichiometric coefficient of intracellular metabolite i in the reaction

j, and v represents the flux of reaction j. S_{ij} is positive if metabolite i is a produced and it is negative if the metabolite i is consumed in reaction j, whereas, S_{ij} take a value as 0 if the metabolite i is absent in the reaction j.

In MFA, the reactions are further classified into measured fluxes (extracellular fluxes, S_m) and unmeasured fluxes (extracellular fluxes, S_u). Using this classification Equation (2-1) can be separated into two parts as follows:

$$S_u \cdot v_u = -S_m \cdot v_m \tag{2-2}$$

Typically, MFA is used to calculate unmeasured fluxes for an over-determined system, where available measured fluxes are more than the degrees of freedom of the system. For this case the vector of unmeasured fluxes v_u is calculated by minimizing the sum of square errors between the measured fluxes and the estimated as follows:

$$v_u = -(S_u S_u^T)^{-1} S_m S_m^T v_m \tag{2-3}$$

In MFA model, the measured fluxes are typically nutrition uptake into the cell and metabolite release from the cell, which can be directly evaluated based on the difference between the concentration of metabolites in the cultured medium and collected supernatant from *in vitro* experiments.

Each measured flux is calculated using repeated measurements from different instruments, and is represented by an arithmetic mean plus/minus its standard derivation (mean ± standard derivation). The measured results are associated with gross measurement errors, which ascribes to improper selections of measurement approaches or equipments and

need elimination before performing metabolic flux analysis using the statistic hypothesis test (Wang and Stephanopoulos 1983). Isotopomer analysis by tracing ^{13}C-labeled substrate using nuclear magnetic resonance (NMR) or gas chromatograph/mass spectroscopy (GC/MS) has been used to provide additional measurements (Riascos et al. 2005; Wiechert 2001) and to validate the flux estimation from MFA (Zupke and Stephanopoulos 1995).

For the hepatic metabolism, MFA has been used to investigate the effects of a combination treatment (hormone and amino acid supplementation) on intracellular fluxes and liver-specific functions of cultured hepatocytes during plasma exposure (Chan et al. 2003b). The results showed that the high level of insulin in pre-conditioning impacts the hepatocyte behavior during subsequent plasma exposure. Moreover hormone and amino acid supplementation during plasma exposure enhances the liver-specific functions by reducing the lipid accumulation in the cells. MFA was also used to investigate the metabolic state change specifically after acute liver failure (Arai et al. 2001) and burn injury (Lee et al. 2000a; Lee et al. 1999).

Metabolic flux analysis provides a comprehensive view of intracellular metabolism based on measurements of extracellular fluxes and stoichiometric mass balance at the pseudo-steady state. By comparing the intracellular fluxes in different environmental conditions, MFA can be used to investigate the metabolic state change due to external stimuli. However, the main difficulty in applying MFA is to get the necessary measurements that result in an over-determined system. Another shortcoming of MFA is

that it does not incorporate the reaction directionality, which is very important and may change in different conditions.

2.3.3 Flux Balance Analysis (FBA)

Flux balance analysis (FBA) has been used to calculate the intracellular fluxes under the optimization of a specific objective function restricted by mass balances equations at the pseudo-steady state and other constraints. FBA better compensates the issue of under-determined system where measurements are not sufficient. However, it is possible that alternative flux distributions exist that produce the same optimization solution in which a subset of the reactions exhibits different values (Lee et al. 2000b). Therefore, finding appropriate objectives for the cell (Gianchandani et al. 2008; Khannapho et al. 2008; Schuetz et al. 2007) and imposing a set of reasonable constraints (Bonarius et al. 1997) are important aspects for the current developments of FBA.

2.3.3.1 Metabolic Objectives of Flux Balance Analysis

The traditional FBA framework optimizes a single objective over a feasible region. Common objective includes maximization of growth rate of *Escherichia coli* (Varma and Palsson 1994b), maximization of ATP production in the mitochondrion (Ramakrishna et al. 2001), maximization of a specific function of mammalian cell under exceptional culture conditions (Sharma et al. 2005), or maximization of the formation of the key liver anti-oxidation glutathione (GSH) (Yoon and Lee 2007). Recently, urea maximization has been chosen as an objective function for analysis of cultured hepatocytes of BAL devices (Sharma et al. 2005), and for determination of amino acid supplementation in hepatocyte

culture using a rational design approach (Yang et al. 2009).

Traditional FBA employs linear programming since both objective function and constraints are linear. In this case, investigation of the uniqueness and identification of all alternative optimal solutions are very important to analyze alternative pathways via different flux distribution patterns with the same objective value. A recursive mixed-integer programming problem has been developed to find all alternative optima by introducing two binary variables, one to separate the basic variables from non-basic variables, and another to ensure that all non-basic variables are zero (Lee et al. 2000b; Phalakornkule et al. 2001). This approach has been applied to identify alternative pathways for different amino acid supplementations during plasma exposure, and eight different pathways with the same value of maximum urea were determined (Yang et al. 2009).

Since mammalian cells may have more than one objective function, a multi-objective approach modified based on FBA has been developed to identify the flux distribution which optimizes several objectives simultaneously. A weight sum of objective functions is used to convert the multi-objective problem to a single objective by summation of the different objectives with defined various weights and results in a Pareto-optimal set for the multi-objective model. The Pareto-optimal solution has been used to help understand hepatic cellular system with competitive cell functions, such as urea and albumin production/GSH/ATP synthesis (Nagrath et al. 2007; Sharma et al. 2005). Those Pareto-optimal solutions may contribute to operating BLA devices based on the feasible

solutions range obtained from the model, and can help to develop the metabolic control strategy of hepatocytes based on the different Pareto set with various metabolic states.

Another modified FBA framework is a multi-level objective, which optimizes several objectives gradually according to their priorities rather than optimizing them simultaneously. Bi-level programming with two objectives has been used to study the metabolic network, where the constraints of one problem (upper level problem) are defined in part by a second optimization problem (lower level problem). ObjFind, a bi-level optimization problem, minimizes the sum of square errors of measured fluxes between the measured values and those from the model in the upper level and maximizes the sum of weighted fluxes in the lower level (Burgard and Maranas 2003). The advantage of this approach is that it can infer the metabolic objectives which are the most consistent with experimental data using the value of the coefficient of importance rather than starting by postulating an objective. This approach has been used to investigate the metabolic objectives in cultured hepatocytes for BAL devices under a wild range of different culture conditions during plasma exposure (Uygun et al. 2007). Bi-level programming can be reformed into a single-level programming by following the primal-dual strategy which constructs an optimization problem that includes both primal and dual constraints with an equality constraint for primal and dual objective (Burgard and Maranas 2003; Burgard et al. 2003; Pharkya et al. 2003), or replacing the inner optimization problem with its first-order equilibrium constraints and complementary constraints (Raghunathan and Biegler 2003; Raghunathan et al. 2003).

Recently, a number of modified FBA has been developed to predict the cell phenotype after knockout of single or multiple genes. Two examples are minimization of metabolic adjustment (MOMA) that minimizes the Euclidean distance from a wild-type flux distribution (Segre et al. 2002) and regulatory on/off minimization (ROOM) that minimize the number of significant flux changes (Shlomi et al. 2005). These approaches have been used to predict the flux distribution of *E. coli* after a particular gene knockout and help to understand how cell adapts to the loss of a gene by regulation. Both approaches are motivated by the assumptions that cells have minimal changes close to the wild type after gene knockout rather than minimizing the growth rate that is predicted by FBA. OptKnock, a bi-level programming problem, was developed to identify multiple gene knockout strategies in *E. coli* for maximization of the desired production in the upper level and maximization of biomass yield or MOMA in the lower level (Burgard et al. 2003). This approach has been used to identify the reactions whose removal leads to redirect the *E. coli* metabolism towards to maximum amino acid production at maximum biomass yield (Pharkya et al. 2003). However, these approaches have not applied for the cultured hepatocytes, which is possible due to the difficulties to perform gene inhibition experiments.

2.3.3.2 Constraints of Flux Balance Analysis

The hepatic network is complex and thus multiple metabolic states may exist. In the kinetic modeling, the state is separated using kinetic parameters varied with time. In the stoichiometric modeling, the state can be defined using different constraints (Edwards and Palsson 2000). In addition, the constraints help to reduce the feasible region of the

unmeasured flux space.

Various constraints incorporating to the stoichiometric modeling involve environmental (nutrient, physical factor etc.), physicochemical (mass balance, reaction directionality, maximum enzyme capacities), self-imposed regulatory and evolutionary constraints (Covert et al. 2003). Those constraints can be written in term of linear inequality by giving minimum and maximum value for each individual reaction ($v_j^{\min} \le v_j \le v_j^{\max}$) based on the measurement data from the different *in vitro* experiments, which can be further restricted to the minimum value as zero for the reversible reactions ($0 \le v_j \le v_j^{\max}$) and defined as zero associated with the deleted gene ($v_j = 0$) (Edwards and Palsson 2000).

Successfully imposition of constraints on FBA helps to reduce the feasible range for each unmeasured flux in the network dramatically. Recently, three additional thermodynamics constraints using the second law of thermodynamics, including energy balance analysis (EBA), pathway energy balance constraints (PEB) and network-embedded thermodynamic analysis (NET analysis), have been incorporated into the FBA model to reduce the solution space by deleting thermodynamically infeasible ones (Beard and Qian 2005; Kummel et al. 2006; Nolan et al. 2006). There are two major contributions from EBA constraints. One is used to eliminate the internal cycle in the network, which is similar to the basic concept of the voltage loop law: no net flux is possible through these cycles (Beard et al. 2004; Beard et al. 2002; Beard and Qian 2005). Moreover, EBA ensures that entropy production is positive for each reaction, which means that positive Gibbs free energy of a reaction should associate with a negative value of reaction flux

and the other way around. PEB constraints successfully extended the second law of thermodynamics from individual reactions (EBA) to individual pathways. The idea behind PEB constrains is that endergonic reactions ($\Delta G > 0$) can be "powered" by exergonic reactions ($\Delta G < 0$) if those reactions are 'coupled' in the same pathway. Therefore, an overall distribution of Gibbs free energy to the reactions involving pathway analysis and flux distribution is imposed as PEB constraints into FBA model (Nolan et al. 2006). Since metabolic concentration from different metabolic state can greatly affect the real Gibbs free energy of reactions, NET analysis incorporating the concentrations of metabolites as additional constraints, has been used to determine the feasible range of Gibbs free energy of reactions at a certain state (Kummel et al. 2006; Zamboni et al. 2008).

In the hepatic metabolism, there are promising applications by incorporating these thermodynamic-based constraints, including understanding of cellular regulatory of hepatocyte (Beard and Qian 2005), study of drug-drug metabolic interactions between acetaminophen and ethanol (Yang and Beard 2006), investigation of the metabolic objectives of liver hepermetabolism (Nolan et al. 2006) and analysis of anti-diabetes drug toxicity (Yoon and Lee 2007).

2.3.4 Pathway Analysis

In contrast to flux analysis, pathway analysis can be used to identify metabolic pathways and their functional connections by separating the entire network into pathways (sub-network). This analysis can be done without requiring information of flux values or

imposing any objective functions for cellular metabolism (Trinh et al. 2009).

The most commonly used methods for pathway analysis are elementary flux modes (EFM) and extreme pathways (EP) (Schilling et al. 2000; Schuster et al. 1999; Schuster et al. 2000; Wiback and Palsson 2002). In both two approaches, convex analysis is used to identify the convex set of flux vectors that satisfy the linear equations generated from mass balances and inequalities from the reaction directionality. EFMs are the set of all pathways that consist of the minimum of reactions that exist as a function unit. EPs are the system independent and irreducible subset of elementary modes, which do not include pathways non-negatively combined by other extreme pathways. The details of differences and similarities between EFM and EP have been recently reviewed (Klamt and Stelling 2003; Papin et al. 2004; Wagner and Urbanczik 2005).

From a mathematical perspective, the elementary modes of a biochemical network can be defined as the set of flux vectors that satisfy the following equation (Poolman et al. 2004),

$$S \cdot e = 0 \tag{2-4}$$

where **S** is the stoichiometric matrix of the metabolic network, and e is a column vector whose elements indicate the participation of each reaction in that particular modes. A number of software programs for computing elementary modes and extreme pathways are available, such as C programming METATOOL (Pfeiffer et al. 1999), Expa (Bell and Palsson 2005), YANA (Schwarz et al. 2005) and the software package FluxAnalyzer with a user-friend interface based on MATLAB (Klamt et al. 2003).

In addition, flux analysis and pathway analysis can be combined to identify the pathways associated with a certain steady-state flux distribution. The flux distribution that satisfies the stoichiometric matrix and the reaction directionality can be represented as a linear combination of vectors of EFM or EP with non-negative weights as follows,

$$E \cdot w = v \tag{2-5}$$

where **E** is a matrix of elementary modes in which the columns represent the pathways, v is a given flux distribution and w is a vector of weights corresponding to EFM or EP. Several approaches have been developed to reconstruct the metabolic network by calculating the weights which include (a) seeking the weights of each mode (Poolman et al. 2004) or random selected subset modes (Wang et al. 2007) using a least-square solution of the problem; (b) generating the minimum norm of the weighting vector, which, in biological terms, is to find the modes that are closest to the real flux distribution pattern (Schwartz and Kanehisa 2005); (c) calculating a range of possible values of weights (α-spectrum) (Wiback et al. 2003); and (d) identifying the least number of pathways, in biological terms, which is to find minimum number of regulatory routes needed to control the system (Wiback et al. 2003).

Both concepts of EFM and EP have been successfully applied to a number of metabolic networks, including identification of the efficient pathways of human red blood cell (Wiback et al. 2003), definition of the minimal medium requirement for *H. pylori* (Schilling et al. 2002) and study of the growth behavior of *E.coli* central metabolism (Stelling et al. 2002). For hepatic network analysis, the majority of pathway analysis

publications are used to analyze the robustness of amino acid anabolism in human hepatocyte (Behre et al. 2008) and to investigate the network flexibility of hepatic metabolism (Nolan et al. 2006; Yoon and Lee 2007). However, tremendous number of elementary modes/extreme pathways for the hepatic network with medium-scale and complex interconnection, makes the problem computationally infeasible or brings difficulties to analysis of the overall hepatic network (Klamt and Stelling 2002). Thus, a decomposition algorithm, based on local connection of metabolites, has been presented to automatically decompose the network into smaller subsystems (Schuster et al. 2002b). The application of this approach to decompose the basic hepatic network is still questioned and better logical decomposition rules are expected.

Flux analysis and pathway analysis have been recently reviewed in (Edwards et al. 2002; Kauffman et al. 2003; Lee et al. 2006; Nielsen 2003; Raman and Chandra 2009; Trinh et al. 2009; Varma and Palsson 1994a) and in more detail in (Stephanopoulos et al. 1998; Torres and Voit 2002)

2.3.5 Conclusions

In summary, mathematical modeling is a promising tool for evaluating and predicting fluxes and pathways of the hepatic metabolism associated with different environmental perturbations. It can be extrapolated for *in silico* modeling applications such as design of the ideal culture medium for hepatocytes, understanding xenobiotic detoxification and it can also help develop a genome-scale hepatic network.

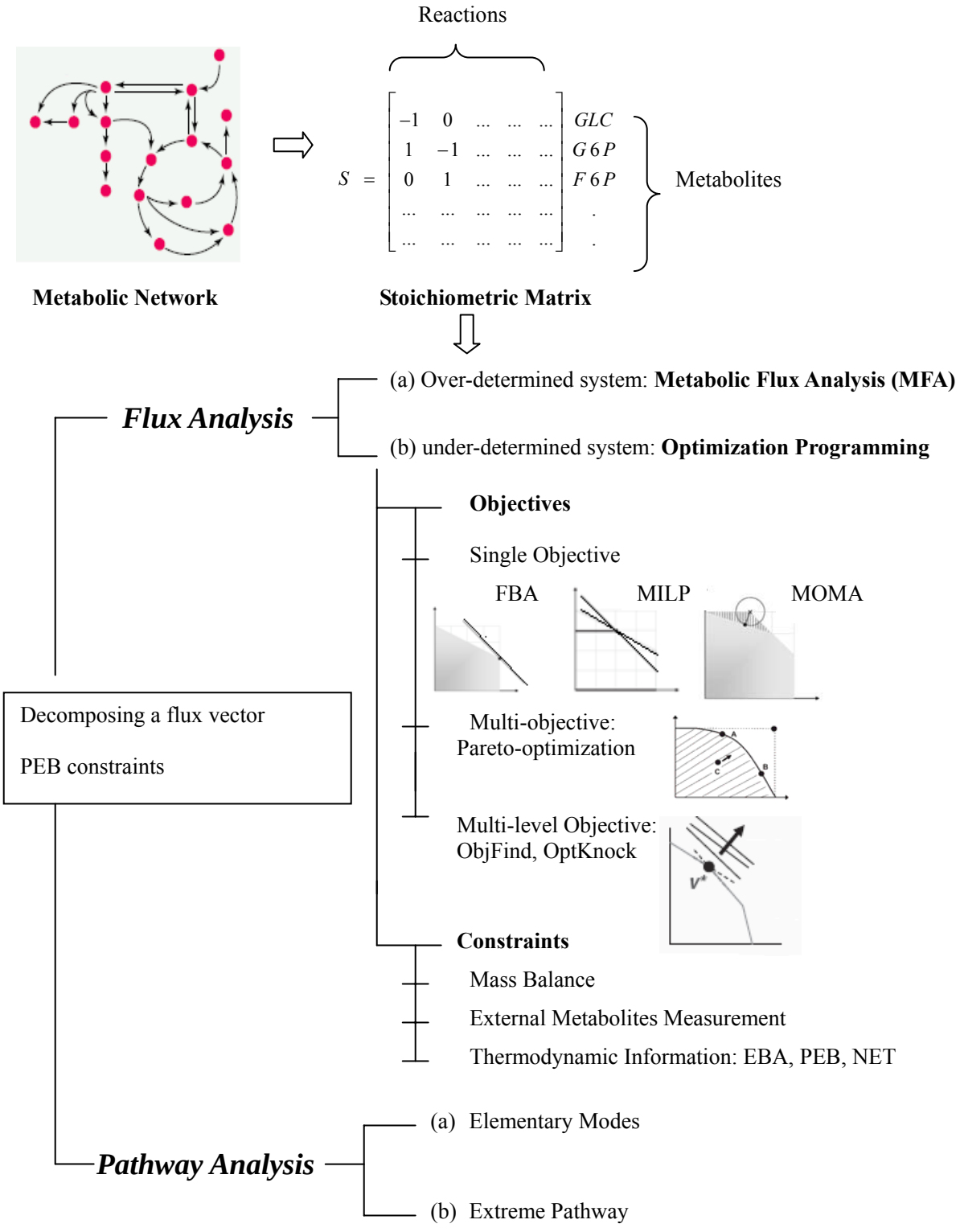

Figure 2.1: Stoichiometric modeling: flux and pathway analysis

Chapter 3

A RATIONAL DESIGN APPROACH

FOR AMINO ACID SUPPLEMENTATION IN HEPATOCYTE CULTURE

Abstract:

Improvement of culture media for mammalian cells is conducted via empirical adjustments, sometimes aided by statistical design methodologies. Chapter 3 demonstrates a proof of principle for the use of constraints-based modeling to achieve the enhanced liver-specific functions of cultured hepatocytes during plasma exposure by adjusting amino acid supplementation and hormone levels in the medium. Flux balance analysis (FBA) is used to determine an amino acid flux profile consistent with a desired output, which is used to design an amino acid supplementation. The morphology, specific cell functions (urea, albumin production) and lipid metabolism of cultured hepatocytes during plasma exposure were measured under conditions of no supplementation, empirical supplementation, and designed supplementation.

Urea production under the designed amino acid supplementation was found to be increased compared with previously reported (empirical) amino acid supplementation. Although not an explicit design objective, albumin production was also increased by designed amino acid supplementation, suggesting a functional linkage between these outputs. In conjunction with traditional approaches to improving culture conditions, the rational design approach described herein provides a novel means to tune the metabolic outputs of cultured hepatocytes.

3.1 Introduction

The metabolic capabilities and constraints of cultured hepatocytes are of great interest for the development of extracorporeal bioartificial liver (BAL) devices to support and extend the life of critically ill patients until a liver transplantation becomes available (Allen and Bhatia 2002; Matthew et al. 1996b; Tilles et al. 2002). Cultured hepatocytes are core components of BAL devices, which have been developed rapidly in recent years (Strain and Neuberger 2002). However, hepatocytes are anchorage-dependent cells, and they rapidly lose liver-specific functions once they are removed from their host and cultured in an artificial environment (Allen et al. 2001). Some culture techniques have been introduced to help stabilize liver-specific *in vitro* functions, which include culturing hepatocytes in sandwich collagen gels (Dunn et al. 1991; Dunn et al. 1992), co-culturing hepatocytes with other types of cells such as 3T3 fibroblasts (Bhatia et al. 1997), culturing hepatocytes on extracellular matrix (Page et al. 2007), and addition of insulin to the culture medium (Li et al. 2004). Maintenance of liver-specific functions in hepatocytes during plasma exposure is very important to BAL devices. Effects of short- or long-term exposure of hepatocytes to plasma, as occurs during clinical application, have been studied recently. Hepatocytes exposed to plasma *in vitro* exhibit a progressive accumulation of lipid droplets, accompanied by a decrease in functional markers such as urea and albumin synthesis (Matthew et al. 1996b; Stefanovich et al. 1996). Subsequent studies demonstrated that supplying amino acids and hormones (insulin and hydrocortisone) during plasma exposure improves synthetic functions as well as cytochrome P450 (detoxification) activities of the rat hepatocytes (Washizu et al. 2000a; Washizu et al. 2001; Washizu et al. 2000b).

Mathematic modeling of hepatic metabolism is increasingly being utilized in tandem with experimental measurements to understand and control the performance of hepatocytes under adverse culture conditions. Metabolic flux analysis (MFA), which provides a comprehensive view of intracellular metabolism based on measurements of extracellular fluxes and stoichiometric mass balances at pseudo-steady-state, has been utilized to investigate the effects of insulin preconditioning and plasma amino acid supplementation on cultured hepatocytes. It was found that a combination of these two treatments promotes hepatic-specific functions (urea and albumin secretion), mediated by an increase in gluconeogenesis and a reduction in the intracellular triglyceride accumulation (Chan et al. 2003a; Chan et al. 2003b; Chan et al. 2003c). Flux balance analysis (FBA) is based on the utilization of linear programming and the pseudo-steady-state assumption to optimize a specific objective function, while satisfying mass balances for all intracellular metabolites and other imposed constraints (Kauffman et al. 2003; Varma and Palsson 1994a). Depending on the system of interest, various objectives may be employed in FBA, including maximization of growth rate (Edwards et al. 2001; Mahadevan et al. 2002; Varma and Palsson 1994b), maximization of specific fluxes in mammalian cells (Marin et al. 2004; Sharma et al. 2005), or minimization of metabolic adjustment (MOMA) (Segre et al. 2002) when experimental data are available for comparison between wild type and gene knockout. In order to extend the understanding of hepatocyte functions relevant to the BAL, constraint-based techniques have been used to characterize the capabilities of the hepatocyte metabolic network. Some recent studies have focused on the overall flux distribution in the central metabolism of primary rat hepatocytes using

FBA (Nagrath et al. 2007; Sharma et al. 2005; Uygun et al. 2007).

We present an approach that uses FBA to design an amino acid supplementation to achieve a specific cellular objective in cultured hepatocytes exposed to plasma, in this case urea production. Urea secretion is easily measured to high accuracy using commercial kits and is a well-established baseline marker of hepatocyte culture, making it a suitable objective for FBA. From the amino acid fluxes corresponding to urea output, a novel amino acid supplementation was designed and used in the culture of cryopreserved hepatocytes with varying insulin levels during preconditioning and hormone levels during plasma exposure. Hepatocyte morphology was observed and specific cell functions (urea, albumin production) and lipid accumulation were measured in order to validate our hypothesis that urea secretion would be augmented using amino acids supplementation calculated theoretically from a mathematical model.

3.2 Methods

3.2.1 Flux Balance Analysis

The basic hepatic network used in this analysis (Appendix A) is based on the network developed for metabolic flux analysis of cultured hepatocytes (Chan et al. 2003a; Lee et al. 2000a; Sharma et al. 2005). The hepatic network considered here involves 45 intracellular metabolites and 76 reactions (33 irreversible reactions and 43 reversible reactions, labeled in Appendix A), including gluconeogenesis, tricarboxylic acid cycle (TCA), urea cycle, amino acid uptake and catabolism, oxygen uptake, electron transport system, pentose phosphate reactions (as a lumped group), ketone body synthesis, fatty

acid, triglyceride (TG) and glycerol metabolism. Although this hepatic network doesn't account for protein degradation, energy balance, nucleotide and transport metabolism, it covers a majority of central carbon and nitrogen metabolism and has been used extensively for analysis of the hepatic metabolism both *in vitro* and *in vivo* (Chan et al. 2003a; Chan et al. 2003b; Chan et al. 2003c; Lee et al. 2003; Nagrath et al. 2007; Sharma et al. 2005; Uygun et al. 2007).

The following FBA model is developed for the maximization of urea output, constrained by 45 mass balances for the intracellular metabolites and flux bounds of measured and irreversible reactions based on the hepatic network of Appendix A, as follows:

$$\begin{aligned} Max \quad & v_{urea} \\ s.t. \quad & \sum_{j=1}^{N} S_{ij} v_j = 0 \qquad i \in M \\ & v_j^{\min} \le v_j \le v_j^{\max} \qquad j \in N \end{aligned} \tag{I}$$

where S_{ij} is the stoichiometric coefficient of metabolite i in the reaction j; v_j refers to the flux of reaction j, v_{urea} is urea flux; M is the number of metabolites; K is the number of constrained reactions (based on measurements and/or irreversibility), and N is the total number of reactions involved in the hepatic network. Model (I) corresponds to a linear programming (LP) problem since the objective and the constraints are linear functions of the involved variables.

The main assumptions for the development of the FBA model are as follows:

1) Although it exists many of hepatic functions, urea production is the one often used as a marker of hepatocyte function that typically correlates with a healthy, differentiated

phenotype (Chan et al. 2002; Higuchi et al. 2006; Kane et al. 2006; Li et al. 2004; Washizu et al. 2000a; Washizu et al. 2000b) and the one of liver-specific functions that hepatocytes may seek to satisfy directly or indirectly. Therefore, urea maximization is a reasonable case study for the approach.

2) One can assume a pseudo-steady state for the hepatic metabolic network, which means that the rate of change of intracellular compositions is small (Stephanopoulos et al. 1998). This assumption is valid because the concentrations of intracellular metabolites are very small (~nmol/million cell) compared to their turnover, relative flux (~μmol/million cell/day) x measurement time (one day) (Marin et al. 2004).

3) We assume that the designed supplementation fine tunes rather than radically alters hepatocyte metabolism. Therefore, we can use a prior set of experimental measurements and calculated fluxes as representative of the physiological space state of hepatocytes. The prior data considered include: high/low insulin preconditioning followed by unsupplemented plasma cultures (HI_NAA_NH/LI_NAA_NH), and high/low insulin preconditioning followed by amino acid-supplemented plasma cultures (HI_RAA_NH/LI_RAA_NH) (see Table 3.1 for details of experimental conditions). The range of experimental data (Chan et al. 2003c) defines the minimum and maximum values (bounds) of measured fluxes in the model (Appendix B).

4) The reversibility of each reaction is determined based on the information given in the metabolic map of KEGG (Kanehisa and Goto 2000). Reversible reactions are allowed to take either positive or negative values, whereas irreversible reactions are restricted to positive values (Appendix B).

The FBA Model (I) leads to one flux distribution that maximizes the objective function and is consistent with the imposed constraints; however, it is possible that alternative flux distributions exist that produces the same maximal output but in which a subset of the reactions exhibits different values or reaction directionalities (Price et al. 2004). The need to search for all alternative solutions has been demonstrated previously for the central metabolism of *E. coli* (Lee et al. 2000b). The solution strategy involves a recursive mixed integer linear programming (MILP) to enumerate all solutions. To apply this approach, model (I) is first reformulated to its canonical form (Chvatal 1983) by introducing slack variable s^L, s^U for the lower and upper bounds of v, respectively.

$$\begin{aligned} Max \quad & \alpha^T \\ s.t. \quad & Bz = q \\ & z \geq 0 \end{aligned} \tag{II}$$

where $z = \begin{bmatrix} s^L \\ s^U \end{bmatrix}$, $\alpha = \begin{bmatrix} c \\ 0 \end{bmatrix}$, $B = \begin{bmatrix} S & 0 \\ I & I \end{bmatrix}$, $q = \begin{bmatrix} -Sv^{\min} \\ v^{\max} - v^{\min} \end{bmatrix}$; c is an N-dimensional column vector, but only the element related to urea production is equal to 1, and the others are zero.

Next, two types of binary variables are introduced to make sure that all different bases are examined. Binary variable y is used to identify a new basis set in each iteration, whereas another binary variable w represents the variable that does not belong to the basis and takes the value of zero. Therefore, model (II) is rewritten as MILP problem as follows,

$$
\begin{aligned}
Max \quad & \alpha^T z \\
s.t. \quad & Bz = q \\
& \sum_{i \in NZ^{P-1}} y_i \geq 1 \\
& \sum_{i \in NZ^{p}} w_i \leq \left| NZ^{p} \right| - 1 \qquad p = 1, 2, ..., P-1 \\
& 0 \leq z_i \leq U w_i \qquad i \in I \\
& y_i + w_i \leq 1 \qquad i \in NZ^{P-1} \\
& z \geq 0
\end{aligned}
\tag{III}
$$

where p is an iteration counter; y_i is a binary variable that takes the value of 1 if z_i is non-zero basic variable at the previous iteration *p-1*, otherwise it takes the value of 0 and remains in the basis; w_i is a binary variable used to ensure that all non-basic variables are zero; and U is the upper bound of z, chosen arbitrarily to exceed the upper bound of the fluxes. In this model (III), it is chosen to take the value of 1000, which is sufficiently greater than the maximum overall flux. There is a new constraint added in each iteration p to eliminate at least one of the nonzero variables of the basis based on the results of the previous iterations, $p = 1, 2, ..., p-1$. The algorithm stops when the objective function in the current iteration is less than that of the previous iteration, which means all solutions with the same objective function value have been found.

All mathematical models in this study are implemented using GAMS version 22.4 and solved by CPLEX 9 on a Dell PC (3 GHz, 1 GB of RAM).

3.2.2 Hepatocyte Culture Media

Dulbecco's Modified Eagle's Medium (DMEM) with 4.5 g/L glucose, fetal bovine serum (FBS), penicillin and streptomycin were purchased from Invitrogen Corporation (Carsbad,

CA). Heparinized human plasma was obtained from Innovative Research Inc (Novi, MI). Glucagon, hydrocortisone, epidermal growth factor, insulin, Modified Eagle's Medium (MEM) vitamin solution, Eagle's Basal Medium (BME) amino acid solution, RPMI 1640 solution, and all other chemicals were purchased from Sigma Chemical (St. Louis, MO).

Standard hepatocyte C+H medium consists of DMEM supplemented with 10% heat inactivated fetal bovine serum, 7.0 ng/mL glucagon, 7.5 g/mL hydrocortisone, 20 g/L epidermal growth factor, 200 U/mL penicillin, 200 g/mL streptomycin, and 500 mU/mL insulin (high insulin, HI) or 0.05 mU/mL insulin (low insulin, LI). Type I collagen was prepared by extracting acetic acid-soluble collagen from rat tail tendons as described previously (Dunn et al. 1991). A collagen gelling solution is prepared by mixing rat type I collagen with DMEM to a final concentration of 1 mg/mL.

L-arginine free medium consists of L-arginine free RPMI 1640 plus 10% fetal bovine serum, and 500 mU/mL insulin with concentrations of glucagon, hydrocortisone, epidermal growth factor, penicillin, streptomycin identical to those in standard hepatocyte C+H medium.

Plasma solution was prepared by mixing 81 mL of heparinized human plasma with 2 mL MEM vitamin solution, 1 mL streptomycin-penicillin solution, and 5 mL buffer solution with 2.56% (w/v) sodium monophosphate and 7.5% (w/v) sodium bicarbonate. Two types of amino acid supplemented plasma were prepared – a "reference" supplementation (RAA) based on previous published work, and a "designed" supplementation (DAA)

based on our FBA predictions. To prepare RAA plasma, 2 mL of 200 mM glutamine, 8 mL (50x) BME amino acid solution were added to the media. To prepare DAA plasma, amino acids were added to the media according to the final compositions based on the calculation from flux balance (see Table 3.2 in Results).

3.2.3 Design of Experiment: Amino Acid Supplementation

Cryopreserved rat hepatocytes were purchased from Xenotech LLP (Lenexa, KS). The Xenotech protocol for thawing cryopreserved hepatocytes was followed. The viability of reconstituted cells was estimated by trypan blue exclusion.

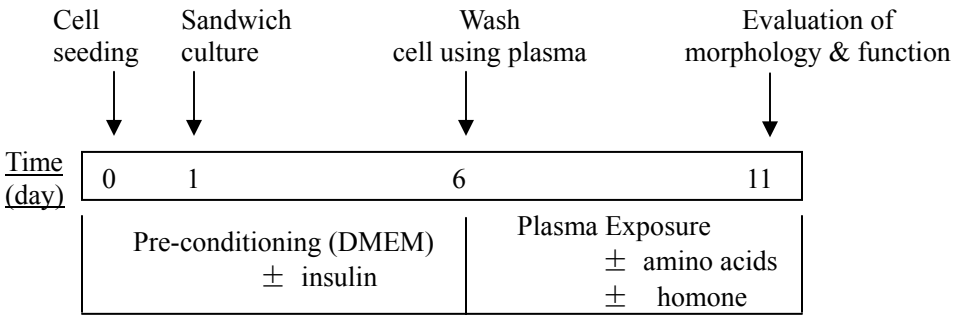

Figure 3.1: Experimental timeline

The experimental timeline is shown in Figure 3.1. A quantity of 0.4 mL of the mixed collagen solution was poured in each well of six-well plates and incubated at 37 °C and 10% CO_2 for at least 90 minutes until the gel solidified. Suspended cryopreserved hepatocytes were seeded in each collagen-coated well at a density of $1x10^6$ cells/mL. After 24 hours incubation, culture medium was aspirated and 0.4 mL of collagen solution was added, which gelled to form a collagen sandwich. After 90 minutes gelation time, 0.8 mL fresh culture medium was added. Fresh medium was exchanged with spent medium

daily for 6 days prior to plasma exposure. The 6-day-old sandwiched hepatocyte cultures were subsequently exposed to either unsupplemented (NAA) plasma, RAA plasma or DAA plasma for an additional 5 days. At the end of the experiment, culture supernatants were collected and stored at 4 °C prior to analysis.

The three independent variables used in the design of the experiments are: (1) the insulin level (500 mU/mL, HI and, 0.05 mU/mL, LI) during pre-conditioning culture with DMEM; (2) amino acid supplementation in the plasma (unsupplemented, NAA, "reference" supplementation, RAA, "designed" supplementation, DAA) and (3) hormone supplementation in plasma including 7.5 g/mL of hydrocortisone and 0.05 mU/mL of insulin (WH) or without hormone supplementation (NH) during plasma exposure. Twelve treatment combinations are listed in Table 3.1.

Table 3.1: Treatment conditions

Treatment Condition	Medium Preconditioning	Amino Acid Supplementation	Hormone Supplementation
HI_NAA_NH	High insulin (+)	Unsupplemented (-)	Unsupplemented (-)
LI_NAA_NH	Low insulin (-)	Unsupplemented (-)	Unsupplemented (-)
HI_RAA_NH	High insulin (+)	Reference supplemented (R)	Unsupplemented (-)
LI_RAA_NH	Low insulin (-)	Reference supplemented (R)	Unsupplemented (-)
HI_DAA_NH	High insulin (+)	Designed supplemented (D)	Unsupplemented (-)
LI_DAA_NH	Low insulin (-)	Designed supplemented (D)	Unsupplemented (-)
HI_NAA_WH	High insulin (+)	Unsupplemented (-)	Supplemented (+)
LI_NAA_WH	Low insulin (-)	Unsupplemented (-)	Supplemented (+)
HI_RAA_WH	High insulin (+)	Reference supplemented (R)	Supplemented (+)
LI_RAA_WH	Low insulin (-)	Reference supplemented (R)	Supplemented (+)
HI_DAA_WH	High insulin (+)	Designed supplemented (D)	Supplemented (+)
LI_DAA_WH	Low insulin (-)	Designed supplemented (D)	Supplemented (+)

After 5 days exposure to the various plasma conditions, the morphology of the hepatocytes cultured in a collagen sandwich medium was captured using an Olympus CKX41 microscope. Urea was measured using a standard, commercial kit (Sigma, St. Louis, MO). Albumin concentrations were determined by enzyme-linked immunosorbent assay (ELISA) using purified rat albumin (MP Biomedicals, Solon, OH) and peroxidase-conjugated antibody for detection (MP Biomedicals, Solon, OH). Free fatty acids were measured in the presence of the enzyme acetyl-COA synthetase using a commercial enzymatic colorimetric kit (Roche, Indianapolis, IN). Triglyceride levels were measured with a commercial kit (Stanbio, Boerne, TX) based on the release of glycerol catalyzed by lipoprotein lipase. β-hydroxybutyrate was quantified using a commercial kit (Stanbio, Boerne, TX) based on the appearance of NADH in the conversion to acetoacetate by adding β-hydroxybutyrate dehydrogenase, and acetoacetate

were quantified based on the disappearance of NADH in the conversion to β-hydroxybutyrate by adding the same enzyme in a different pH buffer (Chan et al. 2003a). Each flux value was calculated by subtracting the supernatant concentration from the unconditioned medium concentration and dividing by the cell number and the time interval over which the medium was exposed to cells.

At the end of experiment, live cells were distinguished by green fluorescence generated by the fluorogenic reagent calcein AM (Molecular Probes, Eugene, OR), and dead cells were identified by red fluorescence resulting from nucleic acids bound with ethidium homodimer (Molecular Probes, Eugene, OR). Cell viability was calculated as the ratio of the number of live cells to the total number of cells, which was quantified after killing all of the cells using 75% methanol at the end of the experiment.

3.2.4 Design of Experiment: Supplementation of Arginine

Hepatocytes isolated from adult F344 male rat were suspended in standard C+H medium and cultured in a collagen sandwich configuration at a density of $1x10^6$ cells/mL for two days. Hepatocytes were subsequently switched to media with varying L-arginine concentration (0.2, 0.4, 1, 2, 4 and 8 mM) for three days. Fresh medium was exchanged with spent medium and supernatant was collected daily. At the end of the experiment, urea production was measured using a standard commercial kit (Sigma, St. Louis, MO).

3.3 Results

3.3.1 Rational Design of Amino Acid Supplementation

The FBA model predictions maximize urea secretion while maintaining exchange fluxes

within bounds based on prior experimental observations and satisfying the constraints of material balance at pseudo-steady-state. The solution of model III (Appendix C) offers insights into the flux distribution of exchange reactions (primarily amino acid transport) required for optimization of urea production and allows analysis of the flexibility of the hepatic network via the computation of multiple solutions. With the resulting distribution of exchange fluxes, a level of urea production is predicted (6.81 μmol/million cells/day) that is increased more than two fold compared with urea production reported in the literature for hepatocytes exposed to plasma (Chan et al. 2003a; Chan et al. 2003c). Eight fluxes distributions are found using model (III) that each satisfies all the metabolic constraints and results in the same maximal urea flux. Eleven out of 76 reactions in the overall network illustrate some flexibility, including gluconeogenesis (R1-8), palmitate uptake (R72), production of glyceraldehyde-3-P (R73) and cholesterol eater consumption (R75). These are summarized in Appendix C. Further analysis illustrates that in all cases the difference between the flux value of reaction 6 (oxaloacetate transformation to phosphoenolpyruvate) and reaction 7 (pyruvate transformation to oxaloacetate) is identical, so that the net flux of oxaloacetate entering the TCA cycle and urea cycle is constant. Each of the remaining fluxes has the same value in all eight flux distributions, suggesting that overall the network is not very flexible in attaining the theoretically optimal urea secretion.

The amino acid uptake/secretion rates (v_{18}, v_{22}, v_{24}, v_{26}, v_{29}, v_{35}, v_{37}, v_{44}, v_{58}-v_{68}) associated with theoretically optimal urea production (Appendix C) constitute target fluxes, v_{target}, which are used to calculate the necessary concentration of amino acids in

the media (i.e., supplementation) by assuming a linear relationship between amino acid supplementation and corresponding fluxes in the model (Sharma et al. 2005). This extrapolation is likely to be a reasonable first-order approximation because the designed amino acid supplementation (DAA) is a perturbation from the reference supplementation (RAA), and amino acid flux data are available for both the non-supplemented (NAA) and RAA states as well as for culture in medium only (Chan et al., 2003b; 2003c) (Fig. 3.2).

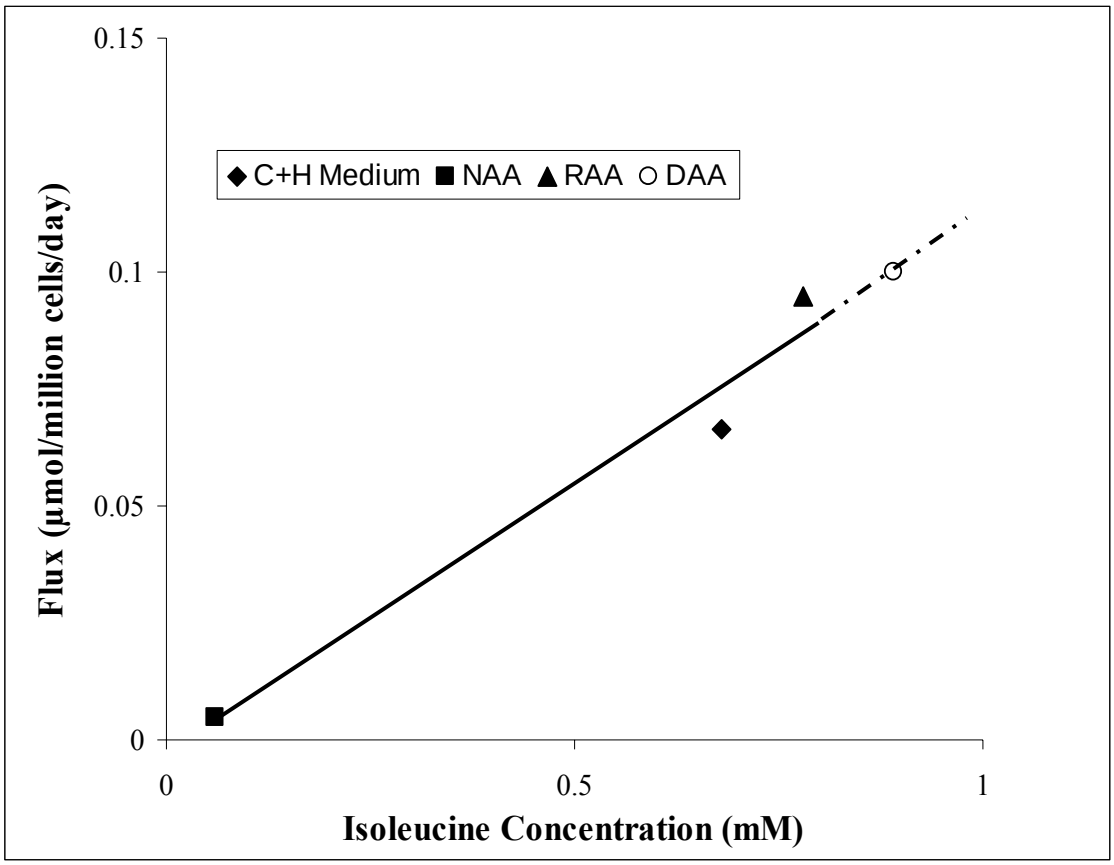

Figure 3.2: Calculation of designed amino acid supplementation levels. For example, isoleucine concentration in the designed amino acid supplementation is calculated as an extrapolation point of the linear relation between isoleucine supplementation in the medium (axis x) and isoleucine uptake fluxes (axis y) ($y = 0.1159x - 0.0032$, $R^2=0.9656$).

Comparing the reference supplementations of amino acids (Table 3.2), three groups of amino acids are identified. Compared with reference supplementation (Chan et al., 2003b), the designed supplementation levels of eleven amino acids are greater by at least 10%. In particular, serine and glycine supplementation levels are 260% and 140% increased, respectively, compared to reference levels. The designed arginine supplementation is a more modest one-third higher than reference level. As arginine is directly transformed to urea production in the urea cycle, it is clear that increasing arginine supplementation should increase the urea production, and this would be a trivial route to increased urea production. However, the other amino acids collectively promote urea production via the TCA cycle, which is linked to the urea cycle by the metabolite fumarate, and an increased turnover of the TCA cycle can help to balance production of fumarate in the state of high urea cycle activity. Thus, optimization of urea production requires activation of multiple, independent pathways that require amino acids as substrates, supporting the hypothesis that amino acid supplementation can directly modulate urea production capabilities in hepatocytes.

The designed supplementation of three amino acids, namely lysine, aspartate and cysteine, is similar to reference values. Moreover, supplementations for methionine, glutamine, phenylalanine, glutamate and asparagine are predicted to be lower than the experimental value. Many of these amino acids also can feed the TCA cycle; thus, their lower values shouldn't be interpreted as meaning that they cannot lead to urea production but rather that they are either less efficiently transformed to urea or are already present in sufficient quantities for a balanced metabolism. For those amino acids, the DAA was formulated

with identical amounts to the RAA.

Table 3.2: Composition of designed amino acid supplementation

	Reference AA*	***Designed AA****
Serine	0.10	0.36
Glycine	0.17	0.41
Tyrosine	0.40	0.72
Valine	0.87	1.49
Alanine	0.29	0.46
Threonine	0.79	1.18
Arginine	0.42	0.56
Histidine	0.35	0.44
Proline	0.18	0.22
Leucine	0.83	1.02
Isoleucine	0.78	0.89
Lysine	0.75	0.79
Aspartate	0.01	0.01
Cysteine	0.13	0.13
Methionine	0.20	0.14
Glutamine	6.85	6.12
Phenylalanine	0.42	0.32
Glutamate	0.11	0.09
Asparagine	0.09	0.01

* amino acid supplementation in the medium during plasma exposure (mM)

3.3.2 Effect of Amino Acid Supplementation on Hepatocyte Exposed to Plasma

The behavior of cryopreserved rat hepatocytes exposed to heparinized plasma was compared among groups receiving no amino acid supplementation (beyond what is normally in plasma, labeled NAA), reference supplementation (RAA) and designed

supplementation (DAA) of amino acids. Each of these amino acid supplementations was evaluated for cells preconditioned in either high (HI) or low (LI) levels of insulin. Furthermore, groups were evaluated with (WH) and without (NH) hormone supplementation consisting of hydrocortisone and insulin during plasma exposure (Table 3.1). The preconditioning and hormone additions have been found previously to influence the metabolism of fresh, primary rat hepatocytes exposed to plasma (Chan et al. 2003a; Chan et al. 2003c).

First, the morphology of hepatocytes was examined over the course of a 5 day exposure to heparinized plasma under each treatment condition for the appearance of intracellular lipid droplets, a manifestation of stored triglycerides (TG) (Stefanovich et al. 1996). Control cells, which were preconditioned in low-insulin medium and never exposed to plasma, did not exhibit any change in morphology, even after 11 days of culture (Fig. 3.3g). During unsupplemented plasma exposure, the nuclei of hepatocytes became enlarged and were obscured by lipid droplets (Fig. 3.3a, d). However, after plasma exposure with RAA supplementation (Fig. 3.3b, e) or DAA supplementation (Fig. 3.3c, f), the boundaries between hepatocytes were more clear and bright, formed fewer large lipid droplets, and exhibited similar morphology as in the standard medium of low-insulin precondition (Fig. 3.3g). This suggests that the amino acid supplementation drives metabolism in a way that leads to reduced lipid accumulation. Hormone (insulin and hydrocortisone, designated as WH)) addition along with amino acids during plasma exposure augmented the ability of amino acid supplementation to maintain native hepatocyte morphology (compare Fig 3.3e, f to 3.3b, c). The morphological trends after

high insulin preconditions were very similar to those after low insulin preconditioning (data not shown).

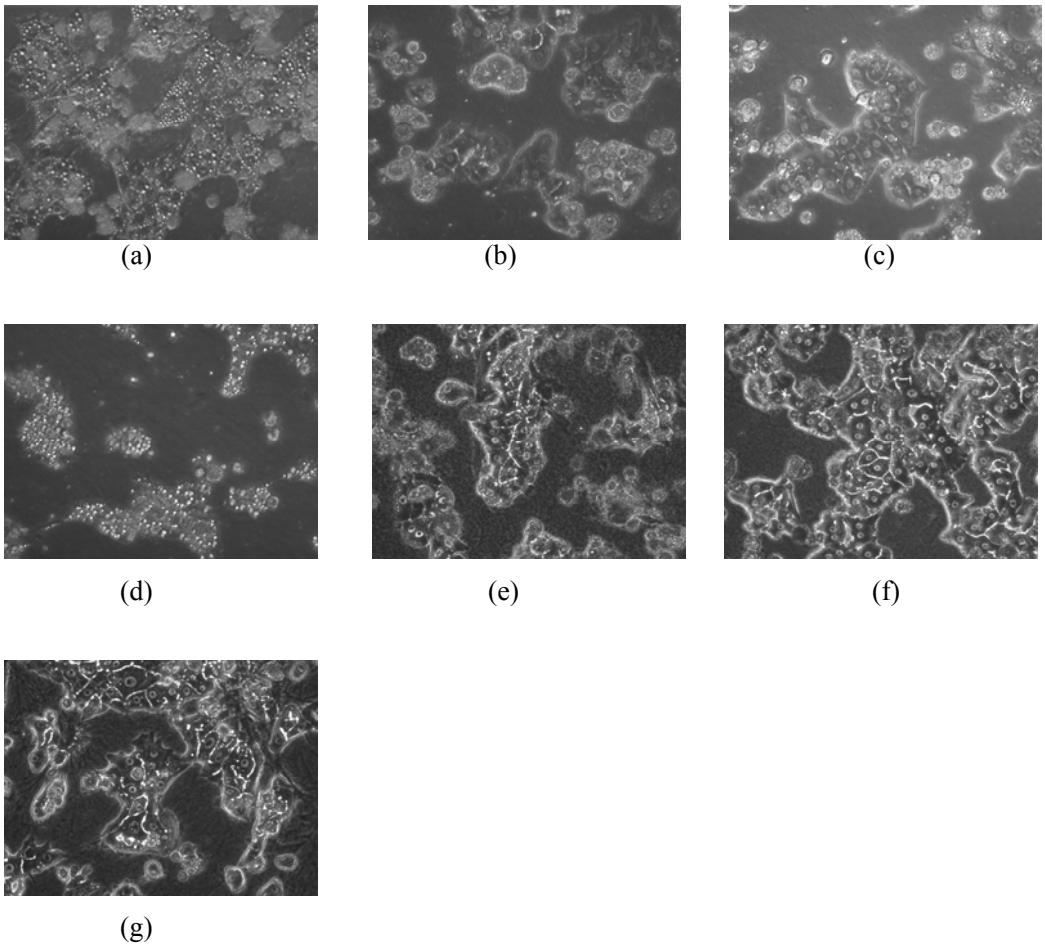

(a) (b) (c)

(d) (e) (f)

(g)

Figure 3.3: The morphology of hepatocytes was examined on day 11, following six days of preconditioning and five days of plasma exposure under each treatment condition: (a) LI_NAA_NH (b) LI_RAA_NH (c) LI_DAA_NH (d) LI_NAA_WH (e) LI_RAA_WH (f) LI_DAA_WH (g) control cells, which were preconditioned in low-insulin medium and never exposed to plasma. Scale Bar, 100 μm

A major concern in the use of cryopreserved hepatocytes is loss of viability following the thawing process. To ensure that the various culture conditions, i.e., amino acid and hormone supplementation regimens, did not impact differentially on viability, we measured the cell viability using calcein/ethidium staining at the end of the experiment, Day 11, corresponding to 6 days of pre-conditioning and 5 days of plasma exposure. After this extended period of culture, much of it in the challenging conditions of plasma exposure, a significant loss of viability at the end of our experiments was observed compared with 75% viability immediately after thawing cryopreserved rat hepatocytes (Fig. 3.4). However, cell viabilities were similar in all of the exposure conditions at the end of our experiments, simplifying interpretation of changes in metabolic outputs. Nonetheless, the values of all functional markers are normalized to the number of viable cells in a given sample.

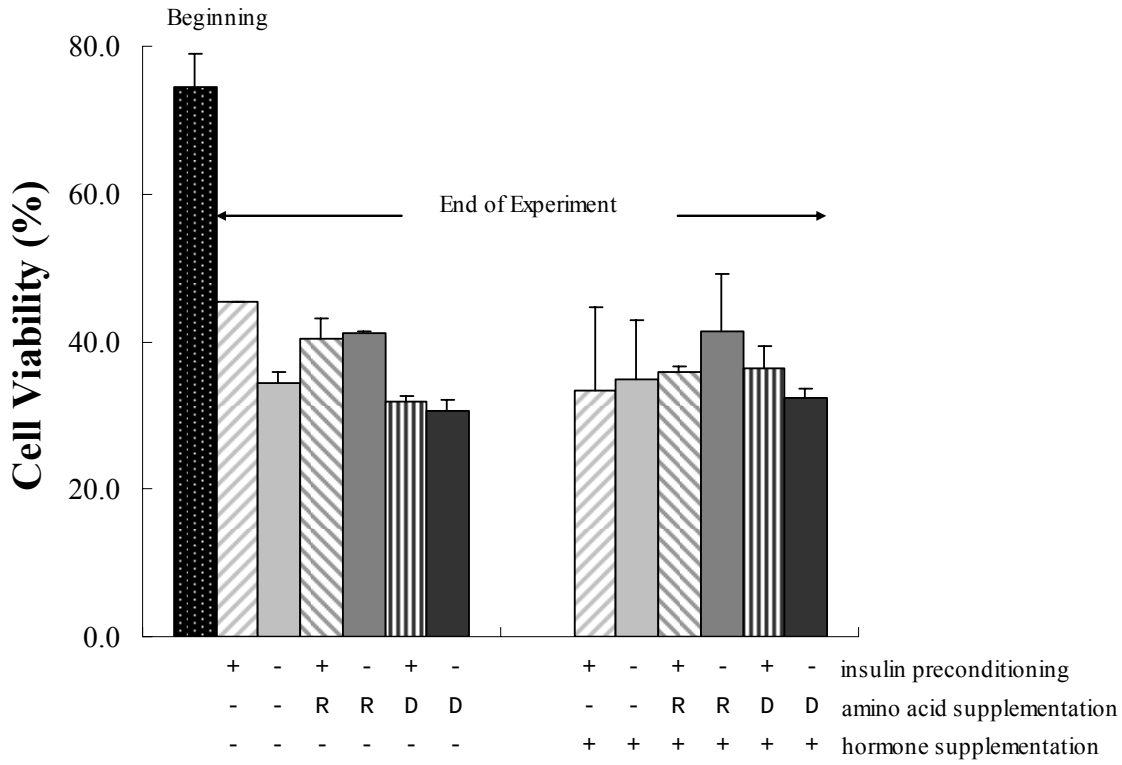

Figure 3.4: Cell Viability. After 11 days of culture, the hepatocyte viability was quantified using calcein/ethidium staining for all twelve culture conditions.The percentage of viable cells is calculated as the ratio of live cells to total cells. The viability after thawing of the cryopreserved hepatocytes, which was determined using trypan blue exclusion assay, is also indicated.

Urea and albumin synthesis were measured after five days exposure to plasma using each of the supplementation protocols (Fig. 3.5a, b). Hepatocytes exposed to plasma without amino acid supplementation suffered significant impairment of urea and albumin production regardless of their preconditioning or hormone supplementation status. When either the RAA or DAA supplementation was employed, preconditioning of rat hepatocyte cultures in high insulin medium prior to plasma exposure increased albumin production, but did not significantly change urea production. Reference amino acid supplementation results in a marked increase in urea and albumin production compared to unsupplemented plasma, and this increase is augmented further by the use of the designed amino acid supplementation. Hormone plus amino acid supplementation during plasma exposure resulted in comparable urea and further increased albumin production compared with the corresponding conditions without any hormone.

Figure 3.5 a

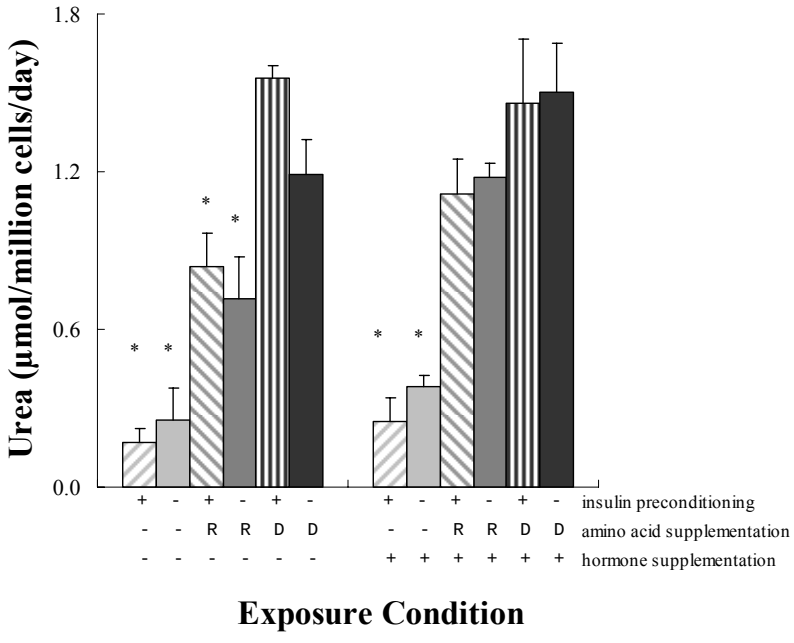

Figure 3.5 b

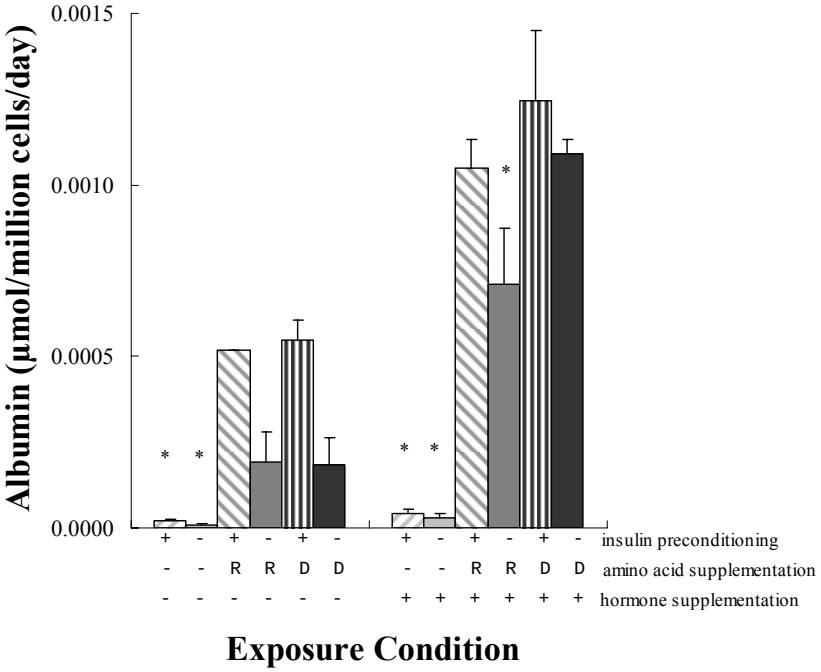

Figure 3.5: Urea (a) and albumin (b) production under the twelve experimental conditions: insulin preconditioning level (+ supraphysiological insulin, - physiological insulin), plasma amino acid level (- without supplementation, R "reference" supplementation, D "designed" supplementation) and hormone supplementation (- without hormone, + with hormone) during plasma exposure. Values shown represent means ± standard deviation of three independent measurements. Asterisks (*) indicate significant difference ($p<0.05$) between the designed supplementation and either the reference supplementation or non-supplemented control for the same insulin precondition and the same hormone supplementation during plasma exposure.

Because of the strong role for lipid metabolism in mediating the effects of various modifiers (i.e., hormones and amino acids) on differentiated functions of cultured hepatocytes exposed to plasma (Chan et al. 2002; Li et al. 2004), we measured lipid uptake and ketone body formation in this system. Total lipid uptake (TG and palmitate) was not significantly affected by either insulin preconditioning prior to plasma exposure or amino acids/hormone supplementation during plasma exposure. Ketone body synthesis (ketogenesis) is a recognizable step of lipid metabolism, and its final products include β-hydroxybutyrate and acetoacetate. The β-hydroxybutyrate production was reduced by supplementing amino acids to plasma independent of hormone supplementation (Fig 3.6a). Both the RAA and DAA supplementations were equally effective in reducing β-hydroxybutyrate production. The acetoacetate production was reduced by supplementing hormone to plasma independent of insulin precondition or of amino acid supplementation during plasma exposure (Fig. 3.6b).

Figure 3.6 a

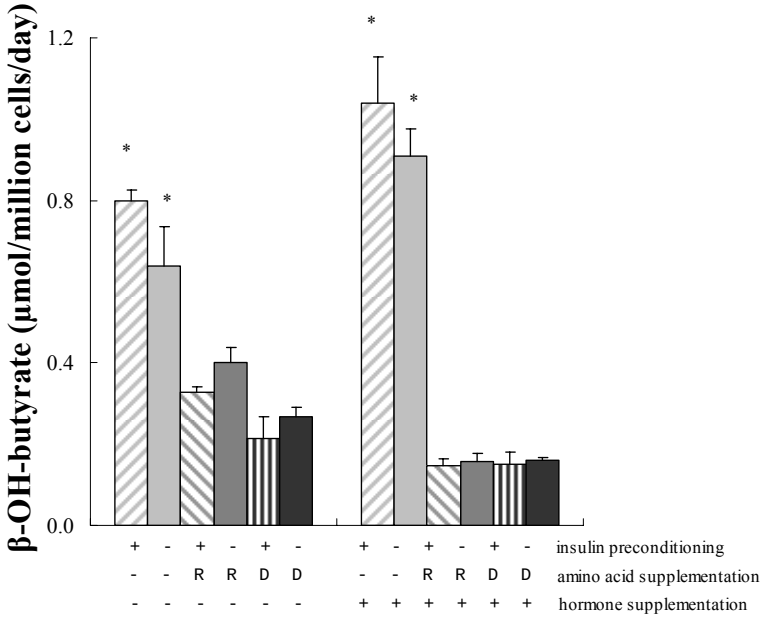

Figure 3.6 b

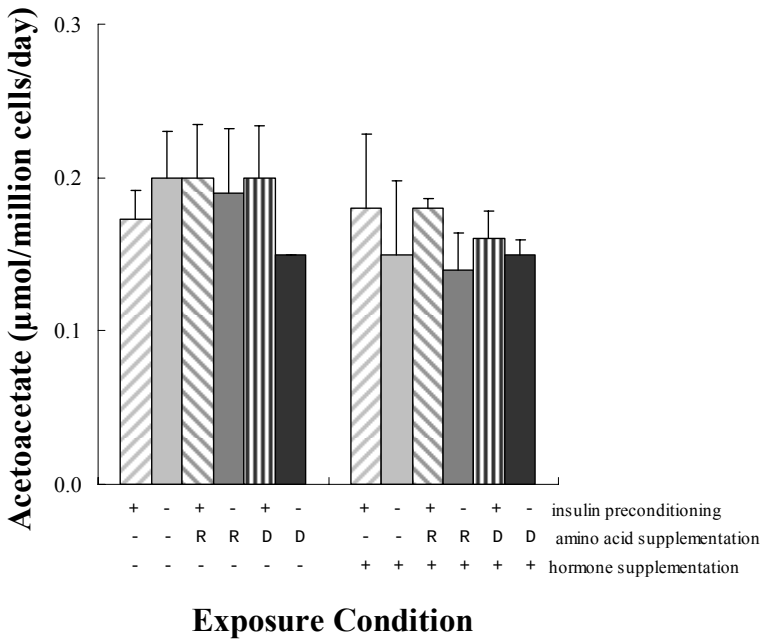

Figure 3.6: β-hydroxybutyrate (a) and acetoacetate (b) production under each of the experimental conditions as indicated in Figure 3.5. Values shown represent means ± standard deviation of three independent measurements. Asterisks (*) indicate significant difference ($p<0.05$) between the designed supplementation and either the reference supplementation or non-supplemented control for the same insulin precondition and the same hormone supplementation during plasma exposure.

3.3.3 Effect of Arginine Supplementation on Urea Production

In order to determiner whether the observed increase in urea production in supplemented media is due simply to channeling of arginine, rat hepatocytes were cultured in media supplemented with a wide range of arginine levels, holding all other medium components constant. Urea production was found to be linearly increased with increase of arginine supplementation (0.2 mM~4mM) in the medium (Fig. 3.7). However, the rate of increase in urea production becomes smaller as arginine concentration increases beyond 4 mM and reaches a maximum peak.

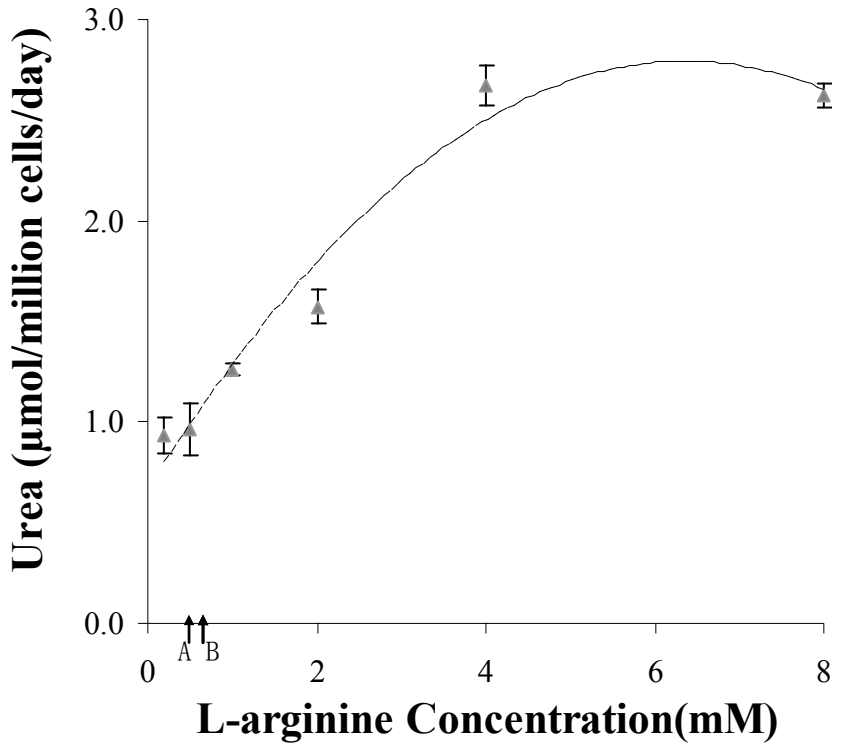

Figure 3.7: Urea production under arginine exclusive supplementation. Hepatocytes were cultured in L-arginine free medium with the addition of L-arginine at the concentrations specified. Arginine concentration in RAA and DAA is represented in A, and B, respectively.

Using arginine as supplementation alone, urea production could only increase by 0.052 μmol/million cells/day when arginine concentration is increased from 0.42 mM to 0.56 mM (Fig. 3.7, point A and B), which is arginine concentration in RAA and DAA design, respectively. Instead, FBA model shows urea production could be increased more than two fold, and experimental data of amino acid supplementation show that urea production could increase more than 0.3 μmol/million cells/day for same addition of arginine supplementation, but with the addition of other amino acid supplementation.

3.4 Discussion

3.4.1 Rational Design Method for Amino Acid Supplementation

The effects of supplemented amino acids and hormones to plasma on liver-specific functions have been investigated in previous studies using freshly isolated rat hepatocytes (Chan et al. 2003a); however, the exact composition of the supplementation was derived empirically. The RAA supplementation was derived by addition of glutamine, deemed to be a critical amino acid for hepatocyte metabolism, mixed with a commercial amino acid supplementation, Basal Medium Eagle (BME). This has proven to be an effective starting point; however, we hypothesized that it could be fine-tuned using a rational design strategy based on FBA. It is not feasible to merely supplement all amino acids at arbitrarily high levels, as such a concentrated medium with amino acid supplementation would become harmful to cells due to high osmolarity (Washizu et al. 2000a). On the other hand, it has been shown that addition to plasma of single amino acids, such as glycine or glutamine, is insufficient to maintain hepatocyte-specific functions (Washizu et al. 2000a). We found here that addition of arginine is not enough to significantly improve

urea production. These studies suggest that a balanced supplementation is necessary to improve liver-specific functions, but it is not clear from such studies how to design an effective amino acid supplementation from data on addition of a single amino acid. As such, a quantitative, rational design methodology for amino acid supplementation would be very useful for metabolic engineering. Our studies represent a first attempt to use flux balance analysis to quantitatively design amino acid supplementation to the plasma for cultured hepatocytes.

This rational design method accounts for multiple flux variables and their interconnections considering a complex hepatic network of interdependent chemical reactions by using linear programming and mixed integer linear programming. In accordance with a number of previous studies, the network includes those reactions and pathways known to play a significant role in nitrogen metabolism (Chan et al. 2003a; Chan et al. 2003b; Chan et al. 2003c; Lee et al. 2003; Nagrath et al. 2007; Sharma et al. 2005; Uygun et al. 2007). From this standpoint, the production and degradation of protein is a potentially important consideration. Albumin production, by far the most abundantly produced secreted protein and the only protein included in the network, exhibits a flux that is very small compared to other fluxes. Protein degradation was examined in a previous study by adding breakdown of apolipoprptein B into the system (Chan et al. 2003a), with the result that it was found to play a negligible role in hepatic network. An overall nitrogen balance calculated as the difference between nitrogen uptaken and excreted in the forms of amino acids, ammonia, urea and albumin production closes within 10%, which suggests that other forms of nitrogen not included in the model

(mainly protein and nucleic acids) play an insignificant role in the overall nitrogen balance. Although energy balance was not explicitly due to the fact that many ATP consuming reactions were not included in the network, thermodynamic constraints were included by giving positive flux bounds for each irreversible reaction in the FBA model. To confirm that the results are thermodynamically feasible, each flux calculated from FBA model was multiplied by the Gibbs free energy change (ΔG) and the summation $\sum_j \Delta G_j v_j$ was evaluated and found to be negative.

3.4.2 Multiple-Objective Optimization: Effects of Amino Acid Supplementation on Urea and Albumin Production

The single objective of urea synthesis was chosen for flux balance analysis in this study. In FBA, a single objective can be achieved via multiple, distinct flux distributions. In this case, FBA produced eight different flux distributions that achieve the same urea production and satisfy the same constraints. However, these distributions differed primarily in their glucose utilization and not at all in their amino acid uptake. Therefore, only one designed amino acid supplementation was generated (Table 3.2).

While urea synthesis is only one of many functions that hepatocytes must perform, a high level of urea production is generally regarded as indicative of healthy, metabolically active hepatocytes. Utilizing the idea of multi-objective optimization, previous work has shown that another liver specific function, albumin production, is compromised when reaching the highest possible urea production (Nagrath et al. 2007; Sharma et al. 2005). However, high levels of both functions are quite feasible. In Figure 3.8, point A presents

the result from FBA model which is the global maximum urea production, corresponding to very low albumin production. However, in moving from point A to C through point B, albumin production is increased dramatically with very little decrease in urea synthesis. On the boundary containing points D and C, albumin production is maximal, with a wide range of possible values for the urea production. These points illustrate the Pareto set (Fig. 3.8), which defines the feasible solution space for the FBA model.

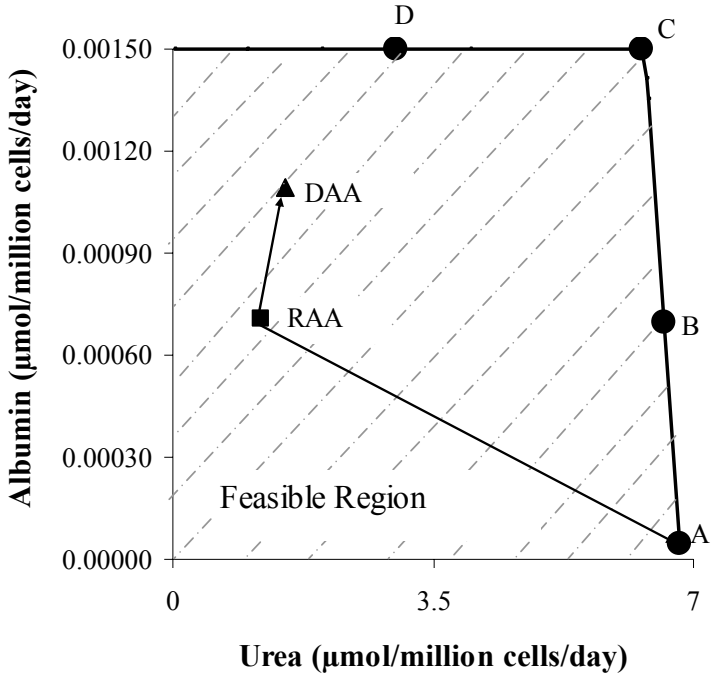

Figure 3.8: Pareto-set for bi-objective problem of urea and albumin synthesis. The black circles are results calculated from multi-objective model, and point A is the result for maximization of urea production in the FBA model. RAA and DAA are experimental results as defined before. The hashed area corresponds to the feasible region of the model.

Experimentally, we found that albumin secretion was either unaffected or somewhat increased, depending on the hormone exposure, as urea production increased in going from the RAA to DAA supplementation. This finding remains consistent with the metabolically feasible region shown in Figure 3.8. Given that the liver performs a myriad of metabolic functions in vivo, it is likely that the regulatory program of hepatocytes is geared towards maintaining many functions at sub-optimal levels rather than any particular function at its apparent maximum.

3.4.3 Effects of Hormone Supplementation on Hepatocyte

Hormone levels either during preconditioning of hepatocytes or during plasma exposure may affect their metabolic functions. Previous studies using freshly isolated rat hepatocytes showed that insulin preconditioning does not significantly affect urea synthesis in the absence of amino acids; however, when supplemented with amino acids, low insulin preconditioning resulted in increased urea production compared with that of high insulin preconditioning (Li et al. 2004). In our studies using cryopreserved rat hepatocytes, the level of insulin did not affect urea production significantly regardless of amino acid composition. On the other hand, albumin production was enhanced by supraphysiological insulin preconditioning (Fig. 3.5b).

Previous studies found that physiological levels of hydrocortisone (50-250 ng/mL) in the culture medium in pre-condition are necessary to maintain differentiated functions of hepatocytes in sandwich culture (Dunn et al. 1991). However, we found that hydrocortisone supplementation without amino acid supplementation during plasma

exposure did not alter the morphological appearance of cryopreserved hepatocytes or their production of urea and albumin. Rather, supplementation of amino acids in combination with hormone preconditioning is required to increase urea synthesis and albumin production. The synergistic effects of hormone addition and amino acid supplementation could be due to hormonal regulation of amino acid transport systems in primary rat hepatocytes. For example, hydrocortisone has been observed to upgrade transport system N for glutamine, histidine and asparagine (Gebhardt and Kleemann 1987).

3.4.4 Cryopreservation Hepatocytes

Cryopreservation is a necessary step for the practical application of hepatocytes as a resource for in vitro analysis (Garcia et al. 2003) and bioartificial liver devices (Park and Lee 2005; Watanabe et al. 1997), since cryopreserved hepatocytes can be stored indefinitely, transported to any site, and utilized when desired. In our study, the metabolic state of cryopreserved rat hepatocytes was evaluated under plasma exposure utilizing various cell culture supplementation conditions. A negative consequence of utilizing cryopreserved hepatocytes is the loss of viability from the summed processes of freezing, storage, thawing and culturing (Lloyd et al. 2003). Indeed, we observed a significant loss of viability (32 to 45 %) at the end of our experiments compared with 75% viability at the beginning (Fig. 3.4). However, we find that the surviving hepatocytes are robust in their ability to adopt morphologies akin to freshly isolated hepatocytes (Fig. 3.3) and to produce levels of differentiated markers only slightly reduced from their freshly isolated counterparts (Chan et al. 2003a).

The decline in liver-specific functions of hepatocytes during plasma exposure without amino acid supplementation may be due partially to cell death (Washizu et al., 2001). However, calcein and ethidium homodimer staining of the cells indicates similar proportions of viable cells in all of the exposure conditions (Fig. 3.4). The loss of function during human plasma exposure is associated with intracellular triglyceride (TG) accumulation. We observed microscopically high lipid accumulation in plasma without amino acid supplementation for cultured cryopreserved hepatocytes and a reduced rate of TG accumulation with amino acid supplementation. The accumulation of TG in non-supplemented cultures can be attributed to the increased uptake of lipids in plasma (Matthew et al. 1996b) and/or to a reduction in free fatty acids oxidation by cultured hepatocytes (Stefanovich et al. 1996). Therefore, we evaluated the correlation between urea synthesis and lipid accumulation through free fatty acids pathway. Total lipid (TG and FFA) uptake by cryopreserved hepatocytes was invariant with any of the experimental variables (Fig. 3.6). It is thus more likely that the lowered lipid accumulation under supplemented conditions was due to an increase in fatty acids conversion to acetyl-CoA. One of the end products of acetyl-CoA is ketone bodies (Fig. 3.6). The decrease in ketone body production suggests that more acetyl-CoA enters into the TCA cycle and produces urea, which is consistent with FBA predictions and experimental observations.

3.4.5 Improvements of FBA in the Future Work

It is significant that, despite the approximations made in the FBA model, the DAA

supplementation did indeed lead to a higher urea production. The fact that albumin production was increased and β-hydroxybutyrate decreased in the DAA conditions compared with exposure condition without amino acid supplementation suggests that the resulting physiological state is a metabolically healthy one for the cultured, previously cryopreserved, hepatocytes used in this study. Nonetheless, the observed synthesis rate of urea was still lower than the value predicted by the linear programming model. It is likely that one factor contributing to a lower than predicted urea output is that some designed amino acid fluxes might not be achieved due to deviations from the linear extrapolation used to design the supplementation or due to competitive transport limitations, since some amino acids make use of a common transporter. For example, alanine, serine, and glutamine use the same neutral transport system A in cell culture of rat hepatocytes (Joseph et al. 1978). Regulation by amino acid transporters is an important area for future investigation, as the resulting flux-supplementation functions, which may be nonlinear in the presence of transport limitations, can be added to FBA as capacity constraints to recalculate the amino acid supplementation for maximal urea production. Furthermore, new pretreatments can be designed to enhance the capacity of needed amino acid transporters, such as adjusting sodium concentration or the hormone level (Gu et al. 2005; Kitiyakara et al. 2001).

3.5 Summary

In summary, this study presents a novel approach to design rationally an amino acid profile for enhanced hepatocyte functions during plasma exposure. The fact that the DAA promoted a metabolically healthy phenotypic with higher levels of liver-specific functions (urea and albumin synthesis), represents a proof of principle for the approach.

Near-term improvements may be made in the hepatocyte cultures employed here by incorporating the amino acid transport mechanism and hormone effects regarding the metabolic capacity into the model so that a more accurate amino acid and hormone supplementation can be derived. As we characterize and incorporate such additional system constraints into the model, the approach will move closer to the ultimate goal of achieving a supplementation that is optimal for hepatocyte cultures the general case yet also can be tuned to meet variations in operating conditions.

Chapter 4

ANALYSIS OF AMINO ACID SUPPLEMENTATION EFFECTS ON HEPATOCYTE CULTURES USING FLUX BALANCE ANALYSIS

Abstract:

When cultured hepatocytes are exposed to challenging environments such as plasma exposure, they frequently suffer a decline in liver-specific functions. Media supplements are sought to reduce or eliminate this effect. A rational design approach for amino acid supplementation in hepatocyte culture has been developed in our prior work, and designed amino acid supplementation (DAA) was found to increase urea and albumin production.

To fully characterize the metabolic state of hepatocytes under different amino acid supplementations, a number of metabolite measurements are performed in this work and used in a metabolic network flexibility analysis framework including thermodynamic constraints to determine the range of values for the intracellular fluxes. A metabolic objective prediction model is used to infer the metabolic objectives of the hepatocytes and to quantify the intracellular flux distribution for three different amino acid supplementations.

The results illustrate that DAA leads to greater fluxes in TCA cycle, urea cycle and fatty acid oxidation concomitant with lower fluxes in intracellular lipid metabolism compared with empirical amino acid and no amino acid supplementation for hepatocytes during plasma exposure. It is also found that hepatocytes exhibit flexibility in their metabolic

objectives depending on the composition of the amino acid supplementations. By incorporating both experimental data and thermodynamic constraints into the mathematical model, the proposed approach leads to identification of metabolic objectives and characterization of fluxes' variability and pathway changes due to different cultured conditions.

4.1 Introduction

There are a number of studies in the literature regarding the use of primary hepatocyte cultures to study drug detoxification (Gebhardt et al. 2003; Nussler et al. 2001; Tuschl et al. 2008), and as the basic for artificial cell-based devices (Chan et al. 2003b; Flendrig et al. 1998; Wurm et al. 2009). In recent years, better understanding of isolation and cryopreservation techniques (Lloyd et al. 2003; Stefanovich et al. 1996), advances in hepatocyte-matrix interaction (Dunn et al. 1991; Hosagrahara et al. 2000) and improved liver function performance in culture medium (Chan et al. 2002; Sand and Christoffersen 1988; Zupke et al. 1998) have improved our understanding of hepatocyte physiology. In particular, recent studies have shown that amino acid supplementation resulted in improvement of synthetic functions as well as cytochrome P450 (detoxification) activities during plasma exposure as occurs in clinical application of bioartificial liver devices (Washizu et al. 2000a; Washizu et al. 2001; Washizu et al. 2000b). However, the exact composition of previous supplementations were derived empirically. Recent work in our group represented a first attempt to use flux balance analysis to quantatitavely design amino acid supplementation to the plasma for cultured hepatocytes (Yang et al. 2009), and liver-specific functions (urea and albumin) under designed amino acid

supplementation were found to be increased compared with previously reported (empirical) amino acid supplementation (Chan et al. 2003c) and also resulted in reduced lipid accumulation. The present study builds on the prior work by contributing a detailed analysis of the metabolic phenotypes observed under amino acid supplementation, integrating a set of metabolite measurements with the flux balance analysis framework.

Computational modeling of hepatic metabolism is increasingly being utilized in tandem with experimental measurements to understand and control the performance of hepatocytes under adverse culture conditions (Chalhoub et al. 2007; Chan et al. 2003c). In mathematical modeling of cell metabolism, a comprehensive network, with a large number of interconnecting reactions in the cell, is built to mimic the actual cell phenomena. Mathematic modeling for flux analysis can be classified into metabolic flux analysis (MFA) (Arai et al. 2001; Chan et al. 2003a; Vallino and Stephanopoulos 1994) and flux balance analysis (FBA) (Edwards et al. 2002; Kauffman et al. 2003; Lee et al. 2006; Varma and Palsson 1994a). In both approaches, mass balance equations are written for each internal metabolite with the assumption of pseudo-steady state. If the system is overdetermined, MFA is used to calculate all unknown fluxes and evaluate the gross measurement error using redundant information (Wang and Stephanopoulos 1983). If the system is underdetermined, FBA uses constrained optimization to identify the flux distribution of the metabolic network (Lee et al. 2006). Using appropriate metabolic objectives that cell strives to achieve (Gianchandani et al. 2008; Khannapho et al. 2008; Schuetz et al. 2007) and considering valid constraints that reduce the feasible region (Bonarius et al. 1997) are important issues in application of FBA. Since the cellular

objectives may not be known or easily hypothesized, optimization frameworks have been developed to infer the metabolic objectives (Burgard and Maranas 2003), applied to the hypermetabolic state of the liver (Nolan et al. 2006) and to cultured hepatocytes (Uygun et al. 2007).

The consideration of various constraints, describing environmental (nutrients, physical factors etc.), physicochemical (mass balance, thermodynamic of internal reactions, maximum enzyme capacities), self-imposed regulatory and evolutionary constraints, allows to reduce the feasible region of an FBA problem (Covert et al. 2003), and to determine the state of the cell (Edwards and Palsson 2000). Recently, energy balance analysis (EBA) (Beard and Qian 2005) and pathway analysis have been developed to eliminate the thermodynamically infeasible solutions from FBA space. The idea has been used to identify the intracellular fluxes for the case of liver metabolism (Nolan et al. 2006). Network-embedded thermodynamic analysis (NET analysis) has been developed to determine the range of Gibbs energy of reactions and feasible range of metabolite concentration for the entire network utilizing the second law of thermodynamics, the reaction directionalities and metabolite concentrations within an optimization model (Kummel et al. 2006; Zamboni et al. 2008).

In this work, the framework utilized includes mass balance constraints, reaction reversibility restrictions based on experimentally determined values, experimental measurements of extracellular fluxes that impose bounds on flux values, and three different pathways energy balance constraints in order to determine the range of flux

distribution that describes the metabolic state of the cell. In addition, a bi-level programming problem is developed to derive the metabolic objectives. The developed optimization tools are applied to hepatocyte metabolism in order to investigate the amino acid supplement effect on cell functions during plasma exposure. Specifically, the roles of lipid metabolism and TCA cycle in regulating urea production are elucidated.

4.2 Methods

4.2.1 Hepatocye Culture with Amino Acid Supplementation

Hepatocytes were cultured using the well-established collagen sandwich method (Dunn et al. 1991; Yang et al. 2009). Prior to initiating the cultures, 0.4 mL of collagen mixture solution was added to each well of six-well plates and incubated at 37 °C and 10% CO_2 until the gel solidified. Cryopreserved rat hepatocytes purchased from Xenotech LLP (Lenexa, KS) were thawed following the Xenotech protocol and reconstituted to a density of 10^6cells/mL in C+H standard medium, which consists of DMEM supplemented with 10% heat inactivated fetal bovine serum (FBS), 7.0 ng/mL glucagon, 7.5 g/mL hydrocortisone, 20 g/L epidermal growth factor, 200 U/mL penicillin, and 200 g/mL streptomycin. Reconstituted hepatocytes were seeded on a plate with collagen gel for 24 h, at which time another 0.4 mL of collagen gel was added, resulting in a double sandwich configuration. After the second gel layer solidified, 0.8 mL fresh C+H medium with 0.05 mU/mL insulin was added. This maintenance medium was exchanged with spent medium every day for 6 days preconditioning.

To begin the experiment, 6-day-old sandwiched hepatocyte cultures were exposed to plasma with hormone supplementation including 7.5 g/mL of hydrocortisone and 0.05

mU/mL of insulin. Treatment groups varied in the amino acid supplementation in the plasma, comparing “designed” amino acid supplementation (DAA) based on a rational design approach described in our previous work (Yang et al. 2009), “reference” amino acid supplementation (RAA) based on published data (Chan et al. 2003c), and no amino acid supplementation (NAA). The concentrations corresponding to each amino acid supplementation are given in the supporting material (Appendix D). Those media were exchanged with spent media every day for 5 days plasma exposure. At the end of the experiment, culture supernatants were collected and stored at 4 °C prior to analysis.

4.2.2 Biochemical Assay

Albumin production was quantified by an enzyme-linked immunosorbent assay (ELISA) using purified rat albumin (MP Biomedicals, Solon, OH) and peroxidase-conjugated antibody for detection (MP Biomedicals, Solon, OH). The concentrations of urea, glucose, lactate, glycerol, and glutamine were measured colorimetrically using commercial test kits (Sigma, St. Louis, MO). Enzymatic kits were utilized for the measurement of cholesterol (BioAssay System, Hayward, CA), acetoacetate, β-hydroxybutyrate, triglycerides (Stanbio, Boerne, TX), and free fatty acids (Roche, Indianapolis, IN).

Amino acids and ammonia were labeled fluorescently with the AccQ reagent (Waters Corporation, Milford, MA) and separated by gradient elution from 100% buffer A (10% acetonitrile, 6% formic acid, and 84% ammonium formate in water) to 100% buffer B (60% acetonitrile, 40% micropore water) in 33 minutes at 1 ml/min flow rate on an AccQ-Tag C18 column (150 mm × 3.9 mm I.D, Waters Corporation, Milford, MA) with a fluorescence detector (Waters 470, Waters Corporation, Milford, MA) using

excitation/emission at 250/395 nm, respectively. Serial dilutions of standards were used to construct a calibration curve for each analyte, with the linear portion utilized for measurements. The concentrations of amino acid/ammonia in the fresh or spent medium were determined using these standard curves, with sample dilutions performed as necessary to operate within the linear range.

Statistics. All measurement results were expressed as mean ± standard deviation for three replicate culture plates. To evaluate the effect of amino acids supplementation on extracellular fluxes of hepatocytes, data were analyzed with Tukey's test using SAS software (SAS institute Inc., Cary, NC). Significant differences were accepted as significant at $p < 0.05$.

4.2.3 Hepatic Network

The major reactions of hepatic metabolism were considered in a highly interconnected stoichiometric network that includes glycolysis/gluconoegenesis, tricarboxylic acid cycle (TCA), urea cycle, amino acid uptake/secretion and catabolism, oxygen uptake, electron transport system, pentose phosphate reactions (as a lumped group), ketone body synthesis, fatty acid, triglyceride (TG) and glycerol metabolism. This network builds upon previously reported hepatic networks and involves 46 intracellular metabolites (Chan et al. 2003c; Lee et al. 2003; Nagrath et al. 2007; Sharma et al. 2005; Uygun et al. 2007), and 78 reactions (30 reactions with measurement data, 48 reactions with unknown fluxes as labeled in Appendix E).

4.2.4 Pathway Energy Balance (PEB) Constraints

Thermodynamic constraints were applied by allowing the sharing of free energy along elementary pathways connecting metabolic inputs and outputs. The standard Gibbs free energies of metabolites (ΔG_f^0) were estimated using a group-contribution method (Mavrovouniotis 1991; Nolan et al. 2006). The standard Gibbs free energy of reaction (ΔG_{RXN}^0), defined in a standard state (pH 7, 1 atm, 25 °C, concentration 1 M, dilute aqueous solution), is calculated as follows:

$$\Delta G_{RXN}^0 = \sum_p \upsilon_p \Delta G_{f_p}^0 - \sum_r \upsilon_r \Delta G_{f_r}^0 \tag{4-1}$$

where υ_p and υ_r are the apparent stoichiometric number of products, and reactants in the biochemical reaction, respectively.

Ignoring activity coefficient corrections, the Gibbs free energy of reaction away from equilibrium is given by (Mavrovouniotis 1993):

$$\Delta G_{RXN} = \Delta G_{RXN}^0 + RT \ln \prod_j C_j^{\upsilon_j} \tag{4-2}$$

where R is the ideal gas constant, T is the temperature (K); and C_j are the metabolite concentrations.

Extracellular concentrations are supplied by the metabolite measurements reported in this work and have a range corresponding to the measured experimental uncertainty; intracellular concentrations are estimated from literature values and are also expressed as a range corresponding to the range of values reported or estimated. Because a range of

concentration values is used, minimum and maximum values of the Gibbs free energy of an intracellular reaction are calculated as follows,

$$\Delta G_{RXN}^{Min} = \Delta G_{RXN}^{0} + RT \ln \left[\frac{\prod_{p \in \text{products}} C_{p,\min}^{\upsilon_p}}{\prod_{r \in \text{reactants}} C_{r,\min}^{\upsilon_r}} \right] \tag{4-3a}$$

$$\Delta G_{RXN}^{Max} = \Delta G_{RXN}^{0} + RT \ln \left[\frac{\prod_{p \in \text{products}} C_{p,\max}^{\upsilon_p}}{\prod_{r \in \text{reactants}} C_{r,\max}^{\upsilon_r}} \right] \tag{4-3b}$$

For metabolite uptake from or secretion into the culture medium, the standard Gibbs energy is considered as zero ($\Delta G_{RXN}^{0} = 0$) and only the second term in Equations 4-3a-b are used.

Metabolic reactions are assumed to be able to utilize chemical potential from other reactions within their elementary pathways, which were consequently enumerated. The elementary modes are determined using elementary flux algorithm (Schuster et al. 2000; Schuster et al. 2002a), implemented in Matlab *Fluxanalyzer* (Klamt et al. 2003). The matrix of elementary modes E ($P \times N$ dimension) is multiplied by the Gibbs energy of each reaction element-by-element, to form a matrix of pathway weighted by Gibbs energy of reactions, ΔG_p ($P \times N$ dimension).

$$\Delta G_{p}^{0,\min,\max} = E \cdot \Delta G_{RXN}^{0,\min,\max} \tag{4-4}$$

where the superscript 0, min, and max represent the standard, minimum, and maximum Gibbs free energy of the reaction, respectively.

Given the weighted pathway energy ΔG_p and the flux vector v, the pathway energy balance constraints can be formed for each of the pathways of the network (Nolan et al. 2006):

$$\sum_{j}^{N} \Delta G_p^{(0,\min,\max)} \cdot v_j \leq 0 \qquad p \in P \tag{4-5}$$

Those three types of pathway energy balance constraints involving standard, minimum and maximum Gibbs free energy of the reaction are separately incorporated into the optimization problem to eliminate the thermodynamic infeasible flux distribution. More details on the construction of pathway energy balance constraints are given in the supporting material (Appendix F).

4.2.5 Metabolic Network Flexibility Analysis (MNFA)

The range of each unknown flux is estimated using Metabolic Network Flexibility Analysis (MNFA), in which system constraints are imposed but no metabolic objective is assumed or inferred. According to this approach the optimization problem (I) is solved for each unknown flux to determine the minimum and maximum feasible flux values.

$$\begin{aligned} & \underset{j \in E}{Max / Min} && \mathrm{v}_j \\ & s.t. && \sum_{j=1}^{N} S_{ij} v_j = 0 \qquad i \in M \\ & && v_j^{\min} < v_j < v_j^{\max} \qquad j \in K \end{aligned} \tag{I}$$

where v_j is the reaction rate of reaction j; S_{ij} is the stoichiometric coefficient of metabolite i in reaction j; $v_j^{\min}$ and $v_j^{\max}$ are lower and upper bound of reaction j, respectively; M is the set of metabolites; N is the total number of reactions involved in the hepatic

network; K is the set of constrained reactions (based on measurements and/or irreversibility), and E is the set of unknown reactions. The main assumptions for the development of MNFA model (I) are as follows: (1) The internal metabolites are assumed to be maintained at pseudo-steady state, which means their rate of change is small compared to their turnover; (2) the constraints for irreversible reactions, $v_j \geq 0$ are imposed based on the information given in the metabolic map of KEGG (Kanehisa and Goto 2000); (3) the value of each measured flux was constrained by an interval $[\, v_{\min} , v_{\max} \,]$ based on the average and standard derivation of measurements using triplicates.

Pathway energy balance (PEB) constraints (Equation 4-5) can be also added to reduce and more accurately describe the feasible range of intracellular fluxes based on the Gibbs free energy statement of the second law of thermodynamics. In this case the resulted optimization model including pathway energy balance constraints is as follows:

$$
\begin{aligned}
& \underset{j \in E}{Max / Min} \quad v_j \\
& s.t. \qquad \sum_j^N S_{ij} v_j = 0 \qquad i \in M \\
& \qquad\quad v_j^{\min} < v_j < v_j^{\max} \qquad j \in K \\
& \qquad\quad \sum_j^N \Delta G_p^{(0,\min,\max)} \cdot v_j \leq 0 \qquad p \in P
\end{aligned}
\tag{II}
$$

4.2.6 Metabolic Objective Prediction (MOP) Modeling

Where a cellular objective can be identified in terms of metabolic fluxes, it can be used as a driving force to identify a consistent flux distribution within system constraints. However, for mammalian cells, the cellular objectives are manifold, dynamic, and

generally unknown. Thus we applied a metabolic objective prediction (MOP) approach, adopting a bi-level programming model similar to Objfind (Burgard and Maranas 2003) and incorporating minimum PEB constraints to infer the metabolic objectives of hepatocytes under varying amino acid supplementations as follows:

$$
\begin{aligned}
&\underset{c_j}{Min} \quad \sum_{j}^{L} (v_j - v_{j-\exp})^2 \\
&s.t. \qquad c_j \geq 0 \\
&\qquad \sum_{j=1}^{N} c_j = 1 \\
&\qquad \underset{v_j}{Max} \quad \sum_{j}^{N} c_j v_j \\
&. \qquad\quad s.t \quad \sum_{j}^{N} S_{ij} v_j = 0 \qquad\quad i \in M \\
&\qquad\qquad\quad v_j^{\min} < v_j < v_j^{\max} \qquad j \in K \\
&\qquad\qquad\quad \sum_{j}^{N} \Delta G_p^{\min} \cdot v_j \leq 0 \qquad\quad p \in P
\end{aligned}
\tag{III}
$$

where c_j is the coefficient of relative importance for each flux v_j, and L is the number of measured fluxes. MOP is a bi-level programming problem in which the upper-level minimizes the sum of squared error between measured fluxes and their predicted values from the model (III), whereas the lower-level maximizes the sum of all possible objectives and weights are chosen from the upper level problem. The measurements restrict the metabolic objectives chosen in the follower's problem since the feasible region of the lower-level problem is restricted by the upper-level decision. The bi-level programming can be reformulated into a single-level nonlinear program either by following the primal-dual strategy (Burgard and Maranas 2003), or using the Karush-Kuhn-Tucker (KKT) conditions of the lower-level problem (Shi et al. 2005). In this work we followed the KKT approach to transform the bi-level programming (III) to a

single level optimization problem that involves the original constraints, the complementary constraints, and the KKT conditions for the upper and lower level constraints as follows:

$$
\begin{aligned}
&\underset{c_j}{Min} \quad \sum_{j}^{L}(v_j - v_{j-\exp})^2 \\
&s.t. \quad
\left\{
\begin{array}{ll}
c_j \geq 0 & \\
\sum_{j=1}^{N} c_j = 1 & \\
\sum_{j}^{N} S_{ij} v_j = 0 & i \in M \\
\sum_{j}^{N} \Delta G_p^{\min} \cdot v_j \leq 0 & p \in P \\
\sum_{j}^{N} \Delta G_p^{\min} \cdot v_j \leq 0 & p \in P \\
v_j^{\min} < v_j < v_j^{\max} & j \in K
\end{array}
\right\} \text{ Original constraints} \\
&\left\{
\begin{array}{l}
u_2(-\sum_{j}^{N} \Delta G_p^{\min} \cdot v_j) = 0 \\
u_3(v_j^{\max} - v_j) = 0 \\
u_4(v_j - v_j^{\max}) = 0
\end{array}
\right\} \text{ Complementary Constraints} \\
&\left\{
\sum_{i}^{M} u_1 S_{ij} - \sum_{p}^{P} u_2 \Delta G_p^{\min} - u_3 + u_4 = -c_j \qquad j \in N
\right\} \text{ KKT condition}
\end{aligned}
\tag{IV}
$$

where u_1, u_2, u_3, u_4 are dual variables for mass balance, pathway energy balance (PEB) constraints and flux bounds, respectively; and u_2, u_3, u_4 are non-negative variables.

All the optimization problems in this study were implemented using GAMS version 22.9, where MNFA solved by CPLEX 9 and MOP solved by SSB solver.

4.3 Results

4.3.1 Extracellular Measurement

After six days of preconditioning, previously cryopreserved rat hepatocytes were exposed to plasma containing medium with varying amino acid supplementation for five days. At this time, the concentrations of extracellular metabolites in the supernatant and in the fresh medium were measured. The production or consumption rate of each extracellular metabolite was calculated by the difference between its concentration in the fresh medium and in the supernatant divided by the number cells in each well and the time interval (one day) over which the medium was exposed to cells. The measured fluxes of metabolites in each amino acid supplementation are listed in Table 4.1.

Table 4.1: Measured fluxes under three amino acid supplementations

	Metabolites	***Measured Flux*** (μmol/million cells/day)		
		NAA	***RAA***	***DAA***
v_{m1}	Glucose	0.22±0.17*	0.55±0.12	0.67±0.35
v_{m2}	Lactate	2.44±0.37*	3.20±0.36*	3.47±0.36
v_{m3}	Urea	0.38±0.05*	1.18±0.05*	1.50±0.18
v_{m4}	Arginine	0.126±0.002*	0.55±0.01*	0.57±0.01
v_{m5}	Ammonia	-0.29±0.12*	-0.780±0.001*	-1.01±0.02
v_{m6}	Ornithine	-0.147±0.005*	-0.336±0.004*	-0.52±0.03
v_{m7}	Alanine	0.19±0.15*	-0.169±0.009*	-0.31±0.01
v_{m8}	Serine	-0.327±0.005*	-0.347±0.006*	-0.68±0.02
v_{m9}	Cysteine	-0.09±0.02*	0.07±0.01*	0.02±0.01
v_{m10}	Glycine	0.063±0.005*	0.246±0.004*	0.530±0.009
v_{m11}	Tyrosine	-0.028±0.008*	0.03±0.01*	-0.23±0.06
v_{m12}	Glutamate	-0.515±0.008*	-1.46±0.02*	-1.75±0.03
v_{m13}	Aspartate	-0.009±0.001*	-0.021±0.001*	-0.030±0.001
v_{m14}	Acetoacetate	0.15±0.05	0.14±0.02	0.150±0.009
v_{m15}	β-OH-butyrate	0.91±0.07*	0.16±0.02	0.160±0.009
v_{m16}	Threonine	-0.05±0.01*	0.21±0.02*	-0.45±0.04
v_{m17}	Lysine	-0.12±0.01*	-0.07±0.02*	-0.45±0.03
v_{m18}	Phenylalanine	-0.053±0.002*	0.33±0.01*	0.11±0.01
v_{m19}	Glutamine	0.19±0.13*	2.77±0.54*	1.80±0.72
v_{m20}	Proline	0.68±0.11	0.48±0.04	0.46±0.11
v_{m21}	Methionine	-0.017±0.006	0.01±0.01	-0.05±0.06
v_{m22}	Asparagine	0.18±0.13*	0.081±0.005*	-0.134±0.006
v_{m23}	Valine	-0.175±0.004*	-0.20±0.02*	-0.65±0.03
v_{m24}	Isoleucine	-0.166±0.003*	-0.32±0.02*	-0.47±0.03
v_{m25}	Leucine	-0.075±0.002*	-0.01±0.02*	-0.44±0.04
v_{m26}	Albumin	0.00003±0.0000	0.0007±0.0002*	0.00109±0.00004
v_{m27}	Glycerol	1.77±0.07*	2.13±0.13	2.075±0.007
v_{m28}	Palmitate	0.76±0.46	1.073±0.008	0.981±0.005
v_{m29}	Cholesterol	0.46±0.12	0.67±0.13	0.75±0.21
v_{m30}	TG	0.93±0.02	0.82±0.13	0.92±0.01

* $p<0.05$, significantly different from DAA

It has been shown in the literature that liver does not uptake branched chain amino acids (BCAA: valine, isoleucine and leucine) (Marchesini et al. 2005). However, it was found that hepatocytes release different levels of BCAA depending on the particular amino acid supplementation during plasma exposure. Designed amino acid supplementation results in an increased secretion of valine, isoleucine and leucine compared with the culture conditions with no amino acid supplementation or with reference amino acid supplementation. Increased secretion of the BCAA under designed amino acid supplementation is due to an increased rate of amino acid turnover, which is associated with a healthy hepatocyte phenotype (Marchesini et al. 2005).

The major finding of this experiment is that urea production and albumin synthesis under the designed amino acid supplementation were found to be increased compared with previously reported (empirical) amino acid supplementation or no amino acid supplementation by reducing the lipid accumulation (Yang et al. 2009). However, from the experimental results, it was found that triglyceride (TG) uptake (v_{m30}), free fatty acid (FFA) uptake (v_{m28}), and cholesterol synthesis (v_{m29}) are not significantly different among the different amino acid supplementation conditions. Therefore, intracellular fluxes need to be calculated to further investigate the effects of amino acid supplementation on the metabolic state of hepatocytes.

4.3.2 Metabolic Network Flexibility Analysis (MNFA)

The range of each unknown flux was estimated first using MNFA model (I), which incorporates mass balance, experimental data and reversibility constraints. The numerical

values are provided in Appendix G (Label as 'without ΔG'). The ranges of the unknown fluxes exhibit similar trends in all three different amino acid supplementations. The reactions associated with electron transport (v_{u36}, v_{u37}), and oxygen uptake (v_{u46}) illustrate large flux ranges. The flux ranges of TCA cycle (v_{u7}~ v_{u12}) are also large due to insufficient constraints in the MNFA model. The details for designed amino acid supplementation (DAA) are given in Figure 4.1a labeled as blue bar. The rest of the unknown fluxes exhibit small ranges since they are highly connected to the measured fluxes and are restricted further by the imposed constraints, which are given in Figure 4.1b labeled as blue bar. The determined flux ranges are large, thus the unknown reactions' fluxes cannot be completely compared for different amino acid supplementation during plasma exposure (Fig. 4.2a).

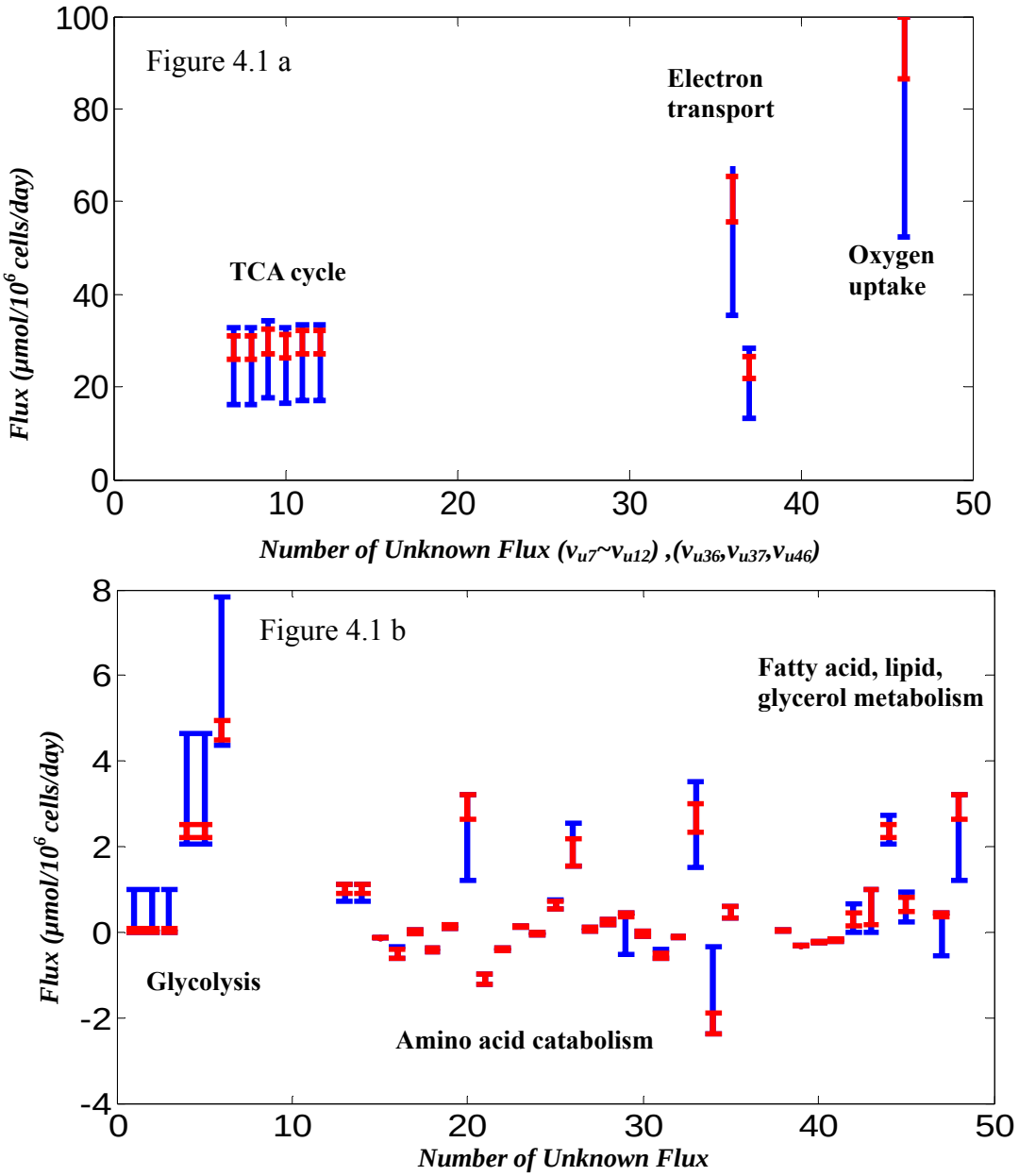

Figure 4.1: Flexibility analysis of hepatic network: ranges for unknown fluxes in designed amino acid supplementation (DAA) were determined using metabolic network flexibility analysis (MNFA): without PEB constraints (blue color), and with minimum PEB constraints (red color). (a) Flux range for oxygen balance (two reactions of relative electron transports (v_{u36}, v_{u37}), oxygen uptake (v_{u46}) and TCA cycle (v_{u7}~ v_{u12}); (b) flux range for the rest of unknown fluxes.

The constraints based on pathway energy balances were imposed on the problem to check our hypothesis that those constraints can help reducing the feasible solution space. In order to construct the PEB constraints, the elementary modes algorithm (Schuster et al. 2000; Schuster et al. 2002a) was first applied for the hepatic network, which is specified for each of three amino acid supplementation (DAA,RAA and NAA) by the reaction irreversibility based on measurement data from experiment (Table 4.1) and flux range of unknown reactions (Appendix G, "without ΔG"). Totals of 65696, 54754 and 90079 elementary modes were identified in DAA, RAA, and NAA, respectively. Next, the Gibbs free energy of reaction is calculated according to Eqn. 4-1, 4-3a and 4-3b by incorporating metabolite concentration bounds given in Appendix H. The pathway energy balance constraints were constructed as described in Eqn. 4-4 and 4-5.

Finally, the range of each unknown flux was estimated using MNFA model (II), which incorporates all the constraints of model (I) and all the feasible PEB constraints. The numerical values are provided in Appendix G (labeled as standard_ΔG, min_ΔG and max_ΔG, respectively). Those results showed that imposing additional pathway energy balances on optimization programming significantly reduces the feasible space of the flux distributions for each of the three different cultured conditions during plasma exposure. Figures 4.1a and 4.1b showed the large reduction achieved in the range of unknown fluxes by the addition of the minimum PEB constraints (red bar) compared with FBA alone (blue bar) in the condition of designed amino acids (DAA) supplementation. Moreover, some unknown fluxes become comparable for different amino acid

supplementation (Fig. 4.2b) with PEB minimum constraints compared with those comparable results without PEB constraints (Fig. 4.2a)

As expected and further illustrated with the results shown in Appendix G, the minimum PEB constraints are the less restrictive of the flux bounds but they also guarantee the system's feasibility. Therefore, we further analyzed the unknown fluxes incorporating minimum PEB constraint in model (II), to investigate the effects of amino acid supplementation on the metabolic state of the hepatocytes. The following results, associate with glycolysis/gluconeogenesis pathway, TCA cycle and urea cycle, are thus obtained.

In previous studies, it was found that glucose metabolism of hepatocytes switches to gluconeogenesis during plasma exposure from glycolysis during medium preconditioning (Chan et al. 2003c). However, we found that this switch only happens in the case with no amino acid supplementation during plasma exposure. For the cases of reference and designed amino acid supplementation, cryopreserved rat hepatocytes maintained the glycolysis phenotype during plasma exposure as in the preconditioning. It is also found that designed amino acid supplementation enhances glucose consumption (v_{m1}) and increases the rate of glucose-6-phosphate dehydrogenation by glucose-6-phosphate dehydrogenase (v_{u38}) and the rate of its storage as glycogen (v_{u43}) compared to that in reference amino acid supplementation (Fig. 4.2c).

Figure 4.2 a

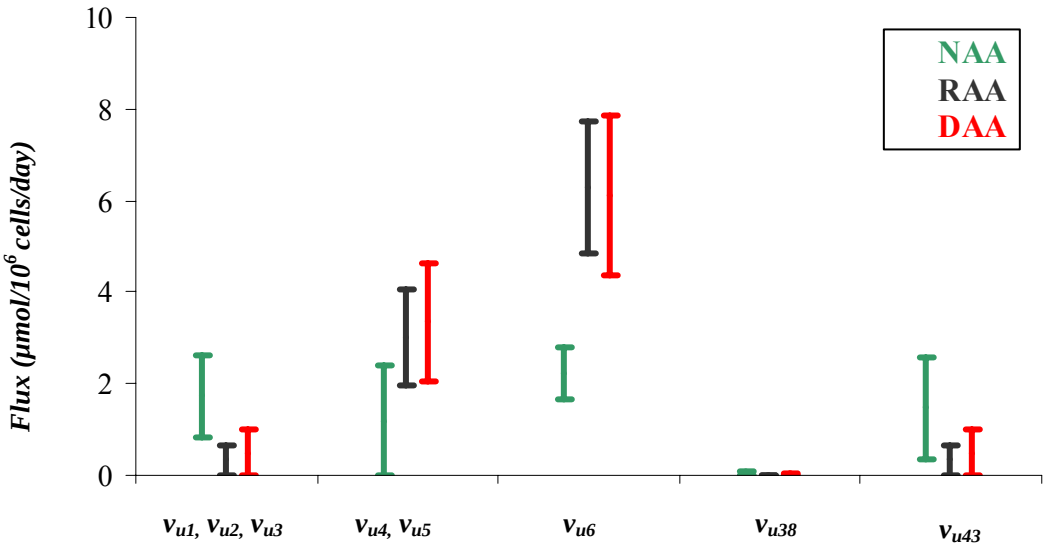

Unknown Fluxes in Gluconeogenesis (in NAA) / Glycolysis (in RAA and DAA) Pathway

Figure 4.2 b

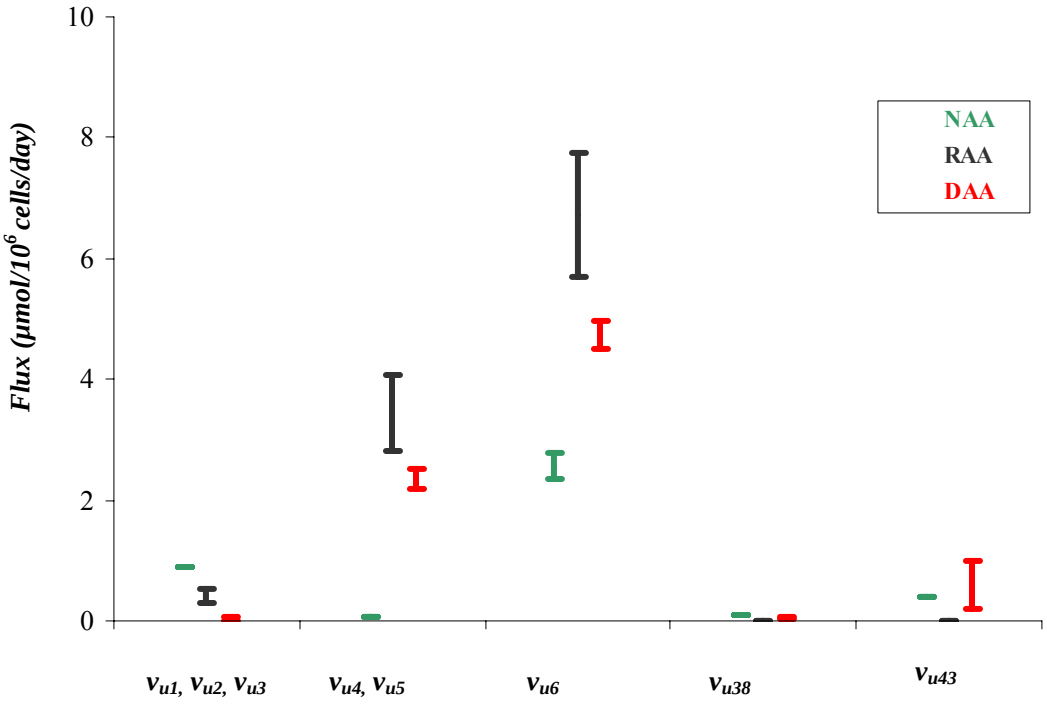

Unknown Fluxes in Gluconeogenesis (in NAA) / Glycolysis (in RAA and DAA) Pathway

Figure 4.2 c

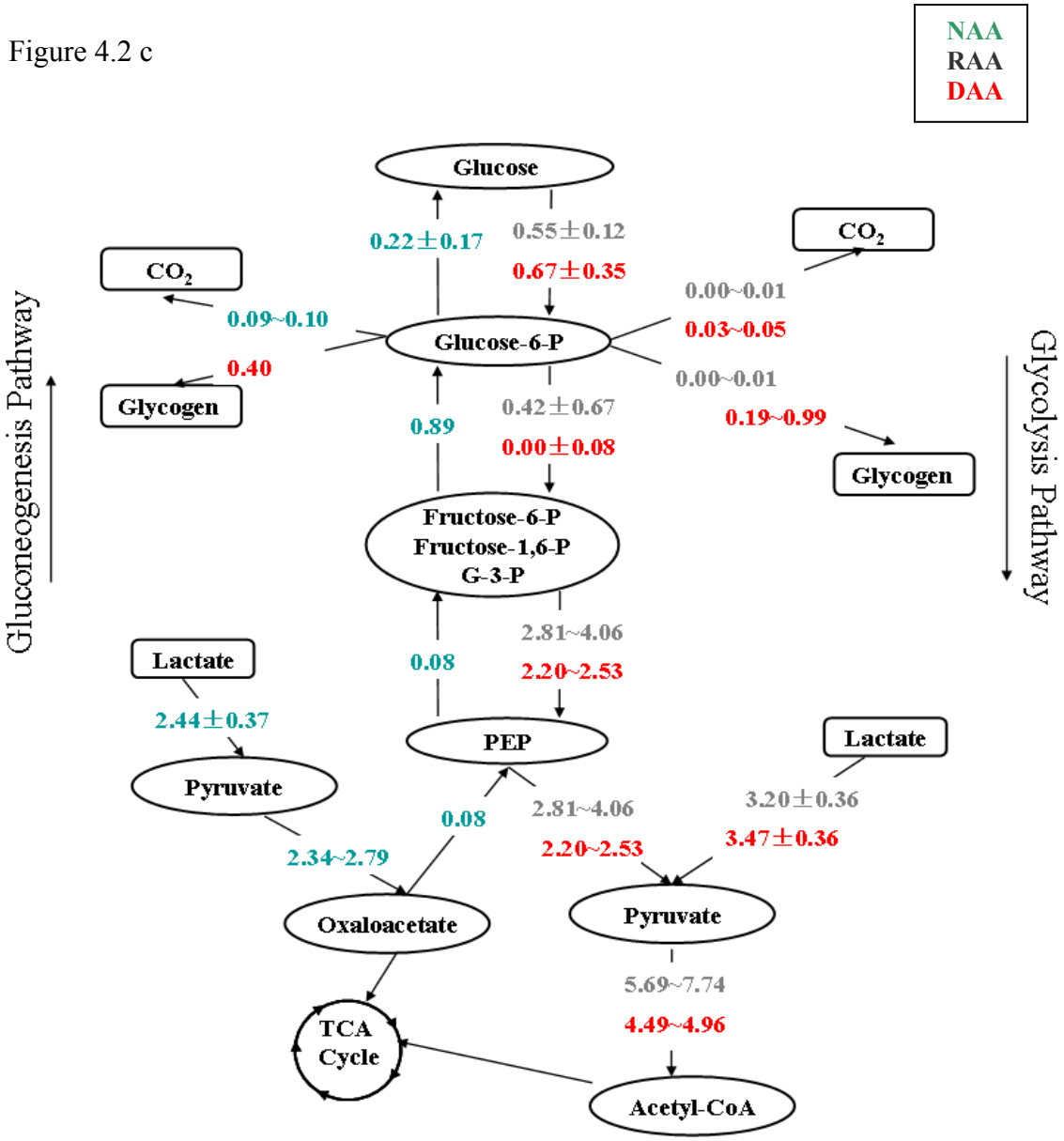

Figure 4.2: MNFA analysis of glycolysis/gluconeogenesis pathway. (a) Unknown flux ranges of glycolysis/gluconeogenesis pathways without PEB constraints; (b) unknown flux ranges of glycolysis/glucogeogenesis pathway with minimum PEB constraints; (c) fluxes in glycolysis/gluconeogenesis pathway: unknown flux range is calculated by metabolic network flexibility analysis (II) with minimal PEB constraints, and extracellular fluxes are measured (average ± standard derivation).

In our previous study, urea production (v_{m3}), a key liver-specific function, was increased in designed amino acid supplementation compared to reference amino acid supplementation and no amino acid supplementation conditions during plasma exposure. Arginine, which is the only amino acid that can be directly converted to urea, can be taken up from the culture medium (v_{m4}), or synthesized from citrulline and aspartate (v_{u14}). This step provides the critical link between urea cycle and TCA cycle. In the presence of ATP, aspartate combines with citrulline to form fumarate and arginine, and fumarate returns to the TCA cycle. The flux distribution results (Fig. 4.3) show that TCA fluxes (v_{u9}~v_{u12}) were increased in designed and reference amino acid supplementation compared with no amino acid supplementation. The majority of urea production from arginine is derived from citrulline (urea cycle, v_{u14}) instead of form arginine uptake from supplementation (v_{m3}), particularly in designed amino acid supplementation.

However, even with the incorporation of PEB constraints, the flux does not constraint sufficiently and do not allow to reach any conclusion regarding the differeces associated with fatty acid, lipid and glycerol metabolism, oxygen uptake and electron transport in the different amino acids supplementation condition. Therefore the minimum PEB constraints were incorporated into the metabolic objective prediction model to calculate a unique flux distribution and infer the cell's metabolic objectives.

Figure 4.3

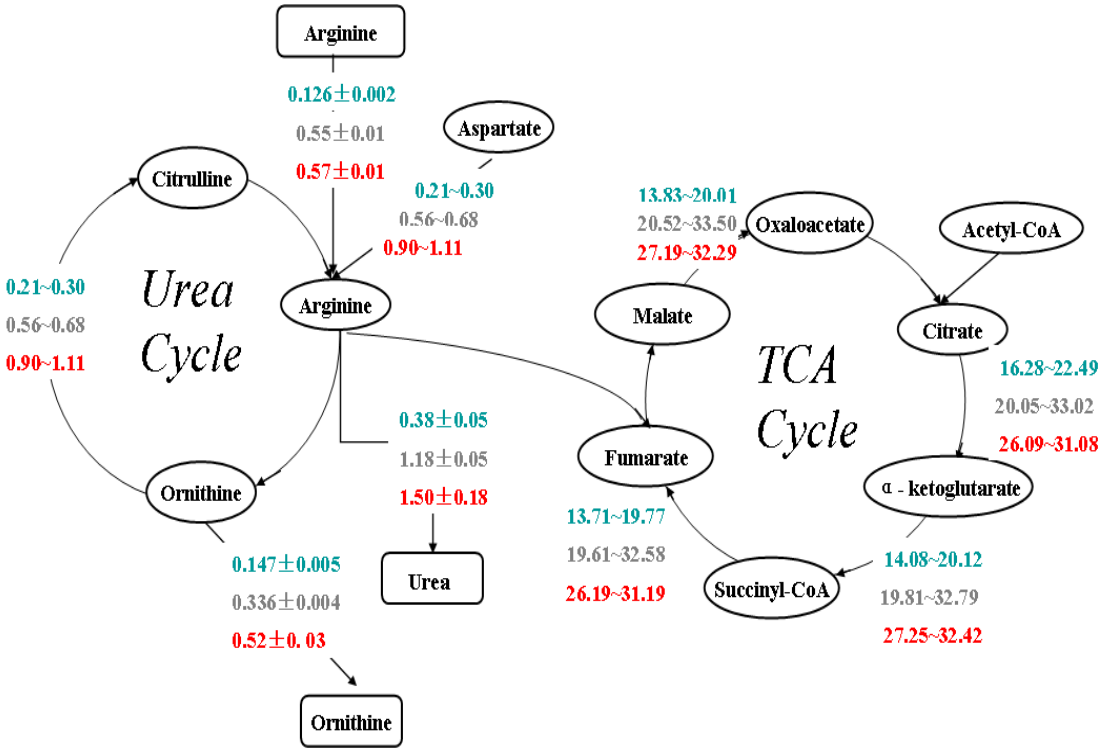

Figure 4.3: Flux distribution in the urea cycle and TCA cycle. Urea production was significantly increased in designed amino acid supplementation by an increase of fluxes in urea cycle compared with those values in reference amino acid supplementation and no amino acid supplementation. TCA fluxes were increased in designed and reference amino acid supplementation compared with no amino acid supplementation. The ranges of unknown fluxes are labeled as "min~max", and extracellular fluxes are labeled "average ± standard derivation".

4.3.3 Metabolic Objective Prediction (MOP)

The Metabolic Objective Prediction model (MOP) is a bi-level program where the upper-level corresponds to minimization of the sum of squared error between measurement fluxes and their calculated value from the model (III), and the lower-level is to identify the metabolic objectives. By applying MOP, objective functions of cultured hepatocytes are obtained for the three different amino acid supplementation conditions. The results for most important reactions ($c_j > 0.1$) are shown in Table 4.2.

Table 4.2: Identification of metabolic objective from MOP model (IV)

Flux #	*NAA*	*RAA*	*DAA*
v_{m4} Arginine Uptake		0.36	
v_{m10} Glycine Uptake		0.12	
v_{m12} Glutamate Secretion		0.13	
v_{m13} Aspartate Secretion		0.16	
v_{m28} Palmitate Uptake	0.46		
v_{m29} Cholesterol ester + H_2O → Cholesterol + Palmitate	0.46		
v_{u33} Palmitate + ATP + 7FAD + 7NAD^+ + 8CoA → 8acetyl-CoA + 7$FADH_2$ + 7NADH + AMP + PP_i		0.11	0.44
v_{u6} Pyruvate + CoA + NAD^+ → Acetyl-CoA + CO_2 + NADH			0.24
v_{m15} Acetoacetate + NADH + H^+ ←→ β-hydrobutyrate + NAD^+			0.23

Note: NAA = no amino acid supplementation; RAA = reference amino acid supplementation; DAA = designed amino acid supplementation.

The analysis implies that hepatocytes prioritize the management of their lipid metabolism by favoring palmitate uptake (v_{m28}), and cholesterol ester transformation to palmitate (v_{m29}) in the case where no amino acids are supplemented. In the condition of reference

amino acid supplementation, the metabolic objectives shift to transport of amino acids and synthesis of ketone bodies via arginine and glycine uptake (v_{m4} and v_{m10}), glutamate and aspartate release (v_{m12} and v_{m13}), and fatty acid oxidation (v_{u33}). Finally in the case of designed amino acid supplementation, hepatocytes' metabolic objectives correspond to fatty acid metabolism: fatty acid oxidation (v_{u33}), transformation of pyruvate to acetyl-CoA (v_{u6}), and formation of the ketone body β-OH-butyrate (v_{m15}).

4.3.4 Flux Distribution: Lipid Metabolism and Electron System

The unknown fluxes are calculated using model (IV) in which the mean squared error from experimental measurements is minimized subject to stoichiometric and minimum pathway energy balance constraints (see Table 4.3). The flux values associated with lipid metabolism and electron transport system are further evaluated in order to investigate amino acid supplementation effects on the metabolic state of hepatocytes.

From the experimental results, it was found that total free fatty acid uptake (triglyceride (TG) uptake (v_{m30}), free fatty acid (FFA) uptake (v_{m28}), and cholesterol synthesis (v_{m29})) are not significantly different among the different amino acid supplementation conditions. However, results from flux distribution indicate that there is lower lipid accumulation in the condition of designed amino acid supplementation due to an increase in TG conversion into fatty acid (v_{u42}), an increase in fatty acid conversion to acetyl-CoA (v_{u33}), and a decrease of TG storage (v_{u45}) compared with other conditions during plasma exposure. These intracellular flux distributions are consistent with the morphological appearance of the cells, in which lipid droplets are apparent in the absence of amino acid

supplementation but are reduced markedly when amino acid supplementation is employed (Yang et al. 2009) .

From the obtained flux distribution (Table 4.3), it also found that the fluxes of oxygen uptake (v_{u33}) and the reactions associated with electron transport (v_{u36}, v_{u37}) were increased under designed amino acid supplementation compared with the other two conditions. From the hepatic energy metabolism aspects, metabolism of amino acids in designed amino acid supplementation increase the amount of NADH and $FADH_2$ through increase of the fluxes in TCA cycle. The NADH and $FADH_2$ are next utilized with O_2 taken from medium to make more ATP via the reactions associated with electron transport.

Table 4.3: Intracellular flux distribution from MOP model (IV)

Flux #	***NAA***	***RAA***	***DAA***
Glycolytic or Gluconeogenic Pathway, PPP, Glycogen storage			
v_{u1}, v_{u2}, v_{u3}	0.89	0.54	0.00
v_{u4}, v_{u5}	0.08	3.19	2.39
v_{u6}	2.51	6.49	4.89
v_{u38}	0.09	0.001	0.05
v_{u43}	0.40	0.004	0.62
TCA cycle			
v_{u7}, v_{u8}	19.07	22.45	30.48
v_{u9}	16.89	22.17	31.60
v_{u10}	16.54	22.01	30.60
v_{u11}, v_{u12}	16.76	22.98	31.70
Urea Cycle			
v_{u13}, v_{u14}	0.30	0.62	1.11
Amino Acid Catabolism			
v_{u15}	0.10	-0.07	-0.13
v_{u16}	-0.27	0.13	-0.61
v_{u17}	-0.05	0.05	0.03

v_{u18}	-0.04	0.22	-0.46
v_{u19}	0.03	0.48	0.08
v_{u20}	5.85	1.07	3.08
v_{u21}	-0.36	-0.16	-1.00
v_{u22}	-0.12	-0.04	-0.42
v_{u23}	-0.05	0.33	0.15
v_{u24}	-0.04	0.18	0.00
v_{u25}	-1.09	-0.14	0.56
v_{u26}	0.13	2.78	1.77
v_{u27}	-0.03	0.22	0.02
v_{u28}	0.29	0.25	0.27
v_{u29}	-2.34	-2.35	0.46
v_{u30}	-0.02	0.01	0.01
v_{u31}	-0.06	-0.27	-0.61
v_{u32}	0.18	0.09	-0.12
v_{u39}	-0.09	-0.09	-0.30
v_{u40}	-0.08	0.004	-0.21
v_{u41}	-0.04	-0.15	-0.19
v_{u47}	-2.34	-2.36	0.44
v_{u48}	5.85	1.07	3.08
Fatty Acid, Lipid and Glycerol Metabolism			
v_{u33}	1.22	1.74	2.78
v_{u34}	-4.81	-1.03	-2.29
v_{u35}	0.92	0.00	0.38
v_{u42}	0.00	0.00	0.32
v_{u44}	1.70	2.11	2.39
v_{u45}	0.93	0.82	0.60
Oxygen Uptake and Electron Transport System			
v_{u36}	39.77	48.77	64.66
v_{u37}	15.18	17.39	25.68
v_{u46}	72.57	70.66	100.00

Flux rate (μmol/million cells/day). The flux range is in Appendix G.

NAA = no amino acid supplementation; RAA = reference amino acid supplementation; DAA = designed amino acid supplementation.

4.4 Discussion

It has been recognized that amino acids play an important role in regulatory control of hepatic metabolism during plasma exposure such as synthesis/degradation of protein and lipid (Chan et al. 2003c). In our previous work, experimental data showed that designed amino acids supplementation, derived from a rational approach based on linear optimization towards an objective of high urea flux, led to an increase in urea and albumin production compared with reference amino acid supplementation and no supplementation. In this work, metabolite measurements and flux/pathway analysis were used to characterize the hepatocytes' state of metabolism under varying amino acid supplementations.

4.4.1 Unknown Flux Ranges with or without PEB Constraints

In this system, the number of unknown fluxes (48 reactions) is greater than the number of mass balance equations (46 internal metabolites). Therefore, intracellular fluxes cannot be uniquely determined using flux balance analysis (FBA) (Stephanopoulos et al. 1998). Additional constraints are required to reduce the feasible region of an FBA problem. Recently, energy balance analysis (EBA) was proposed to eliminate the thermodynamically infeasible fluxes associated with FBA (Beard et al. 2004; Beard et al. 2002). Nolan et al. (Nolan et al. 2006) incorporated the ΔG^0_{PATH} inequality constraints and successfully reduced the feasible region of FBA for hypermetabolic liver. The ΔG^0_{PATH} inequality constraints express an overall distribution of Gibbs free energy to the reactions involved in an elementary mode, in which endergonic reactions ($\Delta G > 0$) can be "powered" by exergonic reactions ($\Delta G < 0$) if those reactions are "coupled" in the same

elementary modes and the overall free energy change weighted by their fluxes is negative. The approach here differs from that of Nolan et al. (Nolan et al. 2006) in that the latter did not consider the effects of the metabolite concentration from different cultured conditions, which can greatly alter the values of Gibbs free energy of the reaction (Beard and Qian 2005). However, hepatocytes contain a large number of different metabolites which make the analysis and quantification of concentration of every metabolite difficult and tedious. In order to resolve this issue, only the concentrations of the extracellular metabolites are measured and represent the values in the culture medium and in the collected supernatant at the end of experiment (Appendix H). The concentrations for intracellular metabolites are assumed to lie within the range that exist in the literature relative to hepatic metabolism, or within their physiological ranges of the order of μM to mM if no data are available in the literature (Fraenkel 1992) (Appendix H). Although exact measurements of concentrations for intracellular metabolites are not available, the proposed methods take into consideration the effects of metabolite concentration on evaluating the Gibbs free energy rather than relying solely rely on standard conditions.

Depending on the Gibbs free energy evaluation for each reaction (standard, minimum and maximum as shown in equations 4-1, 4-3a, and 4-3b), three types of pathway energy balance (PEB) constraints are investigated in this work. Since PEB constraints are calculated as the summation of the products of the Gibbs free energy times the flux of the corresponding reaction, increase of Gibbs free energy of reaction would result in smaller feasible region in terms of flux values. Maximum and standard PEB constraints generated very tight feasible region for underdetermined hepatic network, whereas minimum PEB

guarantee the flux feasibility resulting in the largest feasible region but with reliable range of concentrations of the metabolites. Therefore, we used minimum PEB constraints to explain the effects of amino acid supplementation and incorporate those constraints into MOP model to infer the metabolic objectives.

4.4.2 Advantages of MOP Modeling

In FBA, a particular flux distribution is determined based on a pre-selected objective, such as maximization of growth rate for a microorganism (Ibarra et al. 2002), or maximization of urea production for primary hepatocytes (Sharma et al. 2005). Schuetz et al., (Schuetz et al. 2007) evaluated different objective/constraints combinations and found that the objectives of *E. coli* change with different environmental conditions or biological occurrences. A Bayesian-based objective function discrimination method has thus been developed to find the most probable objective with a highest posterior probability from a group of spare objectives (Knorr et al. 2007). Recently, an optimization-based framework has been developed to systematically identify and test metabolic objectives (Burgard and Maranas 2003). In this approach, the objective is the most consistent with experimental data and represented by the value of the coefficient of importance (c_j). In this work, we developed a bi-level programming MOP to determine the hepatocyte objectives taking into consideration flux data of external metabolites, mass balances of all internal metabolites and minimum PEB constraints. One of the advantages of this method is that it does not require a pre-selection of a set of objective functions (Burgard and Maranas 2003). Uygun et al., (Uygun et al. 2007) applied a similar approach for objective identification in cultured hepatocytes assuming that the cells exhibit the same objective

under different conditions. Instead, we found that the cellular priorities changed based on the amino acid supplementation (Table 4.2).

4.4.3 Metabolic Objectives under Different Amino Acid Supplementation

The results of MOP analysis reveal some interesting characteristics of hepatocyte cells' behavior under different amino acid supplementations. Previous reports suggested that urea synthesis is reduced during plasma exposure most possibly due to lack of amino acids in the medium (Matthew et al. 1996a), which is represented in our studies by the case of no amino acid supplementation. The results of MOP reveal that in this case the cells uptake free fatty acid (FFA) and transform cholesterol ester to FFA (v_{m28}, v_{m29}), which is supported by the results reported in the literature of increased TG accumulation (Matthew et al. 1996a). When amino acid supplementation was provided in the plasma, TG accumulation was reduced for both reference and designed amino acid supplementation (Chan et al. 2003a; Yang et al. 2009). Given that changes are occurring in pathways beyond the urea cycle, it is not surprising that the metabolic objectives of hepatocytes are changing with varying amino acid supplementations. The solution of the MOP model implies that the metabolic objectives for the case of reference amino acid supplementation are to exchange amino acids (arginine, glycine, glutamate, and aspartate) with cultured medium and to synthesize acetoacetate. For the case of designed amino acid supplementation, arginine and glycine uptake was not selected as cell objectives because the cells have already reached their maximum uptake capacity of arginine and glycine. Excess uptake of any amino acid from the cell can cause build-up of ammonia that should be excreted to avoid toxic effects. Supplying hepatocytes with large amount of glutamine

(6.85 mM in reference and designed amino acid supplementation compared with 0.65 mM in the medium of no amino acid supplementation) results in a large increase of intracellular glutamate via the reaction v_{u26} and aspartate due to reaction v_{u31}. Thus secretion of both glutamate and aspartate were among the objectives identified by MOP for the case of reference amino acid supplementation.

Both reference and designed amino acid supplementation identified fatty acid oxidation as an objective, which is an important step to reduce the rate of TG accumulation during plasma exposure (Stefanovich et al. 1996). The coefficients of importance (c_j) associated with fatty acid oxidation are greater in designed amino acid supplementation ($c_j = 0.44$) than in reference amino acid supplementation ($c_j = 0.11$), which implies that the reduction of TG accumulation is more important in the designed amino acid supplementation. The other two metabolic objectives identified for the case of designed amino acid supplementation are β-hydroxybutyrate production and transformation of pyruvate to acetyl-CoA, which indicates that the decrease in ketone body production results in more acetyl-CoA entering the TCA cycle to produce urea (Yang et al. 2009) . These results indicate that hepatocytes employ different strategies to maintain their survival in environment perturbations.

4.5 Summary

Overall, the presented work leads to better understanding of hepatocyte's behavior under varying amino acid supplementation during plasma exposure. Our data showed that amino acid supplementation plays a central role to increase the flux of free fatty acid

oxidation in hepatic metabolism during plasma exposure, which enables the metabolic manipulation of hepatocytes to improve liver cell function in culture by rational design of amino acid supplementation.

Chapter 5

EFFECTS OF AMINO ACID TRANSPORT LIMITATION ON CULTURED HEPATOCYTES

Abstract:

Amino acid supplementation has been shown to enhance the liver-specific functions of cultured hepatocytes during plasma exposure. However, their transport through the cell membrane may restrict their effects on hepatic metabolism. Such constraints should be included in the design of amino acid supplementation.

In chapter 5, we first investigate the transport constraints related to uptake of the neutral amino acids to understand the transport effects on the liver-specific functions. Using different combinations of alanine, serine and glutamine on supplementation, their transport rate and liver-specific functions (urea and albumin) are measured. The results show that the transport competition exists among these three amino acids and as a result affect the urea and albumin production. Next, regression equations are developed to quantify these effects and then incorporated together with other constraints (mass balance, measured data and reaction directionality) within a multi-objective framework to investigate the effects of transport constraints and predict the amino acid supplementation that can lead to improved hepatocyte functionality.

5.1 Introduction

Cultured hepatocytes are core components of extracorporeal bioartificial liver (BAL) devices, which are being developed with the intent to support patients with liver failure until a liver transplantation becomes available. However, cultured hepatocytes are frequently characterized by a decline in liver-specific functions when they are exposed to unfavorable environments such as plasma, as occurs clinically for BAL devices. Media supplementations are sought to reduce these effects. However, previous studies showed that single amino acid supplementation, such as glycine or glutamine, is insufficient to maintain liver-specific functions during plasma exposure (Washizu et al. 2000a). A balanced supplementation of amino acids, either mixed additional glutamine with a commercial amino acid supplementation, Basal Medium Eagle (BME) (Chan et al. 2003c) or designed amino acid supplementation using a rational optimization approach (Yang et al. 2009), have positive effects on hepatic metabolism. These formulations lead to improvement of liver-specific functions as well as reduction of lipid accumulation of hepatocyes during plasma exposure.

Cellular metabolism of amino acids depends on its capacity to transport them through the cell membrane, which is mediated by the transporters that recognize, bind and transport the amino acids from extracellular environment (cultured medium) to cytoplasm, or vice versa. The transporters with the same recognition properties form a transport system. The characteristics of transport for different amino acids can be distinguished based on their ionic charge: neutral, cationic and anionic, which are mediated by independent transport systems with overlapping specificities (Hyde et al. 2003; Malandro and Kilberg

1996; Palacin et al. 1998). In brief, the main transport systems for neutral amino acids are known as system A, ACS, N and L. System A mediates small aliphatic neutral amino acids (alanine, serine and glutamine) with Na^+ ion and pH sensitive, such as alanine, serine and glutamine. Perfect amino acids for ACS transport system, which is Na^+ dependent and not pH sensitive, are alanine, serine and cysteine. System N transports glutamine, asparagine and histidine. Because transport system A and N share comment sequential and functional properties, they are recently reclassified as a single family-system A/N transport (SNAT) family (Gu et al. 2000; Gu et al. 2005). System L transports branched-chain and other aromatic amino acids. System Gly is specific for glycine. Cationic amino acid transporters (CATs) mediate arginine, lysine, and ornithine. Anionic amino acids transporters (EAATs) mediate glutamate and aspartate.

An excess of one amino acid for a particular transport system may inhibit the uptake of any other amino acids which are mediated by the same transport system (Joseph et al. 1978). It has been shown that the transport rate is a control step for alanine metabolism (Fafournoux et al. 1983), and a similar conclusion was drawn for glutamine (Haussinger et al. 1985). It was also shown that alanine and glutamine are mediated by the same transport system A with serine (Christensen et al. 1965).

In our study, first the transport rate of alanine, serine and glutamine are measured under different concentrations to investigate the transport limitations. Next, the experimental results are used to model mathematically the amino acid transport constraints using a least-square regression equation, which explain the variance and dependence in amino

acids transport fluxes (alanine, serine and glutamine). Finally, these amino acid transport constraints are incorporated together with other constraints including mass balances, measured data and reaction directionality within a multi-objective metabolic flux balance model to investigate the effect of transport constraints and predict the amino acid supplementation of alanine, serine and glutamine for maximum urea production and fatty acid oxidation.

5.2 Methods

5.2.1 Design of Experiment: Amino Acids Transport

Hepatocytes were isolated from adult male Fisher F344 rat (150-200g) based on the two-step collagenase-perfusion method via the portal vein described previously (Dunn et al. 1991). Cells were cultured on sandwich collagen at a density of $1x10^6$ cells/mL at the six-well plates. Initially, hepatocytes were cultured in the standard hepatocyte C+H medium, which consists of DMEM supplemented with 10% heat inactivated fetal bovine serum (FBS), 7.0 ng/mL glucagon, 7.5 g/mL hydrocortisone, 20 g/L epidermal growth factor, 200 U/mL penicillin, 200 g/mL streptomycin, and 500 mU/L insulin. This C+H medium was treated to hepatocytes at the beginning of three days with changing the medium every day.

The RMPI_1600, plus 10% FBS with same concentration of Glucagon, EGF, insulin, and glucose as C+H medium, was used to wash hepatocytes three times with 1 hour interval. Then cells were cultured in conditional medium (Table 5.1) with different combinations of alanine, serine and glutamine supplementation (total 33 combinations), in additional

three days with changing medium every day. At the end of experiment, the supernatant was collected and stored in 4℃ for assay

Table 5.1: Conditional medium of transport experiment

	*Alanine**	*Serine**	*Glutamine**
Alanine & Glutamine	0.2,0.4,0.8	0.1	2
	0.2,0.4,0.8	0.1	4
	0.2,0.4,0.8	0.1	6
	0.2,0.4,0.8	0.1	8
Serine & Glutamine	0.1	0.2,0.4,0.6	2
	0.1	0.2,0.4,0.6	4
	0.1	0.2,0.4,0.6	6
	0.1	0.2,0.4,0.6	8
Alanine & Serine	0.2	0.2,0.4,0.6	1.5
	0.4	0.2,0.4,0.6	1.5
	0.8	0.2,0.4,0.6	1.5

* supplied concentration in the cultured medium (mM)

5.2.2 Design of Experiments: Amino Acids Supplementation

Hepatocytes were cultured using the well-established collagen sandwich method (Dunn et al. 1991) as described Chapters 3 and 4. After the second gel layer solidified, 0.8 mL fresh C+H medium (described in section 5.2.1) with 0.05 mU/mL insulin (LI) or 500 mU/mL (HI) was added. Medium was exchanged every day for 6 days preconditioning.

After 6 days of preconditioning, hepatocyte cultures were exposed to plasma with hormone supplementation including 7.5 g/mL of hydrocortisone and 0.05 mU/mL of insulin (WH) or without hormone supplementation (NH). Treatment groups varied in the

amino acid supplementation in the plasma, comparing "designed" amino acid supplementation (DAA) based on a rational design approach described in our previous work (Yang et al. 2009), and "reference" amino acid supplementation (RAA) based on published data (Chan et al. 2003c). The concentrations corresponding to each amino acid supplementation are given in Appendix D. Those media were exchanged with spent media every day for 5 days plasma exposure. At the end of the experiment, culture supernatants were collected and stored at 4 °C prior to analysis.

5.2.3 Biochemical Assays

At the end of both experiments (amino acid transport and amino acid supplementation during plasma exposure), urea was measured using a commercial kit (Sigma, St. Louis, MO) which is based on the reaction of diacetyl monoxime with urea. Albumin production was quantified by an enzyme-linked immunosorbent assay (ELISA) using purified rat albumin (MP Biomedicals, Solon, OH) and peroxidase-conjugated antibody for detection (MP Biomedicals, Solon, OH).

Amino acids were labeled fluorescently with the AccQ reagent (Waters Corporation, Milford, MA) using a Beckman Coulter HPLC system with a fluorescence detector (Waters 470, Waters Corporation, Milford, MA) scanning fluorescence detector at 250/395 nm excitation/emission (detail described in Chapter 4). Serial dilutions of standards were used to construct a calibration curve for each analyte, with the linear portion utilized for measurements. The concentrations of amino acid/ammonia in the fresh or spent medium were determined using these standard curves, with sample

dilutions performed as necessary to operate within the linear range.

In addition, for the experiment of the amino acid supplemention during plasma exposure, the concentrations of glucose, lactate, glycerol, and glutamine were measured colorimetrically using commercial kits (Sigma, St. Louis, MO). Enzymatic kits were utilized for the measurement of cholesterol (BioAssay System, Hayward, CA), acetoacetate, β-hydroxybutyrate, triglycerides (Stanbio, Boerne, TX), and free fatty acids (Roche, Indianapolis, IN).

5.2.4 Transport Constraints: Nonlinear Equations

A quadratic model is developed to simulate the transport limitations that exist between amino acid uptake/secretion and their concentrations in the cultured medium, as follows:

$$\begin{aligned} v &= f(C_{Ala,}C_{Ser},C_{Gln}) \\ &= \beta_0 + \beta_1 C_{Ala} + \beta_2 C_{Ser} + \beta_3 C_{Gln} + \beta_{11} C_{Ala}{}^2 + \beta_{22} C_{Ser}{}^2 + \beta_{33} C_{Gln}{}^2 \\ &\quad \beta_{12} C_{Ala} C_{Ser} + \beta_{13} C_{Ala} C_{Gln} + \beta_{23} C_{Ser} C_{Gln} + e \end{aligned} \tag{5-1}$$

where β 's are parameters which are estimated from a set of known values of concentrations of alanine (C_{Ala}), serine (C_{Ser}), and glutamine (C_{Gln}) supplied in the medium and their corresponding uptake/secretion fluxes (v) using the methods of least squares, which minimizes the sum of the squares of the error e. SAS software (SAS Institute, Inc., Cary, NC) is used to identify which terms ones contribute significantly to the flux values. Terms with $p<0.05$ are considered to be significant, while the others are excluded from the model.

5.2.5 Multi-objective Modeling

The basic hepatic network used in the analysis builds upon previously reported hepatic networks (Chan et al. 2003c; Lee et al. 2003; Nagrath et al. 2007; Sharma et al. 2005; Uygun et al. 2007) and involves 46 intracellular metabolites, and 78 reactions (30 reactions with measurement data, 48 reactions with unknown fluxes as labeled in Appendix E). Gluconeogenesis pathway instead of glycolysis is used in this work, which is the case for amino acid supplementation. The other reactions included are tricarboxylic acid cycle (TCA), urea cycle, amino acid uptake/secretion and catabolism, oxygen uptake, electron transport system, pentose phosphate reactions (as a lumped group), ketone body synthesis, fatty acid, triglyceride (TG) and glycerol metabolism.

The constraints derived to express the transport limitations of amino acids are then incorporated in the optimization framework to investigate the effects of amino acid supplementation on urea production and fatty acid oxidation. The optimization model is as follows:

$$
\begin{aligned}
& Max\{v_{urea}, v_{Fatty\ Acid\ Oxidation}\} \\
& s.t. \qquad \sum_{j=1}^{N} S_{ij} v_j = 0, \qquad i \in M \\
& \qquad\quad v_j^{\min} < v_j < v_j^{\max} \qquad j \in K \\
& \qquad\quad v_k = f(C_{Ala}, C_{Ser}, C_{Gln}) \qquad k \in K'
\end{aligned}
\tag{I}
$$

where S_{ij} is the stoichiometric coefficient of metabolite i in reaction j; $v_j^{\min}$ and $v_j^{\max}$ are lower and upper bound of reaction j, respectively; M is the set of metabolites; N is the total number of reactions involved in the hepatic network; K is the set of constrained reactions (based on measurements from amino acid supplementation

experiment and/or irreversibility); and K' is the set of additional transport constraints generating by nonlinear least-square regression equation 5-1. The main assumptions for the development of model (I) are as follows:

(1) Urea maximization is a reasonable objective since it is often used as a marker of hepatocyte function that typically correlated with a health phenotype of hepatocytes (Yang et al. 2009). Fatty acid oxidation was identified as an additional metabolic objective to represent the reduction of lipid accumulation with amino acid supplementation in Chapter 4. Therefore, both of them are considered in the objective functions in this study.

(2) Based on our previous results using amino acid supplementation, in this work we derived the bounds in model (I) using the measurements of the conditions with amino acid supplementation (DAA and RAA) but varying with insulin precondition (HI and LI) and hormone supplementation during plasma exposure (NH and WH). The range of these experimental measurements defines the flux bounds which cover all eight experiment settings.

(3) The reversibility of each reaction is determined based on the information given in the metabolic map of KEGG (Kanehisa and Goto 2000). Reversible reactions are allowed to take either positive or negative values, whereas irreversible reactions are restricted to positive values if the reaction directions are same with KEGG, or to negative values if the reaction directions are different from KEGG.

(4) Albumin synthesis which is one of the most important liver-specific functions (Nagrath et al. 2007; Sharma et al. 2005; Yang et al. 2009) is considered constant in model (I) and equal to the value at the designed amino acid supplementation.

Model (I) corresponds to a nonlinear programming (NLP) problem since the transport constraints are nonlinear functions and is solved by ε-constraint method (Haimes et al. 1971) which maximizes a primary objective while it converts another objective into a constraint as follows:

$$
\begin{aligned}
& Max \quad v_{urea} \\
s.t. \quad & \sum_{j=1}^{N} S_{ij} v_j = 0, && i \in M \\
& v_j^{\min} < v_j < v_j^{\max} && j \in K \\
& v_k = f(C_{Ala}, C_{Ser}, C_{Gln}) && k \in K' \\
& v_{Fatty\ Acid\ Oxidation} \geq \varepsilon
\end{aligned}
\qquad \text{(II)}
$$

Choosing a different value of parameter ε results in the determination of a set of Pareto-optimal solutions where urea production and the flux of fatty acid oxidation are best compromised.

5.3 Results

5.3.1 Amino Acid Transport Constraints

In the amino acid transport experiment, at the initial three days, hepatocytes were cultured by C+H medium which is changed every day. Then the different combinations of alanine, serine and glutamine supplementation with RMPI_1600 medium are supplied to cultured hepatocytes for additional three days with changing medium every day. At the end of the experiment, alanine, serine and glutamine fluxes are calculated from their measured concentrations in the collected supernatants (Appendix I).

Hepatocytes uptake alanine from the supplied medium when concentration of glutamine

is low, however, it switches to secretion into the medium when the concentration of glutamine increases (Fig. 5.1a). Similar phenomena are observed for serine transport rate (Fig. 5.1b), which suggests the effect of transport competition among these amino acids. It is further shown that hepatocytes have limited uptake capacity for glutamine and that the rate of glutamine uptake is roughly constant when glutamine supplementation in the medium is increased up to 4 mM (Fig. 5.2a and 5.2b). This effect is independent of alanine and serine supplementation in the medium. Moreover the results illustrate that under low level of supplementation of alanine and serine (<1 mM) no competition exists (Appendix I).

It is found that glutamine inhibits the uptake of alanine and serine when high level of glutamine is supplied to the culture medium. Therefore, the effect of this inhibition on the liver-specific functions, such as urea and albumin, was investigated further. Under different combinations of alanine and glutamine supplementations, it was found that urea production is increased with the increase of glutamine supplementation, but gets its maximum value when the glutamine concentration is close to 4 mM (Fig. 5.3a). Higher levels of glutamine supplementation lead to a decline in the urea production. However, urea production is not affected significantly by varying levels of serine and glutamine supplementation (Fig. 5.3b). Albumin synthesis decreases with increasing glutamine supplementation and it is independent of alanine and serine supplementation in the cultured medium (Fig. 5.4 a, b).

Figure 5.1 a

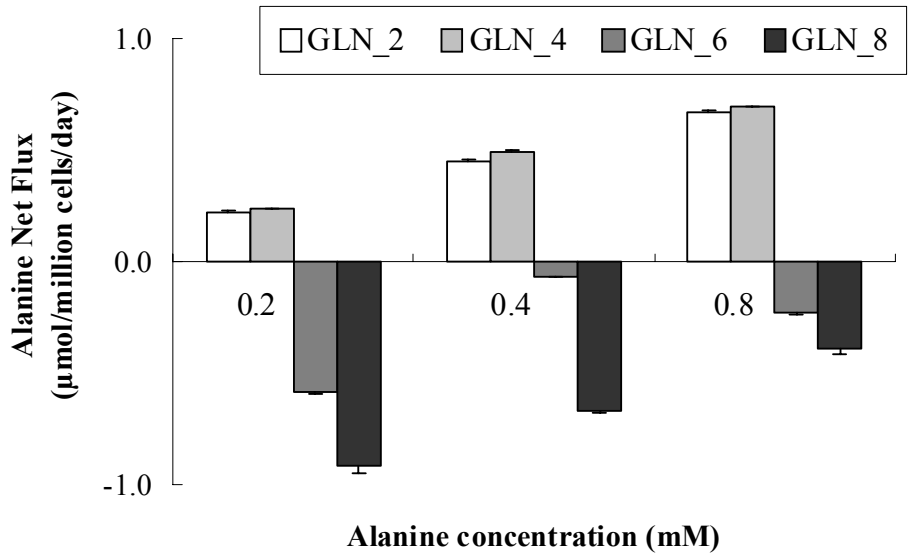

Figure 5.1 b

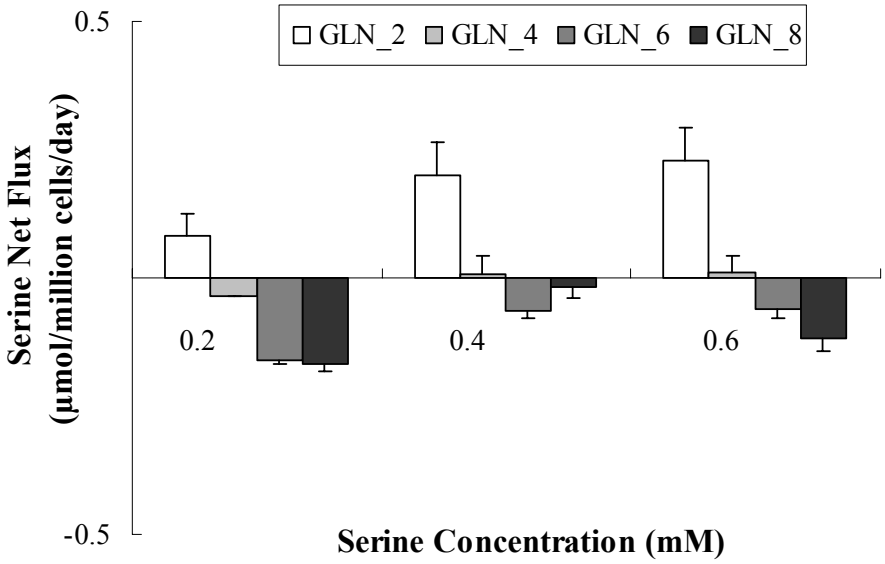

Figure 5.1： Net fluxes of alanine and serine affected by glutamine supplementation. (a) Alanine net fluxes under different combinations of alanine and glutamine in the medium; (b) serine net fluxes under different combinations of serine and glutamine in the medium.

Figure 5.2 a

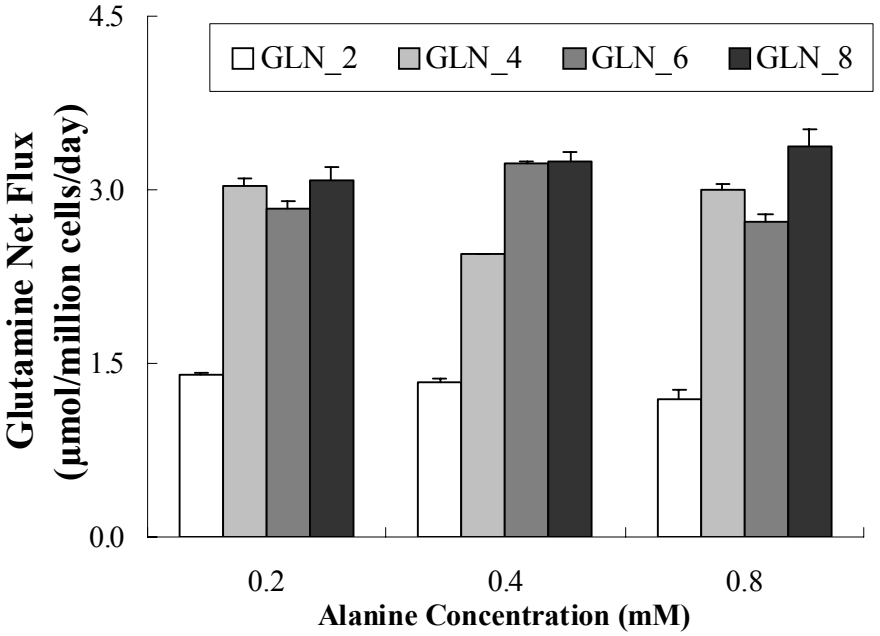

Figure 5.2 b

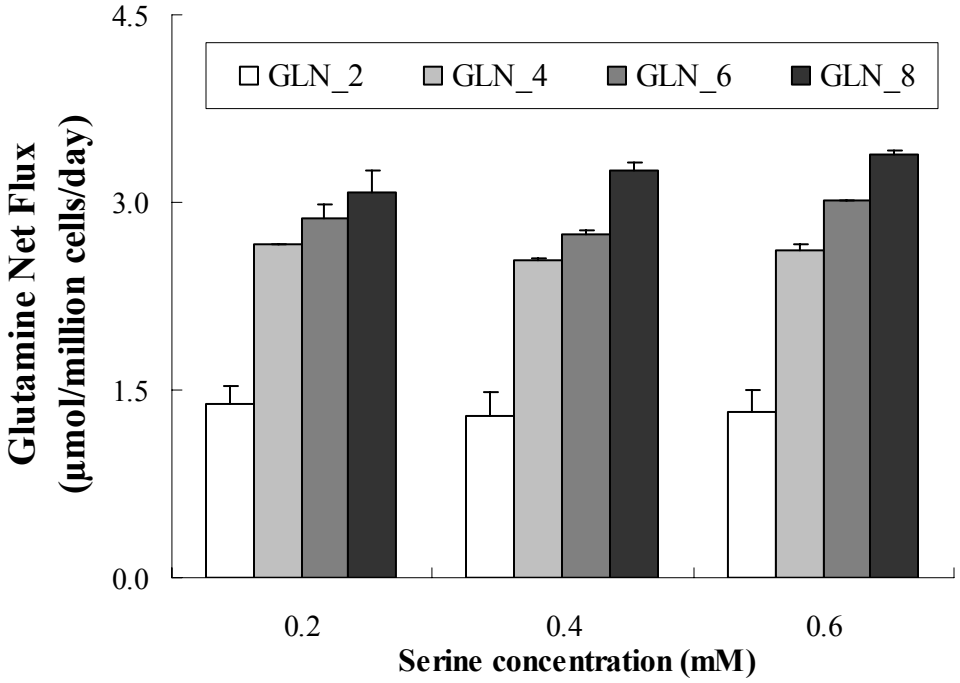

Figure 5.2: Results on Glutamine uptake. (a) Glutamine uptake under different combinations of alanine and glutamine in the medium; (b) glutamine uptake under different combinations of serine and glutamine in the medium.

Figure 5.3 a

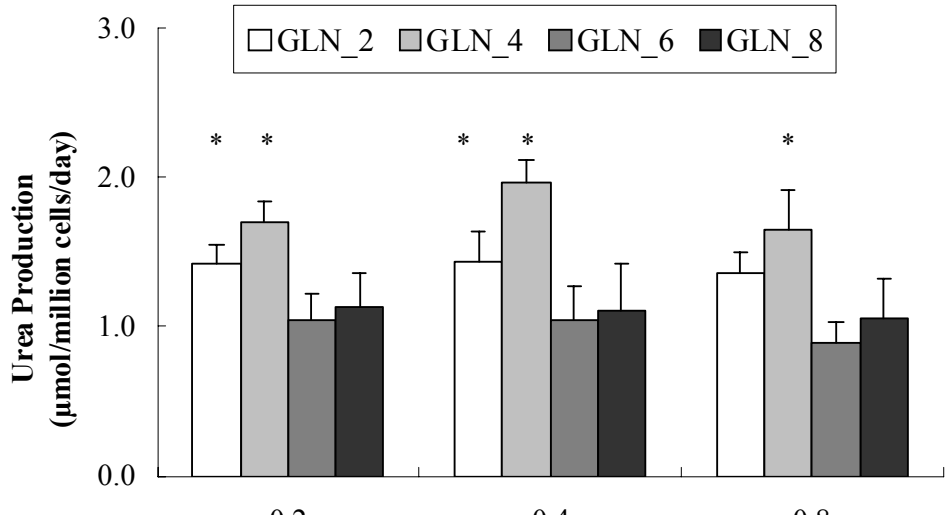

Figure 5.3 b

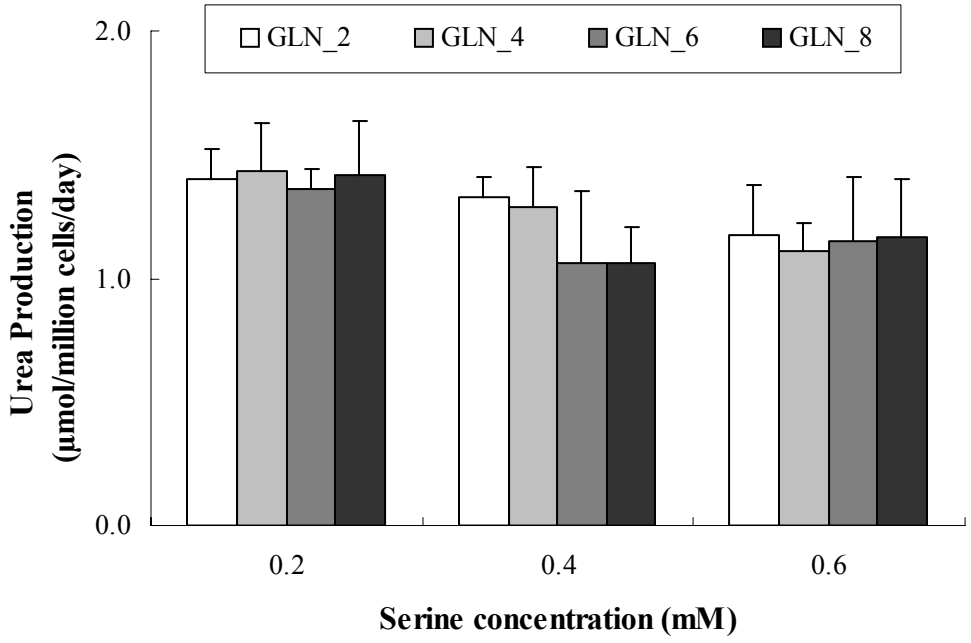

Figure 5.3: Urea production (a) under different combinations of alanine and glutamine supplementation; (b) under different combinations of serine and glutamine supplementation. Asterisks (*) indicate significant different ($p<0.05$) between the different supplied glutamine lever and supplied glutamine level of 6 mM for the same alanine and serine supplementation.

Figure 5.4 a

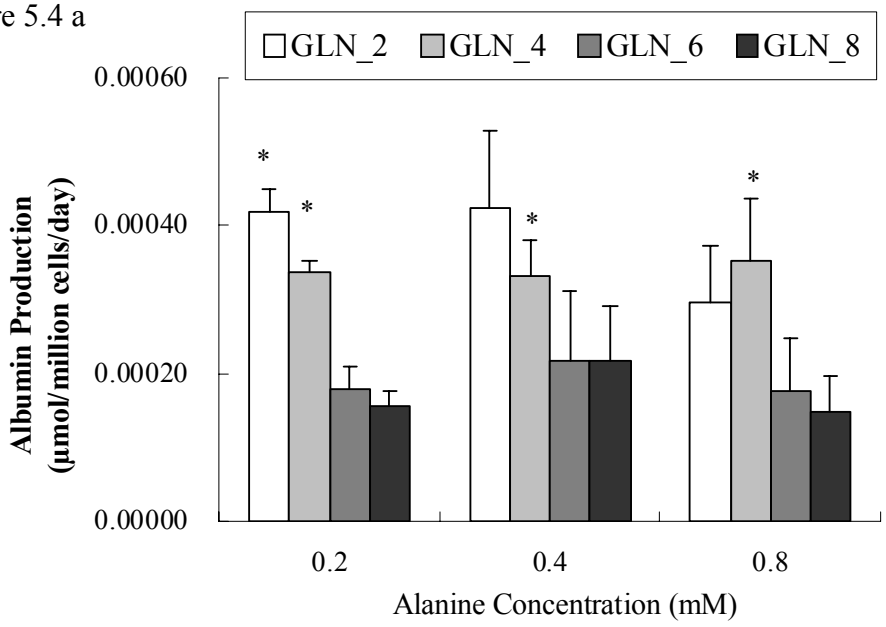

Figure 5.4 b

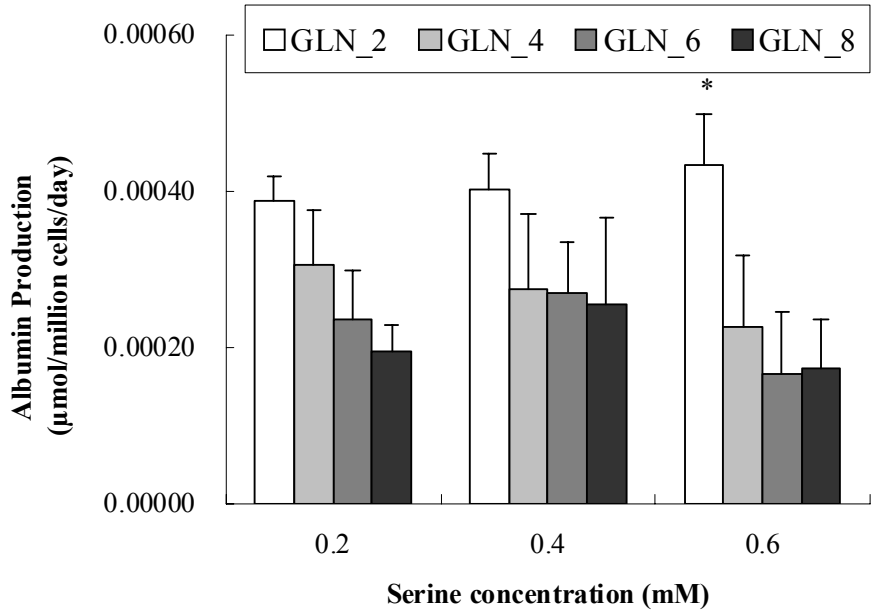

Figure 5.4: Albumin synthesis (a) under different combinations of alanine and glutamine supplementation; (b) under different combinations of serine and glutamine supplementation. Asterisks (*) indicate significant different ($p<0.05$) between the different supplied glutamine lever and supplied glutamine level of 6 mM.

In order to investigate the effects of these restrictions on the hepatic network during plasma exposure, a non-linear regression model is used to fit these three amino acid fluxes with their supplied concentrations in the medium and further those equations are incorporated to flux analysis model as constraints. All the experimental data in Appendix I are used to calculate the parameters in the regression model (Eqn.5-1), and only those significant parameters (with p value less than 0.05) are shown for nonlinear transport constrains as follows,

$$v_{Ala-uptake} = -0.218 + 2.910C_{Ala} - 1.859C_{Ala}^{\ 2} - 0.019C_{Gln}^{\ 2} - 1.538C_{Ala}C_{Ser} + 0.062C_{Ser}C_{Gln} \quad (5\text{-}2)$$

$$v_{Ser-uptake} = -0.323 + 2.189C_{Ala} - 2.185C_{Ala}^{\ 2} + 4.000C_{Ser} - 4.832C_{Ser}^{\ 2} - 0.210C_{G\ln} + 0.017C_{G\ln}^{\ 2} \quad (5\text{-}3)$$

$$v_{Gln-uptake} = -0.620 + 1.118C_{Gln} - 0.081C_{Gln}^{\ 2} + 0.005C_{Ala}C_{Gln} - 0.042C_{Ser}C_{Gln} \quad (5\text{-}4)$$

The high value of coefficient of determination (R^2) for these nonlinear regression models ($R^2 \geq 0.88$) imply that most of the variability in amino acid transport rate (v) can be explained by quadratic functions of the concentrations of alanine, serine and glutamine supplied in the medium.

5.3.2 Reduction of Feasible Space using Additional Transport Constraints

In the experiment of amino acid supplementation, after six days of preconditioning with high or low insulin provided, cultured hepatocytes were exposed to plasma containing medium with varying amino acid and hormone supplementation for five days. At this time, the concentrations of extracellular metabolites in the supernatant and in the fresh

medium were measured. The production or consumption rate of each extracellular metabolite was calculated by the difference between its concentration in the fresh medium and in the supernatant divided by the number of cells in each well and the time interval (one day) over which the medium was exposed to cells. The measured fluxes of metabolites in each culture condition are listed in Appendix J. The range of these experimental measurements defines the flux bounds （$v_{\min} \le v \le v_{\max}$）which cover all eight experiment settings (in Table 5.2).

In order to investigate the role of transport constraints on flux space, the bi-objective Pareto-optimal solutions (Model I) were first determined by finding different combinations of urea production and fatty acid oxidation in cultured hepatocytes without transport constraints. The outline of the feasible range without transport constraints is represented by the line A'B'C'D' (Fig. 5.5), which shows the changes of flux values and directions from one objective to the other. By incorporating the transport constraints (Eqn. 2, 3 and 4) to the bi-objective model (I), the feasible range of flux space is significantly reduced, which is represented by the line ABCD (Fig. 5.5).

Table 5.2: Minimum and maximum values for measured fluxes

	Metabolites	Flux Bounds*	
v_{m1}	Glucose	1.02	2.635
v_{m2}	Lactate	2.108	3.827
v_{m3}	Urea	0.562	10
v_{m4}	Arginine	0.105	0.647
v_{m5}	Ammonia	-1.311	0.025
v_{m6}	Ornithine	-0.556	-0.127
v_{m7}	Alanine	-10	10
v_{m8}	Serine	-10	10
v_{m9}	Cysteine	-0.00813	0.219
v_{m10}	Glycine	0.115	0.585
v_{m11}	Tyrosine	-0.76	0.207
v_{m12}	Glutamate	-1.783	-0.45
v_{m13}	Aspartate	-0.049	0.01
v_{m14}	Acetoacetate	0.116	0.235
v_{m15}	β-hydroxybutyrate	0.119	0.437
v_{m16}	Threonine	-0.887	0.664
v_{m17}	Lysine	-0.684	0.624
v_{m18}	Phenylalanine	-0.404	0.506
v_{m19}	Glutamine	0.23	100
v_{m20}	Proline	-1.843	0.574
v_{m21}	Methionine	-0.202	0.187
v_{m22}	Asparagine	-0.361	0.158
v_{m23}	Valine	-1.092	0.223
v_{m24}	Isoleucine	-0.937	-0.092
v_{m25}	Leucine	-0.8481	-0.003
v_{m26}	Albumin	0.000103	0.001452
v_{m27}	Glycerol	1.958	2.234
v_{m28}	Palmitate	0.796	1.093
v_{m29}	Cholesterol	0.543	2.216
v_{m30}	TG	0.694	0.946

*μmol/million cells/day

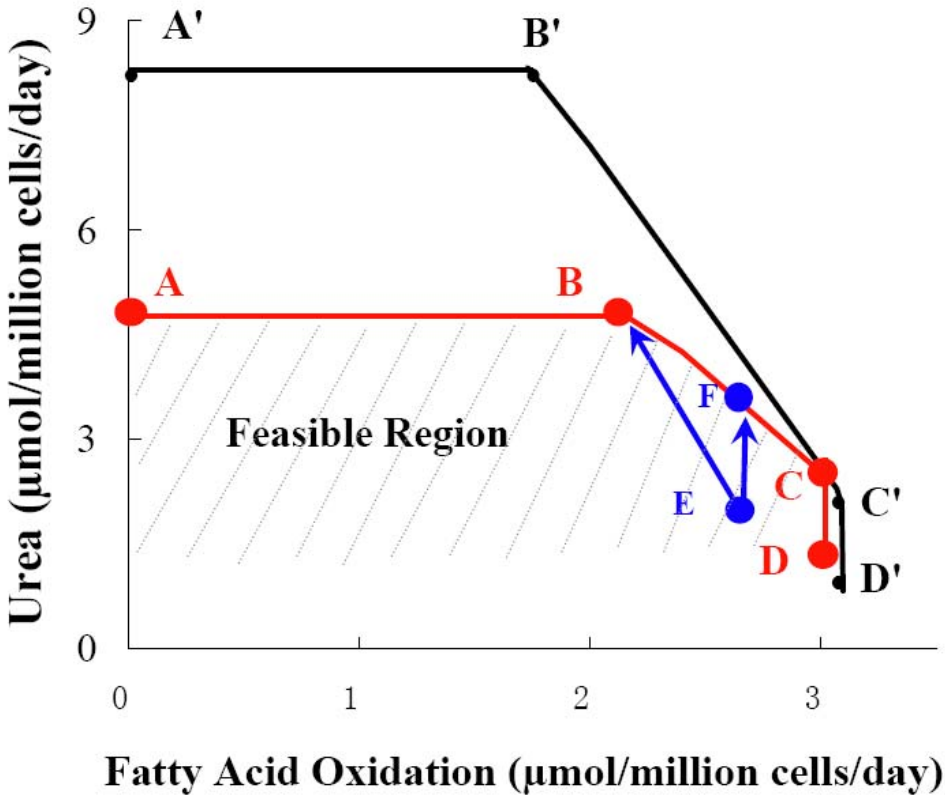

Figure 5.5: Pareto-optimal solution for bi-objective problem in cultured hepatocytes: urea production vs. fatty acid oxidation. No amino acid transport constraints (in black), and with amino acid transport constraints (in red).

5.3.3 Amino Acid Supplementation and Flux Distribution

The additional transport constraints significantly reduce the feasible region of Pareto-optimal solution. By examining the whole feasible region in Figure 5, from point A to B and from point C to D, an increase in urea production has a small effect on the reduction of fatty acid oxidation flux However, the effects are more pronounced between point B and C where an increase in urea production requires a large decrease in fatty acid oxidation. Point E in the feasible region corresponds to the results of the experiment which hepatocytes were cultured with the designed amino acid supplementation. Urea

production and flux of fatty acid oxidation can be further improved towards the boundary of the feasible region (Fig. 5.5, red line).

In this study, parameter ε was chosen as the different value to drive the hepatocyte culture towards higher urea production in the feasible solutions: point B (maximum urea production with highest value of fatty acid oxidation fluxes) and point F (maximum urea production by maintaining the flux of fatty acid oxidation as that of estimation from metabolic objective prediction model in our previous work with designed amino acid supplementation). Urea production, flux fatty acid oxidation and the concentration of alanine, serine and glutamine are calculated from the multi-objective model (II) and listed in Table 5.3, where it is compared with the experimental results with reference and designed amino acid supplementation (the flux distribution for Point F is listed in Appendix K).

Table 5.3: Amino acid supplementation of alanine, serine and glutamine

	Model (II)		*Experiments*	
	Point B	*Point F*	*DAA*	*RAA*
Urea Production*	4.746	3.513	<1.7	<1.2
Fatty Acid Oxidation*	2.167	2.780	2.78	1.74
Alanine (mM)	0.57	0.50	0.46	0.29
Serine (mM)	0.33	0.41	0.36	0.10
Glutamine (mM)	2.67	3.38	6.85	6.85

* flux rate (μmol/million cells/day)

5.4 Discussion

It has been proved that a mixture of amino acid supplementation plays an important role on the improvement of liver-specific functions during plasma exposure (Chan et al. 2003c) (Yang et al. 2009). However, the observed flux of urea production in the *in vitro* experiment was still lower than the predicted urea output from the mathematical modeling, which may be due to transport limitation among the amino acids supplied to plasma.

5.4.1 Transport Competition among Alanine, Serine and Glutamine

Compared with other amino acid supplementation (< 1.5 mM), glutamine is supplied at a very high level to the plasma (6.85 mM) in both reference and designed amino acid supplementation. In the cultured hepatocytes, glutamine is a key amino acid used to produce urea by deamidation of glutamine to glutamate via glutaminase, while glutamine requirements need to be increased for the patients with liver disease (Darmaun 2000). However, in this study, it is found that a high level of glutamine supplementation (>6 mM in the reference and designed amino acid supplementation) is not required due to its transport capacity. It is also found that higher concentration of glutamine inhibits the uptake of alanine and serine (Fig. 5.1) since these three amino acids share transport system A, which catalyzed the Na^+-dependent net uptake of neutral amino acids (Christensen et al. 1965; Joseph et al. 1978). Reduction in flux uptake of alanine and serine is likely to reduce the liver-specific functions of culture hepatocytes (Fig. 5.3 and 5.4). Although hepatic glutamine transport is also mediated by system N which also mediates the uptake of histidine and asparagine, their effects are not considered in this

study since asparagine is supplied in a low level in both reference and designed amino acid supplementation (0.09 mM) and both histidine and glutamine can conversed to glutamate in the hepatic network.

5.4.2 Advantages of Transport Constraints for Flux Balance Analysis

In order to systematically understand the transport limitation among alanine, serine and glutamine, three nonlinear equations are developed to characterize the dependence between their transport fluxes and concentrations supplied in the cultured medium, which are imposed in the flux balance analysis as transport constraints. To our knowledge, this is the first attempt to construct amino acid transport constraints in the field of flux analysis. The traditional constraints used on the flux analysis include mass balances, reaction directionality and inequalities applied from the second law of thermodynamics on the individual reactions (energy balance analysis, EBA) (Beard and Qian 2005) and on the pathways (pathway energy balance constraints, PEB) without concentration information (Nolan et al. 2006) or with incorporation of metabolites' concentrations in our previous work (Chapter 4). Employment of transport constraints provides an additional way to reduce the feasible range of the flux space and to correctly predict the amount of amino acid supplementation in the medium by using nonlinear relationship among the relevant reaction fluxes and metabolites.

Transport constraints are considered within a multi-objective model and it is found that higher level of alanine, lower level of glutamine with similar value of serine (Point B, and point F, compared to the designed amino acid supplementation in our previous work

(Yang et al. 2009) can be used to produce the maximum urea production while maintaining the flux of fatty acid oxidation at a certain value. According to the results, for example, point F, from multi-objective model (II), glutamine supplementation should be reduced to 3.38 mM from 6.85 mM in reference and design amino acid supplementation. Alanine supplementation should be increased to 0.50 mM from 0.29 mM and 0.46 mM, and serine supplementation should be increased to 0.40 mM from 0.10 mM and 0.36 mM in the reference and design amino acid supplementation, respectively. This amino acid supplementation increases urea production to 3.51 μmol/million cells/day compared with the experiment results (Table 5.3) with the same flux of fatty acid oxidation (2.78μmol/million cells/day), and does not inhibit the uptake of alanine and serine (Appendix K).

5.5 Summary

In summary, this work demonstrated that high levels of glutamine inhibit the uptake of alanine and serine and that the resulting transport limitations affect the liver-specific functions. A nonlinear regression model can accurately describe the transport limitations as constraints, which are incorporated into the multi-objective metabolic flux balance model. It was found that the transport constraints connecting the concentration of amino acids, which share the same transport system with their fluxes, can be used as an additional way to reduce the feasible space. Moreover, the transport constraints can be used to re-evaluate the profile of amino acid supplementation during plasma exposure and understand the interaction between different amino acids. The main contribution of this work is the systematic analysis of the effects of amino acid transport on liver

metabolism since liver plays an important role in regulation of amino acids (Burghardt et al. 1996)

Chapter 6

CONCLUSIONS AND FUTURE WORK

6.1 Conclusions

The central theme of this thesis is the development of *in vitro* experiment and mathematical modeling to design and analyze amino acid supplementation effects on cultured hepatocytes during plasma exposure, and thus enables the metabolic manipulation of hepatocytes to improve the targeted functionalities of hepatocytes. The key conclusions we draw from this study are (1) a novel rational design approach provides an amino acid supplementation which promotes a metabolically healthy phenotype with higher level of liver-specific functions including urea production and albumin synthesis; (2) the metabolic objectives of hepatocytes are more than one and change with varying amino acid supplementation. In the designed amino acid supplementation, fatty acid oxidation plays an important role to reduce lipid accumulation during plasma exposure; (3) the designed amino acid supplementation enhances the liver-specific function by reducing the lipid accumulation, increasing the albumin synthesis, increasing the fluxes in TCA cycle (that results in further increase of urea production), and increasing the electron transport providing more ATP to the hepatic metabolism; (4) transport limitations exist for the amino acids which use the same transport system when one of them supplied in a higher level in the cultured medium during plasma exposure. Those transport limitations result in reduced utilization of amino acids and should be avoided when providing a novel amino acid supplementation; (5) two types of constraints for the flux analysis, pathway energy balance (PEB) constraints and amino acid transport constraints, have been developed and are proved to significantly

reduce the feasible solution space compared with flux balance analysis (FBA) .

6.2 Future Work

6.2.1 Modulation of metabolic pathways by siRNA Technology

Small interference RNAs (siRNAs) are composed of small double-stranded RNA oligonucleotides with overhanging extremities and a length of 21/22 bases. siRNA enters the RNAi induced silencing complex (RISC) followed by its recognition of the targeted mRNA, which is subsequently degraded. Thus, mRNA translation is halted (Bartlett and Davis 2006; Dykxhoorn et al. 2003). siRNAs are wildly used for silencing of gene expression in living cells due to the high efficiency (Hutvagner and Zamore 2002). siRNA silencing *Fas* protected mice from liver failure and fibrosis in two models of autoimmune hepatitis (Song et al. 2003)

siRNA technology may have substantial impact on hepatic metabolism due to its ability to target a specific entity in the network while leaving other unaffected. siRNA can be used to diminish or eliminate the activity of the desired enzyme relative to a particular reaction which is competitive with liver-specific functions. Another basic application of siRNA is to identify the alternative flux distribution from mixed-integer linear programming (MILP). This can be achieved by using siRNA to break down a pathway by inhibiting one enzyme involved in the pathway to determine whether alternative pathway can be utilized in the hepatic metabolism, or whether the computed multiple flux distributions are an artifact of the modeling approach used due to the flux bounds considered.

6.2.2 Drug-drug Metabolic Interaction

Acetaminophen (APAP) is a common over-the-counter (OTC) medication which is used to relief the pain and fever. It is safe when it is provided at therapeutic doses. However, APAP overdose can cause acute liver failure (ALF). Patients with hepatic impairment using extracorporeal bioartificial liver (BAL) devices and patients which are chronic alcoholics may increase this risk. In the future, the mathematic model generated in this study can be used to analyze the interactions of acetaminophen and ethanol metabolism with the central hepatic metabolism. The mathematical modeling tandem with *in vitro* experiments is used to identify the non-toxic APAP pathway and hepatotoxicity pathway induced by ethanol (Yang and Beard 2006) or possibly by plasma exposure, a clinical application for BAL devices. The results can be used to further administer the therapeutic APAP doses and amino acid supplementation for this special group of patients with chronic alcohol use.

APPENDIX A: Hepatic metabolic network used for Chapter 3

No. and Enzyme	*Stoichiometry*
1 Glucose-6-Pase	Glucose-6-P + H_2O → Glucose + P_i
2 Phosphoglucose isomerase	Fructose-6-P ←→ Glucose-6-P
3 Fructose-1,6-P_2ase-1	Fructose-1,6-P_2 + H_2O → Fructose-6-P + P_i
4 Two Steps	2-glyceraldehyde-3-P ←→ Fructose-1,6-P_2
5 Four Steps	Phosphoenolpyruvate + NADH + H^+ + ATP + H_2O ←→ Glyceraldehyde-3-P + P_i + NAD^+ + ADP
6 PEPCK	Oxaloacetate + GTP → Phosphoenolpyruvate + GDP + CO_2
7 Pyruvate carboxylase	Pyruvate + CO_2 + ATP + H_2O → Oxaloacetate + ADP + P_i +2 H^+
8 Lactate dehydrogenase	Lactate + NAD^+ ←→ Pyruvate + NADH + H^+
9 Citrate synthase	Oxaloacetate + Acetyl-CoA + H_2O → Citrate + CoA + H^+
10 Isocitrate dehydrogenase	Citrate + NAD^+ ←→ α-ketoglutarate + CO_2 + NADH
11 α-ketoglutarate dehydrogenase	NAD^+ + α-ketoglutarate + CoA→ Succinyl-CoA + CO_2 + NADH + H^+
12 Succinyl-CoA synthetase, succinate dehydrogenase	Succinyl-CoA + P_i + GDH + FAD←→ Fumarate + GTP + $FADH_2$ + CoA
13 Fumarase	Fumarate + H_2O ←→ Malate
14 Malate dehydrogenase	Malate + NAD^+ ←→ Oxaloacetate + NADH + H^+
15 Arginase	Arginine + H_2O → Urea + Ornithine
16 Carbamoyl-P-synthetase I, ornithine transcabamylase	Ornithine + CO_2 + NH_4^+ + 2ATP + H_2O ←→ Citrulline + 2ADP + 2P_i + 3H^+
17 Argininosuccinase, Argininosuccinate synthetase	Citrulline + Aspartate + ATP → Arginine + Fumarate + AMP + PP_i
18	Arginine Uptake
19	NH_4^+ Uptake
20	Ornithine Secretion
21 Alanine aminotransferase	Alanine + 0.5 NAD^+ + 0.05 $NADP^+$ + H_2O → Pyruvate + NH_4^+ + 0.5 NADH + 0.5 NADH + H^+
22	Alanine Uptake
23	Serine → NH_4^+ + Pyruvate
24	Serine Uptake
25 3-mercaptopyruvate sulfurtransferase, transminase	Cysteine + 0.5 NAD^+ + 0.5 $NADP^+$ + H_2O + SO_3^{2-} ←→ Pyruvate + Thiosulfate + NH_4^+ + 0.5 NADH + 0.5 NADPH + H^+
26	Cysteine Uptake

No. and Enzyme	*Stoichiometry*
27 Serine hydroxymethyl transferase	Threonine + NAD^+ → Glycine + Acetyl-CoA + NADH
28 Glycine DH, Aminomethytransferase, dihydrolipoyl DH	Glycine + NAD^+ + H_4folate ←→ Serine + N^5,N^{10}-CH_2-H_4folate + NADH + NH_4^+
29	Glycine Uptake
30 Nine Steps	Tryptophan + $3H_2O$ + $3O_2$ + CoA + $3NAD^+$ + FAD → $3CO_2$ + $FADH_2$ + 3NADH + $4H^+$ + NH_4^+ + Acetoacetyl-CoA
31 Three Steps	Propionyl-CoA + ATP + CO_2 → Succinyl-CoA + AMP + PP_i
32 Eight Steps	Lysine + $3H_2O$ + $5NAD^+$ + FAD + CoA → $2NH_4^+$ +$5H^+$ + 5NADH + $2CO_2$ + $FADH_2$ + Acetoacetyl-CoA
33 Phenylalanine hydroxylase	Phenylalanine + H_4biopterin + O_2 → H_2biopterin + Tyrosine + H_2O
34 Five steps	Tyrosine + $0.5NAD^+$ +0.5NADP + H_2O + $2O_2$ → NH_4^+ + $0.5NADH^+$ + 0.5NADPH + H^+ + CO_2 + Fumarate + Acetoacetate
35	Tyrosine Uptake
36 Glutamate dehydrogenase I	Glutamate + $0.5NAD^+$ + $0.5NADP^+$ + H_2O ←→ NH_4^+ + α-ketoglutarate + 0.5NADP + 0.5NADPH + H^+
37	Glutamate Uptake
38 Glutaminase	Glutamine + H_2O → Glutamate + NH_4^+
39 Two steps	Ornithine + NAD^+ + $NADP^+$ + H_2O → Glutamate + NH_4^+ + NADH + NADPH + H^+
40 Three steps	Proline + $0.5O_2$ + $0.5NAD^+$ +$0.5NADP^+$ → Glutamate + 0.5NADH + 0.5NADPH + H^+
41 Four steps	Histidine + H_4folate + $2H_2O$ → NH_4^+ + N5-formiminoH_4folate + Glutamate
42 Five steps	Methionine + ATP + Serine + NAD^+ + CoA → PP_i + P_i + Adenosine + Cysteine + NADH + CO_2 + NH_4^+ + Propionyl-CoA
43 Aspartate aminotransferase	Aspartate + $0.5NAD^+$ + $0.5NADP^+$ + H_2O ←→ Oxaloacetate + NH_4^+ + 0.5NADH + 0.5NADPH + H^+
44	Aspartate Uptake
45 Asparaginase	Asparagine + H_2O → Aspartate + NH_4^+
46 Fatty acid oxidation	Palmitate + ATP + 7FAD + $7NAD^+$ → 8acetyl-CoA + $7FADH_2$ + 7NADH + AMP + PP_i

No. and Enzyme	*Stoichiometry*
47 Thiolase	2Acetyl-CoA ←→ Acetoacetyl-CoA + CoA
48 Two steps	Acetoacetyl-CoA + H_2O → Acetoacetate + CoA
49	Acetoacetate Production
50 β-Hydroxyburate dehydrogenase	Acetoacetate + NADH + H^+ ←→ β-OH-butyrate + NAD^+
51 ECT	NADH + H^+ + $0.5O_2$ + 3ADP → NAD+ H_2O + 3ATP
52 ECT	$FADH_2$ + $0.5O_2$ + 2ADP → FAD + H_2O + 2ATP
53	O_2 Uptake
54 Glucose-6-P dehydrogenase	Glucose-6-P + $12NADP^+$ + $7H_2O$ → $6CO_2$ + 12NADPH + $12H^+$ + P_i
55 Seven steps	Valine + $0.5NADP^+$ + CoA + $2H_2O$ + $3.5NAD^+$ + FAD → NH_4^+ + 0.5NADPH + $3H^+$ +3.5NADH + $FADH_2$ + $2CO_2$ + Propionyl-CoA
56 Six steps	Isoleucine + $0.5NADP^+$ + $2H_2O$ + $2.5NAD^+$ + FAD + 2CoA → NH_4^+ + 0.5NADPH + $3H^+$ + 2.5NADH +$FADH_2$ + CO_2 + Propionyl-CoA + Acetyl-CoA
57 Six steps	Leucine + $0.5NADP^+$ + H_2O + $1.5NAD^+$ + FAD + ATP + CoA → NH_4^+ + 1.5NADH + 0.5NADPH + $2H^+$ + $FADH_2$ + ADP + P_i + Acetoacetate + Acetyl-CoA
58	Threonine Uptake
59	Lysine Uptake
60	Phenylalanine Uptake
61	Glutamine Uptake
62	Proline Uptake
63	Histidine Uptake
64	Methionine Uptake
65	Asparagine Uptake
66	Valine Uptake
67	Isoleucine Uptake
68	Leucine Uptake
69	24ARG + 32ASP + 61ALA + 24SER + 35CYS + 57GLU + 17GLY + 21TRY + 33THR + 53LYS + 26PHE + 25GLN + 30PRO + 15HIS + 6MET + 20ASN + TRP + 35VAL + 13ISO + 56LEU + 2332ATP → Albumin + 2332ADP + 2332 P_i

No. and Enzyme	*Stoichiometry*
70 lipoprotein and hepatic lipase	$TG + 3H_2O \rightarrow Glycerol + 3Palmitate + 3H^+$
71	Glycerol Uptake
72	Palmitate Uptake
73 Three steps	$Glucose\text{-}6\text{-}P + UTP + H_2O \rightarrow Glycogen + 2P_i + UDP$
74 Glycerol-3-P-dehydrogenase	$Glycerol + NAD^+ \leftrightarrow Glyceraldehyde\text{-}3\text{-}P + NADH + H^+$
75 Cholesterol esterase	$Cholesterol\ ester + H_2O \rightarrow Cholesterol + Palmitate$
76	Tryptophan Uptake

Note: For reversible reactions, the symbol $\leftrightarrow$ is used between the reactants and products. For the irreversible reactions, single headed arrow $\rightarrow$ is used.

APPENDIX B: Flux bounds (minimum and maximum values of fluxes for measured fluxes which cover all four experiment setting and unknown fluxed based on reaction reversibility)

#	***Bounds***	
	v_{min}	v_{max}
1	0.00	1.08
2	-100	100
3	0	100
4	-100	100
5	-100	100
6	0	100
7	0	100
8	-0.19	2.17
9	0	100
10	-100	100
11	0	100
12	-100	100
13	-100	100
14	-100	100
15	0	100
16	-100	100
17	0	100
18	0.01	0.33
19	-0.03	0.42
20	0.03	0.23
21	0	100
22	-0.03	0.26
23	0	100
24	-0.29	-0.07
25	-100	100
26	-0.03	0.03
27	0	100
28	-100	100
29	0.06	0.45

#	Bounds	
	v_{min}	v_{max}
30	0	100
31	0	100
32	0	100
33	0	100
34	0	100
35	-0.15	0.14
36	-100	100
37	-0.53	-0.12
38	0	100
39	0	100
40	0	100
41	0	100
42	0	100
43	-100	100
44	0.00	0.00
45	0	100
46	0	100
47	-100	100
48	0	100
49	0.05	0.54
50	0.04	0.31
51	0	100
52	0	100
53	21.89	41.37
54	0.00	0.13
55	0	100
56	0	100
57	0	100
58	-0.38	0.19
59	-0.34	0.25
60	-0.02	0.20
61	-0.09	2.54

#	Bounds	
	v_{min}	v_{max}
62	0	0.14
63	-0.32	0.16
64	0.01	0.14
65	-0.04	0.02
66	-0.46	0.14
67	-0.28	0.10
68	-0.27	0.16
69	0.000048	0.0004
70	0	0.46
71	-0.07	1.28
72	-0.31	0.41
73	0	100
74	-100	100
75	0	0.94
76	-100	100

Note: All flux values are in μmol/million cells/day. A design constraint (-100, 100) indicates lower or upper bound for reversible unknown fluxes.

APPENDIX C: Flux distribution calculated by mixed-integer linear programming III.

#	*Flux Distribution from Model III*							
	D1	***D2***	***D3***	***D4***	***D5***	***D6***	***D7***	***D8***
1	0.00	1.08	1.08	0.00	0.00	1.08	1.08	0.00
2	2.17	2.17	2.17	2.17	3.35	3.35	3.35	3.35
3	2.17	2.17	2.17	2.17	3.35	3.35	3.35	3.35
4	2.17	2.17	2.17	2.17	3.35	3.35	3.35	3.35
5	4.41	4.41	4.41	4.41	6.77	6.77	6.77	6.77
6	4.41	4.41	4.41	4.41	6.77	6.77	6.77	6.77
7	0.66	0.66	0.66	0.66	3.02	3.02	3.02	3.02
8	-0.19	-0.19	-0.19	-0.19	2.17	2.17	2.17	2.17
9	7.50	7.50	7.50	7.50	7.50	7.50	7.50	7.50
10	7.50	7.50	7.50	7.50	7.50	7.50	7.50	7.50
11	10.52	10.52	10.52	10.52	10.52	10.52	10.52	10.52
12	10.89	10.89	10.89	10.89	10.89	10.89	10.89	10.89
13	17.71	17.71	17.71	17.71	17.71	17.71	17.71	17.71
14	17.71	17.71	17.71	17.71	17.71	17.71	17.71	17.71
15	6.81	6.81	6.81	6.81	6.81	6.81	6.81	6.81
16	6.48	6.48	6.48	6.48	6.48	6.48	6.48	6.48
17	6.48	6.48	6.48	6.48	6.48	6.48	6.48	6.48
18	0.33	0.33	0.33	0.33	0.33	0.33	0.33	0.33
19	0.42	0.42	0.42	0.42	0.42	0.42	0.42	0.42
20	0.03	0.03	0.03	0.03	0.03	0.03	0.03	0.03
21	0.26	0.26	0.26	0.26	0.26	0.26	0.26	0.26
22	0.26	0.26	0.26	0.26	0.26	0.26	0.26	0.26
23	0.43	0.43	0.43	0.43	0.43	0.43	0.43	0.43
24	-0.07	-0.07	-0.07	-0.07	-0.07	-0.07	-0.07	-0.07
25	0.17	0.17	0.17	0.17	0.17	0.17	0.17	0.17
26	0.03	0.03	0.03	0.03	0.03	0.03	0.03	0.03
27	0.19	0.19	0.19	0.19	0.19	0.19	0.19	0.19
28	0.64	0.64	0.64	0.64	0.64	0.64	0.64	0.64
29	0.45	0.45	0.45	0.45	0.45	0.45	0.45	0.45
30	3.64	3.64	3.64	3.64	3.64	3.64	3.64	3.64
31	0.38	0.38	0.38	0.38	0.38	0.38	0.38	0.38

#	*Flux Distribution from Model III*							
	D1	***D2***	***D3***	***D4***	***D5***	***D6***	***D7***	***D8***
32	0.25	0.25	0.25	0.25	0.25	0.25	0.25	0.25
33	0.20	0.20	0.20	0.20	0.20	0.20	0.20	0.20
34	0.34	0.34	0.34	0.34	0.34	0.34	0.34	0.34
35	0.14	0.14	0.14	0.14	0.14	0.14	0.14	0.14
36	3.01	3.01	3.01	3.01	3.01	3.01	3.01	3.01
37	-0.12	-0.12	-0.12	-0.12	-0.12	-0.12	-0.12	-0.12
38	2.54	2.54	2.54	2.54	2.54	2.54	2.54	2.54
39	0.30	0.30	0.30	0.30	0.30	0.30	0.30	0.30
40	0.14	0.14	0.14	0.14	0.14	0.14	0.14	0.14
41	0.16	0.16	0.16	0.16	0.16	0.16	0.16	0.16
42	0.14	0.14	0.14	0.14	0.14	0.14	0.14	0.14
43	-6.46	-6.46	-6.46	-6.46	-6.46	-6.46	-6.46	-6.46
44	0.00	0.00	0.00	0.00	0.00	0.00	0.00	0.00
45	0.02	0.02	0.02	0.02	0.02	0.02	0.02	0.02
46	0.00	0.00	0.00	0.00	0.00	0.00	0.00	0.00
47	-3.53	-3.53	-3.53	-3.53	-3.53	-3.53	-3.53	-3.53
48	0.36	0.36	0.36	0.36	0.36	0.36	0.36	0.36
49	0.54	0.54	0.54	0.54	0.54	0.54	0.54	0.54
50	0.31	0.31	0.31	0.31	0.31	0.31	0.31	0.31
51	43.86	43.86	43.86	43.86	43.86	43.86	43.86	43.86
52	15.17	15.17	15.17	15.17	15.17	15.17	15.17	15.17
53	41.37	41.37	41.37	41.37	41.37	41.37	41.37	41.37
54	0.07	0.07	0.07	0.07	0.07	0.07	0.07	0.07
55	0.14	0.14	0.14	0.14	0.14	0.14	0.14	0.14
56	0.10	0.10	0.10	0.10	0.10	0.10	0.10	0.10
57	0.16	0.16	0.16	0.16	0.16	0.16	0.16	0.16
58	0.19	0.19	0.19	0.19	0.19	0.19	0.19	0.19
59	0.25	0.25	0.25	0.25	0.25	0.25	0.25	0.25
60	0.20	0.20	0.20	0.20	0.20	0.20	0.20	0.20
61	2.54	2.54	2.54	2.54	2.54	2.54	2.54	2.54
62	0.14	0.14	0.14	0.14	0.14	0.14	0.14	0.14
63	0.16	0.16	0.16	0.16	0.16	0.16	0.16	0.16
64	0.14	0.14	0.14	0.14	0.14	0.14	0.14	0.14

#	*Flux Distribution from Model III*							
	D1	***D2***	***D3***	***D4***	***D5***	***D6***	***D7***	***D8***
65	0.02	0.02	0.02	0.02	0.02	0.02	0.02	0.02
66	0.14	0.14	0.14	0.14	0.14	0.14	0.14	0.14
67	0.10	0.10	0.10	0.10	0.10	0.10	0.10	0.10
68	0.16	0.16	0.16	0.16	0.16	0.16	0.16	0.16
69	<0.01[a]	<0.01[a]	<0.01[a]	<0.01[a]	<0.01[a]	<0.01[a]	<0.01[a]	<0.01[a]
70	0.00	0.00	0.00	0.00	0.00	0.00	0.00	0.00
71	-0.07	7.50	7.50	7.50	7.50	7.50	7.50	7.50
72	0.00	-0.31	0.00	-0.31	0.00	0.00	-0.31	-0.31
73	2.10	1.02	1.02	2.10	3.28	2.20	2.20	3.28
74	-0.07	-0.07	-0.07	-0.07	-0.07	-0.07	-0.07	-0.07
75	0.00	0.31	0.00	0.31	0.00	0.00	0.31	0.31
76	3.64	3.64	3.64	3.64	3.64	3.64	3.64	3.64

Note: All flux values are in μmol/million cells/day.

[a] Exact value is 0.000048

APPENDIX D: Concentration of amino acid in different culture medium [a]

	NAA	***RAA***	***DAA***
L-arginine	0.08	0.42	0.56
L-alanine	0.10	0.29	0.46
L-serine	0.09	0.10	0.36
L-threonine	0.12	0.79	1.18
L-valine	0.16	0.87	1.49
L-isoleucine	0.06	0.78	0.89
L-leucine	0.10	0.83	1.02
L-histidine	0.15	0.35	0.44
L-glycine	0.16	0.17	0.41
L-lysine	0.11	0.75	0.79
L-proline	0.17	0.18	0.22
L-tyrosine	0.05	0.40	0.72
L-glutamate	0.09	0.11	0.11
L-aspartate	0.01	0.01	0.01
L-cysteine	0.01	0.13	0.13
L-phenylalanine	0.04	0.42	0.42
L-glutamine	0.65	6.85	6.85
L-methionine	0.02	0.20	0.20
L-asparagine	0.09	0.09	0.09

[a] Values shown represent final concentration of amino acid supplementation during plasma exposure in the experimental design. NAA=no amino acid supplementation; RAA=”reference” amino acid supplementation; DAA=”designed” amino acid supplementation.

APPENDIX E: Hepatic metabolic network used for Chapter 4 and 5

No. and Enzyme	*Stoichiometry*
	Measurement Fluxes
v_{m1} Gluocose-6-pase	Glucose-6-P + H_2O → Glucose + P_i
v'_{m1} Hexokinase	Glucose + P_i → Glucose-6-P + H_2O
v_{m2} Lactate dehydrogenase	Lactate + NAD^+ ←→ Pyruvate + NADH + H^+
v_{m3} Arginase	Arginine + H_2O → Urea + Ornithine
v_{m4}	Arginine Uptake
v_{m5}	NH_4^+ Uptake
v_{m6}	Ornithine Secretion
v_{m7}	Alanine Uptake
v_{m8}	Serine Uptake
v_{m9}	Cysteine Uptake
v_{m10}	Glycine Uptake
v_{m11}	Tyrosine Uptake
v_{m12}	Glutamate Uptake
v_{m13}	Aspartate Uptake
v_{m14}	Acetoacetate Production
v_{m15}	Acetoacetate + NADH + H^+ ←→ β-OH-butyrate + NAD^+
v_{m16}	Threonine Uptake
v_{m17}	Lysine Uptake
v_{m18}	Phenylalanine Uptake
v_{m19}	Glutamine Uptake
v_{m20}	Proline Uptake
v_{m21}	Methionine Uptake
v_{m22}	Asparagine Uptake
v_{m23}	Valine Uptake
v_{m24}	Isoleucine Uptake
v_{m25}	Leucine Uptake
v_{m26}	Albumin Synthesis
v_{m27}	Glycerol Uptake
v_{m28}	Palmitate Uptake
v_{m29} Cholesterol esterase	Cholesterol ester + H_2O → Cholesterol + Palmitate
v_{m30}	TG Uptake

No. and Enzyme	*Stoichiometry*
	Unknown Fluxes
v_{u1} Phosphoglucose isomerase	Fructose-6-P ←→ Glucose-6-P
v'_{u1} Phosphoglucose isomerase	Glucose-6-P ←→ Fructose-6-P
v_{u2} Fructose-1,6-P_2ase-1	Fructose-1,6-P_2 + H_2O → Fructose-6-P + P_i
v'_{u2} PFK-1	Fructose-6-P + P_i → Fructose-1,6-P_2 + H_2O
v_{u3} Two Steps	2 Glyceraldehyde-3-P ←→ Fructose-1,6-P_2
v'_{u3} Two Steps	Fructose-1,6-P_2 ←→ 2 Glyceraldehyde-3-P
v_{u4} Four Steps	Phosphoenolpyruvate + NADH + H^+ + ATP + H_2O ←→ Glyceraldehyde-3-P + P_i + NAD^+ + ADP
v'_{u4} Four Steps	Glyceraldehyde-3-P + P_i + NAD^+ + ADP ←→ Phosphoenolpyruvate + NADH + H^+ + ATP + H_2O
v_{u5} PEPCK	Oxaloacetate + GTP → Phosphoenolpyruvate + GDP + CO_2
v'_{u5} Pyruvate kinase	Phosphoenolpyruvate + ADP → pyruvate + ATP
v_{u6} Pyruvate carboxylase	Pyruvate + CO_2 + ATP + H_2O → Oxaloacetate + ADP + P_i +2 H^+
v'_{u6} PDH	Pyruvate + CoA + NAD^+ → Acetyl-CoA + CO_2 + NADH
v_{u7} Citrate synthase	Oxaloacetate + Acetyl-CoA + H_2O → Citrate + CoA + H^+
v_{u8} Isocitrate dehydrogenase	Citrate + NAD^+ ←→ α-ketoglutarate + CO_2 + NADH
v_{u9} α-ketoglutarate dehydrogenas	NAD^+ + α-ketoglutarate + CoA→ Succinyl-CoA + CO_2 + NADH + H^+
v_{u10} Succinyl-CoA synthetase, succinate dehydrogenase	Succinyl-CoA + P_i + GDP + FAD ←→ Fumarate + GTP + $FADH_2$ + CoA
v_{u11} Fumarase	Fumarate + H_2O ←→ Malate
v_{u12} Malate dehydrogenase	Malate + NAD^+ ←→ Oxaloacetate + NADH + H^+
v_{u13} Carbamoyl-P-synthetase I, ornithine transcabamylase	Ornithine + CO_2 + NH_4^+ + 2ATP + H_2O ←→ Citrulline + 2ADP + 2P_i + 3H^+
v_{u14} Argininosuccinase, Argininosuccinate synthetase	Citrulline + Aspartate + ATP → Arginine + Fumarate + AMP + PP_i
v_{u15} Alanine aminotransferase	Alanine + 0.5 NAD^+ + 0.5 $NADP^+$ + H_2O → Pyruvate + NH_4^+ + 0.5 NADPH + 0.5 NADH + H^+
v_{u16}	Serine → NH_4^+ + Pyruvate
v_{u17} 3-mercaptopyruvate sulfurtransferase, transminase	Cysteine + 0.5 NAD^+ + 0.5 $NADP^+$ + H_2O + SO_3^{2-} ←→ Pyruvate + Thiosulfate + NH_4^+ + 0.5 NADH + 0.5 NADPH + H^+
v_{u18} Serine hydroxymethyl transferase	Threonine + NAD^+ → Glycine + Acetyl-CoA + NADH
v_{u19} Glycine DH, Aminomethytransferase, dihydrolipoyl DH	Glycine + NAD^+ + H_4folate ←→ Serine + N^5,N^{10}-CH_2-H_4folate + NADH + NH_4^+
v_{u20} Nine Steps	Tryptophan + 3H_2O + 3O_2 + CoA + 3NAD^+ + FAD → 3CO_2 + $FADH_2$ + 3NADH + 4H^+ + NH_4^+ + Acetoacetyl-CoA
v_{u21} Three Steps	Propionyl-CoA + ATP + CO_2 → Succinyl-CoA + AMP + PP_i

No. and Enzyme	*Stoichiometry*
	Unknown Fluxes
v_{u22} Eight Steps	Lysine + $3H_2O$ + $5NAD^+$ + FAD + CoA → $2NH_4^+$ +$5H^+$ + 5NADH + $2CO_2$ + $FADH_2$ + Acetoacetyl-CoA
v_{u23} Phenylalanine hydroxylase	Phenylalanine + H_4biopterin + O_2 → H_2biopterin + Tyrosine + H_2O
v_{u24} Five steps	Tyrosine + $0.5NAD^+$ +$0.5NADP^+$ + H_2O + $2O_2$ → NH_4^+ + 0.5NADH + 0.5NADPH + H^+ + CO_2 + Fumarate + Acetoacetate
v_{u25} Glutamate dehydrogenase I	Glutamate + $0.5NAD^+$ + $0.5NADP^+$ + H_2O ←→ NH_4^+ + α-ketoglutarate + 0.5NADP + 0.5NADPH + H^+
v_{u26} Glutaminase	Glutamine + H_2O → Glutamate + NH_4^+
v_{u27} Two steps	Ornithine + NAD^+ + $NADP^+$ + H_2O → Glutamate + NH_4^+ + NADH + NADPH + H^+
v_{u28} Three steps	Proline + 0.5 O_2 + $0.5NAD^+$ +$0.5NADP^+$ → Glutamate + 0.5NADH + 0.5NADPH + H^+
v_{u29} Four steps	Histidine + H_4folate + $2H_2O$ → NH_4^+ + N^5-formiminoH_4folate + Glutamate
v_{u30} Five steps	Methionine + ATP + Serine + NAD^+ + CoA → PP_i + P_i + Adenosine + Cysteine + NADH + CO_2 + NH_4^+ + Propionyl-CoA
v_{u31} Aspartate aminotransferase	Aspartate + $0.5NAD^+$ + $0.5NADP^+$ + H_2O ←→ Oxaloacetate + NH_4^+ + 0.5NADH + 0.5NADPH + H^+
v_{u32} Asparaginase	Asparagine + H_2O → Aspartate + NH_4^+
v_{u33} Fatty acid oxidation	Palmitate + ATP + 7FAD + $7NAD^+$ + 8CoA → 8acetyl-CoA + $7FADH_2$ + 7NADH + AMP + PP_i
v_{u34} Thiolase	2Acetyl-CoA ←→ Acetoacetyl-CoA + CoA
v_{u35} Two steps	Acetoacetyl-CoA + H_2O → Acetoacetate + CoA
v_{u36} ECT	NADH + H^+ + $0.5O_2$ + 3ADP → NAD^+ + H_2O + 3ATP
v_{u37} ECT	$FADH_2$ + $0.5O_2$ + 2ADP → FAD + H_2O + 2ATP
v_{u38} Glucose-6-P dehydrogenase	Glucose-6-P + $12NADP^+$ + $7H_2O$ → $6CO_2$ + 12NADPH + $12H^+$ + P_i
v_{u39} Seven steps	Valine + $0.5NADP^+$ + CoA + $2H_2O$ + $3.5NAD^+$ + FAD → NH_4^+ + 0.5NADPH + $3H^+$ +3.5NADH + $FADH_2$ + $2CO_2$ + Propionyl-CoA
v_{u40} Six steps	Isoleucine + $0.5NADP^+$ + $2H_2O$ + $2.5NAD^+$ + FAD + 2CoA → NH_4^+ + 0.5NADPH + $3H^+$ + 2.5NADH +$FADH_2$ + CO_2 + Propionyl-CoA + Acetyl-CoA
v_{u41} Six steps	Leucine + $0.5NADP^+$ + H_2O + $1.5NAD^+$ + FAD + ATP + CoA → NH_4^+ + 1.5NADH + 0.5NADPH + $2H^+$ + $FADH_2$ + ADP + P_i + Acetoacetate + Acetyl-CoA
v_{u42} lipoprotein and hepatic lipase	TG + $3H_2O$ → Glycerol + 3Palmitate + $3H^+$
v_{u43} Three steps	Glucose-6-P + UTP + H_2O → Glycogen + $2P_i$ + UDP
v_{u44} Glycerol-3-P-dehydrogenase	Glycerol + NAD^+ ←→ Glyceraldehyde-3-P + NADH + H^+
v_{u45}	TG store
v_{u46}	O_2 Uptake
v_{u47}	Histidine Uptake
v_{u48}	Tryptophan Uptake

APPENDIX F: Small example of pathway energy balance (PEB) constraints

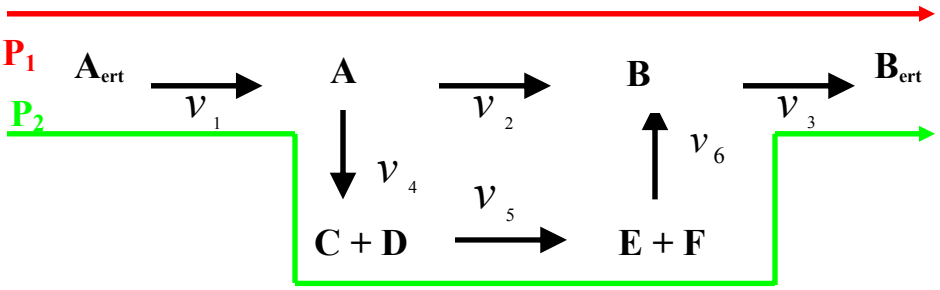

Figure F-1: A small network with 6 reactions (4 intracellular reactions and two transport reactions), and 6 metabolites (A, B, C, E are internal metabolites, and D, F are external metabolites).

Two elementary modes are identified which are determined by implementing this network in Matlab surface software *Fluxanalyzer* (Klamt et al. 2003): one includes reaction 1, 2 and 3, and another involves reaction 1,4,5,6 and reaction 3, described by matrix

$$E = \begin{bmatrix} 1 & 1 & 1 & 0 & 0 & 0 \\ 1 & 0 & 1 & 1 & 1 & 1 \end{bmatrix} \tag{F-1}$$

The Gibbs free energy and flux of each reaction is listed in Table F-1.

Table F-1: Free Gibbs energy of each reaction

	Standard Gibbs	***Real Gibbs (Min)***	***Real Gibbs (Max)***	***Flux***
R1	ΔG_1^0	$RT\ln\frac{[A]_{\min}}{[A]_{ert}}$	$RT\ln\frac{[A]_{\max}}{[A]_{ert}}$	v_1
R2	ΔG_2^0	$\Delta G_2^0 + RT\ln\frac{[B]_{\min}}{[A]_{\max}}$	$\Delta G_2^0 + RT\ln\frac{[B]_{\max}}{[A]_{\min}}$	v_2
R3	ΔG_3^0	$RT\ln\frac{[B]_{ert}}{[B]_{\max}}$	$RT\ln\frac{[B]_{ert}}{[B]_{\min}}$	v_3
R4	ΔG_4^0	$\Delta G_4^0 + RT\ln\frac{[C]_{\min}[D]_{\min}}{[A]_{\max}}$	$\Delta G_4^0 + RT\ln\frac{[C]_{\max}[D]_{\max}}{[A]_{\min}}$	v_4
R5	ΔG_5^0	$\Delta G_5^0 + RT\ln\frac{[E]_{\min}[F]_{\min}}{[C]_{\max}[D]_{\max}}$	$\Delta G_5^0 + RT\ln\frac{[E]_{\max}[F]_{\max}}{[C]_{\min}[D]_{\min}}$	v_5
R6	ΔG_6^0	$\Delta G_6^0 + RT\ln\frac{[B]_{\min}}{[E]_{\max}[F]_{\max}}$	$\Delta G_6^0 + RT\ln\frac{[B]_{\max}}{[E]_{\min}[F]_{\min}}$	v_6

Then the Gibbs free energy of the pathway is calculated by element-by-element multiplication of the Gibbs Free energy of each reaction with the matrix of elementary modes as follows:

$$\Delta G_p^0 = \begin{bmatrix} \Delta G_1^0 & \Delta G_2^0 & \Delta G_3^0 & 0 & 0 & 0 \\ \Delta G_1^0 & 0 & \Delta G_3^0 & \Delta G_4^0 & \Delta G_5^0 & \Delta G_6^0 \end{bmatrix} \tag{F-2}$$

$$\Delta G_p^{\min} = \begin{bmatrix} \Delta G_1^0 + RT\ln\frac{[A]_{min}}{[A]_{ert}} & \Delta G_2^0 + RT\ln\frac{[B]_{min}}{[A]_{max}} & \Delta G_3^0 + RT\ln\frac{[B]_{ert}}{[B]_{max}} & 0 & 0 & 0 \\ \Delta G_1^0 + RT\ln\frac{[A]_{min}}{[A]_{ert}} & 0 & \Delta G_3^0 + RT\ln\frac{[B]_{ert}}{[B]_{max}} & \Delta G_4^0 + RT\ln\frac{[C]_{min}[D]_{min}}{[A]_{max}} & \Delta G_5^0 + RT\ln\frac{[E]_{min}[F]_{min}}{[C]_{max}[D]_{max}} & \Delta G_6^0 + RT\ln\frac{[B]_{min}}{[E]_{max}[F]_{max}} \end{bmatrix}$$

(F-3)

$$\Delta G_p^{\max} = \begin{bmatrix} \Delta G_1^0 + RT\ln\frac{[A]_{\max}}{[A]_{ert}} & \Delta G_2^0 + RT\ln\frac{[B]_{\max}}{[A]_{\min}} & \Delta G_3^0 + RT\ln\frac{[B]_{ert}}{[B]_{\min}} & 0 & 0 & 0 \\ \Delta G_1^0 + RT\ln\frac{[A]_{\max}}{[A]_{ert}} & 0 & \Delta G_3^0 + RT\ln\frac{[B]_{ert}}{[B]_{\max}} & \Delta G_4^0 + RT\ln\frac{[C]_{\max}[D]_{\max}}{[A]_{\min}} & \Delta G_4^0 + RT\ln\frac{[C]_{\max}[D]_{\max}}{[A]_{\min}} & \Delta G_6^0 + RT\ln\frac{[B]_{\max}}{[E]_{\min}[F]_{\min}} \end{bmatrix}$$

(F-4)

Given the matrix of the weighted energies of the pathways and the flux vector, two pathway energy balance constraints with standard Gibbs free energy can be considered as

follows:

$$PEB_1^0 = \Delta G_1^0 \cdot v_1 + \Delta G_2^0 \cdot v_2 + \Delta G_3^0 \cdot v_3 < 0 \quad \text{(F-5a)}$$

$$PEB_2^0 = \Delta G_1^0 \cdot v_1 + \Delta G_3^0 \cdot v_3 + \Delta G_4^0 \cdot v_4 + \Delta G_5^0 \cdot v_5 + \Delta G_6^0 \cdot v_6 < 0 \quad \text{(F-5b)}$$

Given the matrix of the weighted energies of the pathways and the flux vector, two pathway energy balance constraints with minimum Gibbs free energy can be considered as follows:

$$\mathrm{PEB}_1^{\min} = (\Delta \mathrm{G}_1^0 + \mathrm{RTln}\frac{[\mathrm{A}]_{\min}}{[\mathrm{A}]_{\mathrm{ert}}}) \cdot v_1 + (\Delta \mathrm{G}_2^0 + \mathrm{RTln}\frac{[\mathrm{B}]_{\min}}{[\mathrm{A}]_{\max}}) \cdot v_2 + (\Delta \mathrm{G}_3^0 + \mathrm{RTln}\frac{[\mathrm{B}]_{\mathrm{ert}}}{[\mathrm{B}]_{\max}}) \cdot v_3 < 0 \quad \text{(F-6a)}$$

$$\begin{aligned} PEB_2^{\min} &= (\Delta \mathrm{G}_1^0 + \mathrm{RTln}\frac{[\mathrm{A}]_{\min}}{[\mathrm{A}]_{\mathrm{ert}}}) v_1 + (\Delta \mathrm{G}_3^0 + \mathrm{RTln}\frac{[\mathrm{B}]_{\mathrm{ert}}}{[\mathrm{B}]_{\max}}) \cdot v_3 \\ &+ (\Delta \mathrm{G}_4^0 + \mathrm{RTln}\frac{[\mathrm{C}]_{\min}[\mathrm{D}]_{\min}}{[\mathrm{A}]_{\max}}) \cdot v_4 + (\Delta \mathrm{G}_5^0 + \mathrm{RTln}\frac{[\mathrm{E}]_{\min}[\mathrm{F}]_{\min}}{[\mathrm{C}]_{\max}[\mathrm{D}]_{\max}}) \cdot v_5 \\ &+ (\Delta \mathrm{G}_6^0 + \mathrm{RTln}\frac{[\mathrm{B}]_{\min}}{[\mathrm{E}]_{\max}[\mathrm{F}]_{\max}}) \cdot v_6 < 0 \end{aligned} \quad \text{(F-6b)}$$

Given the matrix of the weighted energies of the pathways and the flux vector, two pathway energy balance constraints with maximum Gibbs free energy can be considered as follows:

$$\mathrm{PEB}_1^{\max} = (\Delta \mathrm{G}_1^0 + \mathrm{RTln}\frac{[\mathrm{A}]_{\max}}{[\mathrm{A}]_{\mathrm{ert}}}) \cdot v_1 + (\Delta \mathrm{G}_2^0 + \mathrm{RTln}\frac{[\mathrm{B}]_{\max}}{[\mathrm{A}]_{\min}}) \cdot v_2 + (\Delta \mathrm{G}_3^0 + \mathrm{RTln}\frac{[\mathrm{B}]_{\mathrm{ert}}}{[\mathrm{B}]_{\min}}) \cdot v_3 < 0 \quad \text{(F-7a)}$$

$$\begin{aligned} PEB_2^{\max} &= (\Delta \mathrm{G}_1^0 + \mathrm{RTln}\frac{[\mathrm{A}]_{\max}}{[\mathrm{A}]_{\mathrm{ert}}}) v_1 + (\Delta \mathrm{G}_3^0 + \mathrm{RTln}\frac{[\mathrm{B}]_{\mathrm{ert}}}{[\mathrm{B}]_{\min}}) \cdot v_3 \\ &+ (\Delta \mathrm{G}_4^0 + \mathrm{RTln}\frac{[\mathrm{C}]_{\max}[\mathrm{D}]_{\mathrm{mx}}}{[\mathrm{A}]_{\min}}) \cdot v_4 + (\Delta \mathrm{G}_5^0 + \mathrm{RTln}\frac{[\mathrm{E}]_{\max}[\mathrm{F}]_{\max}}{[\mathrm{C}]_{\min}[\mathrm{D}]_{\min}}) \cdot v_5 \\ &+ (\Delta \mathrm{G}_6^0 + \mathrm{RTln}\frac{[\mathrm{B}]_{\max}}{[\mathrm{E}]_{\min}[\mathrm{F}]_{\min}}) \cdot v_6 < 0 \end{aligned} \quad \text{(F-7b)}$$

APPENDIX G: Comparison of unknown flux ranges predicted by MNFA model

	DAA								RAA								NAA							
	Standard_ΔG		Min_ΔG		Max_ΔG		Without_ΔG		Standard_ΔG		Min_ΔG		Max_ΔG		Without_ΔG		Standard_ΔG		Min_ΔG		Max_ΔG		Without_ΔG	
	min	max	min	max	min	max	min	max	min	max	min	max	min	max	min	max	min	max	min	max	min	max	min	max
1	0.00	0.02	0.00	0.08	0.00	0.01	0.00	1.00	0.00	0.32	0.42	0.67	0.00	0.07	0.00	0.67	0.89	0.89	0.89	0.89	0.89	0.89	0.85	2.63
2	0.00	0.02	0.00	0.08	0.00	0.01	0.00	1.00	0.00	0.32	0.42	0.67	0.00	0.07	0.00	0.67	0.89	0.89	0.89	0.89	0.89	0.89	0.85	2.63
3	0.00	0.02	0.00	0.08	0.00	0.01	0.00	1.00	0.00	0.32	0.42	0.67	0.00	0.07	0.00	0.67	0.89	0.89	0.89	0.89	0.89	0.89	0.85	2.63
4	2.12	2.16	2.20	2.53	2.07	2.12	2.07	4.64	1.98	2.63	2.81	4.06	1.98	2.13	1.98	4.06	0.08	0.08	0.08	0.08	0.08	0.08	0.00	2.38
5	2.12	2.16	2.20	2.53	2.07	2.12	2.07	4.64	1.98	2.63	2.81	4.06	1.98	2.13	1.98	4.06	0.08	0.08	0.08	0.08	0.08	0.08	0.00	2.38
6	4.41	4.45	4.49	4.96	4.36	4.41	4.36	7.84	4.90	5.57	5.69	7.74	4.86	5.02	4.86	7.74	2.42	2.47	2.34	2.79	2.43	2.67	1.68	2.79
7	22.61	22.66	26.09	31.08	22.11	22.61	16.12	32.65	19.35	20.76	20.05	33.02	19.70	20.01	19.20	33.05	16.28	16.38	16.28	22.49	16.28	17.54	7.50	32.93
8	22.61	22.66	26.09	31.08	22.11	22.61	16.12	32.65	19.35	20.76	20.05	33.02	19.70	20.01	19.20	33.05	16.28	16.38	16.28	22.49	16.28	17.54	7.50	32.93
9	24.07	24.12	27.25	32.42	23.47	23.98	17.60	34.13	19.09	20.42	19.81	32.79	19.41	19.71	18.96	32.82	14.08	14.25	14.08	20.12	14.08	15.11	7.49	33.09
10	22.84	22.89	26.19	31.19	22.31	22.83	16.37	32.90	18.90	20.31	19.61	32.58	19.26	19.56	18.76	32.61	13.71	13.88	13.71	19.77	13.71	14.74	7.12	32.72
11	23.61	23.66	27.19	32.29	23.26	23.74	16.94	33.47	19.81	21.29	20.52	33.50	20.19	20.50	19.67	33.53	13.83	14.00	13.83	20.01	13.83	14.90	7.24	32.93
12	23.61	23.66	27.19	32.29	23.26	23.74	16.94	33.47	19.81	21.29	20.52	33.50	20.19	20.50	19.67	33.53	13.83	14.00	13.83	20.01	13.83	14.90	7.24	32.93
13	0.90	0.90	0.90	1.11	0.99	1.07	0.72	1.11	0.56	0.68	0.56	0.68	0.56	0.60	0.56	0.68	0.21	0.23	0.21	0.30	0.21	0.30	0.20	0.30
14	0.90	0.90	0.90	1.11	0.99	1.07	0.72	1.11	0.56	0.68	0.56	0.68	0.56	0.60	0.56	0.68	0.21	0.23	0.21	0.30	0.21	0.30	0.20	0.30
15	-0.13	-0.13	-0.13	-0.12	-0.13	-0.12	-0.13	-0.12	-0.07	-0.06	-0.07	-0.06	-0.07	-0.06	-0.07	-0.06	0.02	0.04	0.02	0.17	0.02	0.13	0.02	0.17
16	-0.50	-0.49	-0.62	-0.40	-0.62	-0.50	-0.62	-0.34	0.12	0.17	0.09	0.17	0.09	0.14	0.09	0.17	-0.29	-0.27	-0.32	-0.27	-0.30	-0.27	-0.32	-0.27
17	-0.03	-0.02	-0.03	0.05	-0.01	0.04	-0.03	0.05	0.04	0.06	0.04	0.06	0.05	0.06	0.04	0.06	-0.07	-0.05	-0.07	-0.04	-0.07	-0.04	-0.07	-0.04
18	-0.46	-0.45	-0.46	-0.37	-0.46	-0.44	-0.46	-0.37	0.22	0.25	0.20	0.25	0.20	0.25	0.20	0.25	-0.05	-0.04	-0.06	-0.04	-0.06	-0.04	-0.06	-0.04
19	0.08	0.09	0.08	0.19	0.08	0.10	0.08	0.19	0.48	0.51	0.45	0.51	0.45	0.50	0.45	0.51	0.02	0.03	0.00	0.03	0.01	0.03	0.00	0.03
20	2.35	2.38	2.64	3.20	2.75	2.82	1.21	3.20	0.86	1.30	0.73	1.43	1.09	1.15	0.73	1.43	5.51	5.58	5.51	6.50	5.51	6.12	1.12	6.77
21	-1.23	-1.23	-1.23	-0.99	-1.22	-1.10	-1.23	-0.99	-0.20	-0.11	-0.21	-0.11	-0.19	-0.11	-0.21	-0.11	-0.37	-0.35	-0.37	-0.34	-0.37	-0.34	-0.37	-0.34
22	-0.42	-0.41	-0.42	-0.36	-0.42	-0.41	-0.42	-0.36	-0.06	-0.02	-0.06	-0.02	-0.06	-0.04	-0.06	-0.02	-0.13	-0.11	-0.13	-0.11	-0.13	-0.11	-0.13	-0.11
23	0.14	0.15	0.12	0.15	0.12	0.15	0.12	0.15	0.33	0.33	0.33	0.33	0.33	0.33	0.33	0.33	-0.05	-0.05	-0.05	-0.05	-0.05	-0.05	-0.05	-0.05
24	-0.06	-0.06	-0.07	0.00	-0.07	-0.04	-0.07	0.00	0.18	0.18	0.18	0.18	0.18	0.18	0.18	0.18	-0.05	-0.04	-0.05	-0.03	-0.05	-0.03	-0.05	-0.03
25	0.73	0.73	0.54	0.73	0.65	0.72	0.54	0.75	-0.17	-0.12	-0.17	-0.11	-0.17	-0.12	-0.17	-0.11	-1.11	-1.06	-1.31	-0.93	-1.24	-1.05	-1.34	0.17
26	2.06	2.08	1.56	2.17	1.78	2.24	1.56	2.54	2.66	3.32	2.24	3.32	2.24	3.32	2.24	3.32	4.75	4.85	0.11	2.93	0.00	0.00	0.00	3.00
27	0.04	0.06	0.02	0.12	0.02	0.12	0.02	0.12	0.21	0.24	0.21	0.24	0.22	0.24	0.21	0.24	-0.03	-0.02	-0.03	-0.01	-0.03	-0.01	-0.03	-0.01
28	0.30	0.30	0.19	0.30	0.29	0.30	0.19	0.30	0.23	0.26	0.23	0.26	0.23	0.26	0.23	0.26	0.29	0.29	0.29	0.34	0.29	0.33	0.29	0.40
29	0.45	0.46	0.37	0.46	0.03	0.46	-0.53	0.46	-3.02	-2.24	-3.02	-1.68	-2.97	-1.77	-3.02	-1.68	-7.00	-6.96	-5.27	-1.99	-2.59	-2.13	-7.00	0.15
30	-0.10	-0.10	-0.10	0.02	-0.09	0.02	-0.10	0.02	0.00	0.02	0.00	0.02	0.02	0.02	0.00	0.02	-0.02	-0.01	-0.02	-0.01	-0.02	-0.01	-0.02	-0.01
31	-0.50	-0.50	-0.61	-0.50	-0.59	-0.54	-0.61	-0.41	-0.30	-0.23	-0.30	-0.23	-0.26	-0.23	-0.30	-0.23	0.00	0.05	-0.13	0.05	-0.09	0.05	-0.13	0.05
32	-0.11	-0.11	-0.12	-0.11	-0.12	-0.11	-0.12	-0.11	0.09	0.10	0.09	0.10	0.09	0.10	0.09	0.10	0.22	0.31	0.05	0.31	0.05	0.31	0.05	0.31
33	2.10	2.11	2.35	2.99	1.92	2.00	1.52	3.51	1.61	1.71	1.61	3.17	1.61	1.63	1.61	3.28	0.98	0.99	0.98	1.48	0.98	1.04	0.98	4.14
34	-1.40	-1.36	-2.36	-1.88	-1.88	-1.77	-2.36	-0.33	-1.24	-0.81	-1.37	-0.72	-1.09	-1.03	-1.37	-0.72	-4.41	-4.36	-5.58	-4.36	-4.95	-4.36	-5.85	0.03
35	0.54	0.57	0.33	0.60	0.50	0.58	0.33	0.60	0.00	0.00	0.00	0.00	0.00	0.00	0.00	0.00	1.00	1.04	0.79	1.04	0.86	1.04	0.79	1.04
36	48.69	48.78	55.67	65.33	47.96	48.93	35.48	69.28	41.61	44.70	43.45	69.80	42.42	43.13	41.33	69.80	34.20	34.49	34.20	46.60	34.20	36.67	16.09	65.71
37	18.96	19.02	21.79	26.43	18.32	18.81	13.20	28.41	15.23	16.46	15.54	27.51	15.52	15.81	15.12	27.89	12.77	12.89	12.77	17.98	12.77	13.70	7.28	31.02
38	0.03	0.04	0.03	0.05	0.03	0.04	0.02	0.05	0.00	0.00	0.00	0.01	0.00	0.00	0.00	0.01	0.09	0.09	0.09	0.10	0.09	0.09	0.00	0.10
39	-0.32	-0.32	-0.32	-0.29	-0.32	-0.30	-0.32	-0.29	-0.10	-0.08	-0.10	-0.08	-0.10	-0.08	-0.10	-0.08	-0.09	-0.08	-0.09	-0.08	-0.09	-0.08	-0.09	-0.08
40	-0.24	-0.24	-0.24	-0.21	-0.24	-0.21	-0.24	-0.21	-0.01	0.01	-0.01	0.01	-0.01	0.01	-0.01	0.01	-0.08	-0.08	-0.08	-0.08	-0.08	-0.08	-0.08	-0.08
41	-0.21	-0.21	-0.21	-0.17	-0.21	-0.21	-0.21	-0.17	-0.15	-0.15	-0.15	-0.15	-0.15	-0.15	-0.15	-0.15	-0.04	-0.04	-0.04	-0.04	-0.04	-0.04	-0.04	-0.04
42	0.05	0.09	0.13	0.44	0.00	0.05	0.00	0.66	0.00	0.03	0.00	0.52	0.00	0.01	0.00	0.55	0.00	0.00	0.00	0.01	0.00	0.00	0.00	1.05
43	0.27	0.67	0.19	0.99	0.26	0.99	0.00	1.00	0.10	0.67	0.00	0.01	0.35	0.67	0.00	0.67	0.40	0.40	0.40	0.40	0.40	0.40	0.36	2.58
44	2.12	2.16	2.20	2.51	2.07	2.12	2.07	2.74	1.98	2.26	1.98	2.74	1.98	2.12	1.98	2.77	1.70	1.71	1.70	1.71	1.70	1.71	1.70	2.89
45	0.82	0.88	0.47	0.80	0.86	0.93	0.25	0.93	0.66	0.95	0.18	0.95	0.69	0.95	0.14	0.95	0.91	0.95	0.91	0.95	0.91	0.95	-0.14	0.95
46	75.00	75.09	86.60	100	75.00	76.22	52.45	100	60.71	65.95	62.47	100	62.53	63.55	59.93	100	63.56	64.14	63.56	84.19	63.56	68.58	26.78	100
47	0.43	0.44	0.35	0.44	0.02	0.44	-0.55	0.44	-3.02	-2.25	-3.02	-1.69	-2.97	-1.78	-3.02	-1.69	-7.00	-6.96	-5.27	-1.99	-2.59	-2.14	-7.00	0.15
48	2.35	2.38	2.64	3.20	2.75	2.82	1.21	3.20	0.86	1.30	0.73	1.43	1.09	1.15	0.73	1.43	5.51	5.58	5.51	6.50	5.51	6.12	1.12	6.77

APPENDIX H: Bounds on metabolite concentrations

Because exact values of metabolite concentrations in hepatocytes are not be easily accessible, feasible ranges for metabolite concentrations [$c_{\min}$, $c_{\max}$] are considered in this study. Intracellular concentrations are estimated from literature values and are expressed as a range of values reported or estimated (Table H-1); extracellular concentrations are supplied by the metabolite measurements reported in this work and have a range corresponding to the measured experiment uncertainty (Table H-2).

The metabolites concentrations (oxaloacetate, acetyl-CoA, NAD^+, NADH, citrate, α-ketoglutarate, succinyl-CoA, fumarate, FAD, $FADH_2$, malate, aspartate, glutamate, $NADP^+$, NADPH, Pi, ATP,ADP, and CoA), are considered separated in cytosol and mitochondria (expressed using subscript 'm') since those metabolites appear both in mitochondria and cytosol (Siess et al. 1978). The concentration ratios are considered for energy-current metabolites (ATP, ADP, AMP, GTP, GDP, UTP, UDP) and cofactors (NAD^+, NADH, FAD, $FADH_2$, $NADP^+$, NADPH) instead of concentration of single metabolite; for example, the ratio of ATP/ADP was specified. Since the intracellular pH remains constant in the range of pH 7.0 to 7.1 while medium pH is around 7.4 (Longmore et al. 1969), the intracellular H^+ concentration is fixed at 0.0001 mM in this study.

For the metabolites' uptake from the medium, their maximum concentrations in the transport reactions are equal to their concentrations in the medium supplementation, and minimum concentrations are assumed in a lower physiological value as 0.001 mM. On the other hand, for the metabolites secreted from the hepatocytes, their minimum intracellular concentrations in the transport reactions are equal to their concentrations in

the medium supplementation, and maximum concentrations attainable are assumed to be 10 mM. Concentrations for some external metabolites (SO_3^{2-}, thiosulfate, H_4folate, N_5, N_{10}-CH_2-H_4folate, N_5-formiminoH_4folate, Adenosine, H_2biopterin, and H_4biopterin, cholesterol ester) are fixed at 1 mM.

Table H-1: Concentration bounds of metabolites based on literature search (mM)

Metabolites	***Min***	***Max***	***Source***
Glucose-6-Phosphate	1	10	(Van Schaftingen et al. 1980)
Fructose-6-Phosphate	0.25	5	(Van Schaftingen et al. 1980)
Fructose-1,6-Phosphate	0.5	5	(Van Schaftingen et al. 1980)
Glyceraldehyde-3-Phosphate	0.0001	0.1	(Berman and Newgard 1998; Burelle
Phospho*enol*pyruvate	0.0001	0.001	et al. 2000; Jones and Mason 1978)
Pyruvate	0.02	0.3	(Jones and Mason 1978)
Oxaloacetate	0.004	0.051	(Siess et al. 1978)
$Oxaloacetate_m$	0.002	0.062	(Siess et al. 1978; Siess et al. 1982; Siess et al. 1984)
NAD+/NADH	1	10	(Williamson et al. 1967)
$(NAD+/NADH)_m$	1	10	(Williamson et al. 1967)
Acetyl-CoA	0.048	0.112	(Siess et al. 1978)
$Acetyl\_CoA_m$	0.63	1.12	(Siess et al. 1978)
Citrate	0.33	1.84	(Siess et al. 1978)
$Citrate\_{m}$	2.54	10	(Siess et al. 1978; Siess et al. 1982; Siess et al. 1984)
α-Ketoglutarate	0.07	0.74	(Siess et al. 1978)
$α\text{-}Ketoglutarate_m$	0.12	1.31	(Siess et al. 1978)
$Succinyl\text{-}CoA_m$	0.05	0.7	(Quant et al. 1989)
Fumarate	0.07	6.002	[bock,1953]
$Fumarate\_{m}$	0.018	0.892	
FAD/ $FADH_2$	1	40	(Beard and Qian 2005)
$(FAD/ FADH_2)_m$	1	40	
Malate	0.35	3.01	(Siess et al. 1978)

Metabolites	*Min*	*Max*	*Source*
$Malate_m$	0.09	4.46	(Siess et al. 1978; Siess et al. 1982; Siess et al. 1984)
Citrulline	1	5	(Boon and Meijer 1991)
$Aspartate_m$	0.19	7.53	(Siess et al. 1978; Siess et al. 1982; Siess et al. 1984)
$Glutamate_m$	11.9	26.69	(Siess et al. 1978; Siess et al. 1982; Siess et al. 1984)
$O_2(g)$	0.007	0.21	(Jones and Mason 1978).
Propionyl-CoA	0.00001	0.0047	(Brass et al. 1990)
Acetoacetyl-CoA	0.00001	0.00003	(Williamson et al. 1968)
$NADP^+/NADPH$	0.1	1	(Williamson et al. 1967)
$(NADP^+/NADPH)_m$	0.01	0.1	(Williamson et al. 1967)
TG	0.289	2.89	(Matthew et al. 1996a)
Pi	5.0	17.8	(Soboll et al. 1978)
Pi_m	7.4	11.3	(Soboll et al. 1978)
PPi	0.027	0.109	(Guynn et al. 1974)
H^+	0.0001	0.0001	(Longmore et al. 1969)
Lactate	0.1	1.6	(Jones and Mason 1978)
[β-OH-butyrate]/[acetoacetate]	0.57	0.78	(Iles et al. 1977)
ATP/ADP	2.1	11.8	(Soboll et al. 1978)
$(ATP/ADP)_m$	0.1	0.7	(Soboll et al. 1978)
ATP/AMP	3.1	12.9	(Soboll et al. 1978)
$(ATP/AMP)_m$	0.3	3.5	(Soboll et al. 1978)
GTP/GDP	0.2	0.4	(Gines et al. 1996)
UTP/UDP	0.033	5	(Arnaud et al. 2003)
CO_2 (g)	2	25	(Beard and Qian 2005; Iles et al. 1977)
Glycogen	0.00001	0.0002	(Garcia-Rocha et al. 2001)
CoA	0.03	0.1	(Siess et al. 1978)
CoA_m	1.4	2.1	(Siess et al. 1978)

Note: The subscript m denotes a metabolite in mitochondria

Table H-2: Concentration bounds of metabolites based on the amino acid supplementation (mM)

Metabolites	***Min***	***Max***
Arginine	0.001	0.08^a, 0.42^b, 0.56^c
Glutamine	0.001	0.65^a, 6.85^b, 6.85^c
Glycine	0.001	0.16^a, 0.17^b, 0.41^c
Proline	0.001	0.17^a, 0.18^b, 0.22^c
Histidine	0.001	0.15^a, 0.35^b, 0.44^c
Aspartate	0.019^a, 0.031^b, 0.040^c	10
Glutamate	0.605^a, 1.569^b, 1.862^c	10
Isoleucine	0.226^a, 1.103^b, 1.359^c	10
Leucine	0.175^a, 0.843^b, 1.461^c	10
Lysine	0.230^a, 0.817^b, 1.241^c	10
Serine	0.417^a, 0.447^b, 1.039^c	10
Valine	0.335^a, 1.067^b, 2.144^c	10
Alanine	0.01^a, 0.459^b, 0.773^c	0.10^a, 10^b, 10^c
Asparagine	0.001^a, 0.001^b, 0.224^c	0.09^a, 0.09^b, 10^c
Cysteine	0.101^a, 0.001^b, 0.001^c	10^a, 0.13^b, 0.13^c
Methionine	0.037^a, 0.001^b, 0.245^c	10^a, 0.20^b, 10^c
Phenylalanine	0.093^a, 0.001^b, 0.001^c	10^a, 0.42^b, 0.42^c
Threonine	0.168^a, 0.001^b, 1.631^c	10^a, 0.79^b, 10^c
Tyrosine	0.078^a, 0.001^b, 0.953^c	10^a, 0.40^b, 10^c
NH_4^+	0.4	10
Ornithine	0.05	10
Tryptophan	0.001	3
Glycerol	0.001	1.21
Palmitate	0.001	0.4
Glucose	0.001^a, 0.68^b, 0.68^c	0.68^a, 10^b, 10^c
Acetoacetate	0.15^a, 0.14^b, 0.15^c	10
Urea	0.38^a, 1.18, 1.54^c	10
Cholesterol	0.455^a, 0.671, 0.753^c	10
Cholesterol ester	0.001	3.6

a: NAA=no amino acid supplementation; b: RAA= reference amino acid supplementation; c: DAA= designed amino acid supplementation

APPENDIX I: Transport rates of alanine, serine and glutamine under different conditional medium

Data Point	*Concentration (mM)*			*Reaction Rate * (Measurement)*			*Reaction Rate* (Estimation)*		
	[Ala]	**[Ser]**	**[Gln]**	**Ala**	**Ser**	**Gln**	**Ala**	**Ser**	**Gln**
1	0.2	0.2	1.5	0.2310	0.3795	1.0988	0.204	0.352	0.864
2	0.2	0.2	1.5	0.2289	0.3805	1.106	0.204	0.352	0.864
3	0.4	0.2	1.5	0.5384	0.4900	1.4665	0.501	0.529	0.865
4	0.4	0.2	1.5	0.5026	0.3893	1.0392	0.501	0.529	0.865
5	0.8	0.2	1.5	0.7856	0.3318	0.8739	0.650	0.373	0.868
6	0.8	0.2	1.5	0.7872	0.3344	0.8973	0.650	0.373	0.868
7	0.2	0.4	1.5	0.2078	0.9054	0.9811	0.161	0.555	0.851
8	0.2	0.4	1.5	0.1982	0.8996	--	0.161	0.555	--
9	0.4	0.4	1.5	0.5384	1.0277	1.4665	0.397	0.732	0.853
10	0.4	0.4	1.5	0.4292	0.8241	0.8739	0.397	0.732	0.853
11	0.8	0.4	1.5	0.516	0.5866	0.6068	0.423	0.576	0.856
12	0.8	0.4	1.5	0.5744	0.5753	0.6013	0.423	0.576	0.856
13	0.2	0.6	1.5	-0.2135	0.4385	0.4789	0.118	0.403	0.838
14	0.2	0.6	1.5	-0.0146	0.4407	0.4431	0.118	0.403	0.838
15	0.4	0.6	1.5	0.114	0.4813	0.5762	0.292	0.580	0.840
16	0.4	0.6	1.5	0.1916	0.4855	0.516	0.292	0.580	0.840
17	0.8	0.6	1.5	0.2144	0.3485	0.1378	0.195	0.424	0.843
18	0.8	0.6	1.5	0.1666	0.3548	0.2532	0.195	0.424	0.843
19	0.2	0.1	2	0.2135	0.0605	1.4193	0.195	0.052	1.286
20	0.2	0.1	2	0.2316	--	1.4005	0.195	--	1.286
21	0.4	0.1	2	0.4568	0.0396	1.3162	0.523	0.229	1.288
22	0.4	0.1	2	0.4553	0.0464	1.3662	0.523	0.229	1.288
23	0.8	0.1	2	0.6619	0.0004	1.1345	0.734	0.073	1.292
24	0.8	0.1	2	0.6805	0.0062	1.2532	0.734	0.073	1.292
25	0.2	0.1	4	0.2386	-0.0119	2.9747	-0.020	-0.147	2.543
26	0.2	0.1	4	0.2398	-0.0673	3.0813	-0.020	-0.147	2.543
27	0.4	0.1	4	0.4987	-0.0832	2.4495	0.308	0.030	2.547
28	0.4	0.1	4	0.486	-0.0003	2.4439	0.308	0.030	2.547
29	0.8	0.1	4	0.6893	-0.0036	2.9721	0.518	-0.126	2.555

Data Point	*Concentration (mM)*			*Reaction Rate * (Measurement)*			**Reaction Rate* (Estimation)**		
	[Ala]	**[Ser]**	**[Gln]**	**Ala**	**Ser**	**Gln**	**Ala**	**Ser**	**Gln**
30	0.8	0.1	4	0.7003	-0.0003	3.0334	0.518	-0.126	2.555
31	0.2	0.1	6	-0.5883	-0.1699	2.7946	-0.388	-0.243	3.153
32	0.2	0.1	6	-0.5734	-0.1519	2.8807	-0.388	-0.243	3.153
33	0.4	0.1	6	-0.0672	--	3.2177	-0.060	---	3.159
34	0.4	0.1	6	-0.0666	--	3.2476	-0.060	---	3.159
35	0.8	0.1	6	-0.2354	-0.1934	2.7653	0.150	-0.222	3.171
36	0.8	0.1	6	-0.2251	-0.178	2.6747	0.150	-0.222	3.171
37	0.2	0.1	8	-0.9394	-0.1504	2.9943	-0.908	-0.236	3.114
38	0.2	0.1	8	-0.8807	-0.1559	3.1568	-0.908	-0.236	3.114
39	0.4	0.1	8	-0.6733	-0.1573	3.2043	-0.579	-0.059	3.122
40	0.4	0.1	8	-0.6595	-0.1448	3.3048	-0.579	-0.059	3.122
41	0.8	0.1	8	-0.4046	-0.1531	3.2694	-0.369	-0.215	3.138
42	0.8	0.1	8	-0.3809	-0.1435	3.4830	-0.369	-0.215	3.138
43	0.1	0.2	2	0.0424	0.1128	1.4834	-0.028	0.134	1.276
44	0.1	0.2	2	0.0181	0.0503	1.286	-0.028	0.134	1.276
45	0.1	0.4	2	0.0019	0.2443	1.427	-0.034	0.337	1.259
46	0.1	0.4	2	-0.0441	0.1554	1.1554	-0.034	0.337	1.259
47	0.1	0.6	2	0.0407	0.2738	1.4501	-0.039	0.185	1.243
48	0.1	0.6	2	0.0011	0.1828	1.2113	-0.039	0.185	1.243
49	0.1	0.2	4	-0.1923	-0.0371	2.6702	-0.231	-0.064	2.524
50	0.1	0.2	4	--	--	--	---	---	---
51	0.1	0.4	4	-0.3981	0.0331	2.5339	-0.212	0.139	2.491
52	0.1	0.4	4	-0.3079	-0.0169	2.5510	-0.212	0.139	2.491
53	0.1	0.6	4	-0.4093	-0.0096	2.5737	-0.193	-0.013	2.457
54	0.1	0.6	4	-0.3037	0.0324	2.6463	-0.193	-0.013	2.457
55	0.1	0.2	6	-0.7439	-0.1664	2.9524	-0.586	-0.160	3.125
56	0.1	0.2	6	--	-0.1537	2.7910	---	-0.160	3.125
57	0.1	0.4	6	-0.7361	-0.0739	2.7299	-0.542	0.042	3.074
58	0.1	0.4	6	-0.6732	-0.0543	2.7700	-0.542	0.042	3.074
59	0.1	0.6	6	-0.392	-0.0748	3.0141	-0.499	-0.110	3.024
60	0.1	0.6	6	-0.7048	-0.0490	3.0051	-0.499	-0.110	3.024
61	0.1	0.2	8	-1.0355	-0.1783	3.0370	-1.093	-0.154	3.077

Data Point	*Concentration (mM)*			*Reaction Rate * (Measurement)*			Reaction Rate* *(Estimation)*		
	[Ala]	**[Ser]**	**[Gln]**	**Ala**	**Ser**	**Gln**	**Ala**	**Ser**	**Gln**
62	62	0.1	0.2	8	-0.96	-0.1586	2.7833	-1.093	-0.154
63	63	0.1	0.4	8	-0.7878	-0.0322	3.1341	-1.025	0.049
64	64	0.1	0.4	8	-0.8291	-0.0034	3.0526	-1.025	0.049
65	65	0.1	0.6	8	-0.9315	-0.1354	3.2511	-0.956	-0.103
66	66	0.1	0.6	8	-0.8231	-0.0978	3.2025	-0.956	-0.103

* flux rate (μmol/million cell/day)

APPENDIX J: Measurement data from experiment of amino acid supplementation

	Flux rate *							
	without hormone supplementation (NH)				with hormone supplementation (WH)			
	RAA		DAA		RAA		DAA	
	HI	LI	HI	LI	HI	LI	HI	LI
1	0.563±0.439	1.284±0.183	1.614±0.609	2.51±0.125	1.003±0.502	0.548±0.121	1.195±0.343	0.668±0.352
2	3.074±0.04	3.013±0.115	2.197±0.089	3.525±0.07	3.107±0.128	3.202±0.36	2.327±0.064	3.467±0.36
3	0.838±0.131	0.718±0.156	1.556±0.049	1.192±0.131	1.117±0.13	1.18±0.051	1.459±0.246	1.504±0.182
4	0.338±0.008	0.396±0.007	0.269±0.023	0.125±0.02	0.611±0.012	0.545±0.012	0.635±0.012	0.565±0.014
5	0.022±0.003	-0.061±0.009	-0.52±0.021	-1.128±0.025	-0.467±0.003	-0.78±0.001	-1.294±0.017	-1.011±0.019
6	-0.548±0.008	-0.286±0.004	-0.442±0.009	-0.376±0.004	-0.132±0.005	-0.336±0.004	-0.349±0.005	-0.521±0.034
7	0.224±0.024	0.243±0.024	-0.041±0.017	-0.203±0.017	0.139±0.006	-0.169±0.009	0.043±0.012	-0.313±0.013
8	-0.389±0.008	-0.238±0.006	-0.779±0.029	-0.738±0.021	-0.075±0.003	-0.347±0.006	-0.341±0.014	-0.679±0.023
9	0.127±0.019	0.211±0.008	0.057±0.005	0.073±0.006	0.111±0.0038	0.0661±0.012	0.0396±0.014	0.0019±0.010
10	0.195±0.006	0.218±0.003	0.32±0.027	0.128±0.013	0.258±0.004	0.246±0.004	0.576±0.009	0.53±0.009
11	-0.185±0.014	0.004±0.011	-0.667±0.046	-0.729±0.031	0.17±0.03	0.028±0.014	0.184±0.023	-0.233±0.059
12	-1.083±0.024	-0.602±0.014	-1.211±0.032	-1.104±0.019	-0.456±0.006	-1.459±0.02	-1.448±0.02	-1.752±0.031
13	-0.014±0.001	-0.005±0.001	-0.027±0.002	-0.047±0.002	0.009±0.001	-0.021±0.001	-0.017±0.001	-0.03±0.001
14	0.2±0.035	0.19±0.042	0.2±0.034	0.15±0.001	0.18±0.006	0.14±0.024	0.16±0.018	0.15±0.009
15	0.328±0.015	0.4±0.037	0.214±0.052	0.267±0.025	0.148±0.015	0.158±0.018	0.15±0.031	0.16±.0009
16	-0.699±0.031	-0.077±0.017	-0.833±0.054	-0.764±0.045	0.643±0.021	0.207±0.023	-0.041±0.03	-0.451±0.044
17	-0.66±0.024	-0.126±0.015	-0.344±0.03	-0.414±0.024	0.604±0.02	-0.067±0.023	-0.094±0.014	-0.451±0.026
18	-0.337±0.015	-0.001±0.009	-0.38±0.024	-0.345±0.017	0.493±0.013	0.326±0.013	0.289±0.012	0.107±0.013
19	2.622±1.283	2.622±1.283	2.846±1.083	2.846±1.083	2.666±0.688	2.768±0.538	2.173±0.777	1.799±0.717
20	-0.816±0.528	-0.763±0.028	-1.094±0.367	-1.289±0.554	0.417±0.033	0.475±0.037	0.419±0.119	0.463±0.111
21	-0.181±0.006	-0.017±0.004	-0.168±0.01	-0.191±0.011	0.122±0.008	0.011±0.01	0.152±0.035	-0.045±0.06
22	-0.088±0.005	0.103±0.055	-0.331±0.03	-0.313±0.01	-0.02±0.005	0.081±0.005	-0.046±0.007	-0.134±0.006
23	-1.072±0.02	-0.356±0.011	-0.778±0.044	-0.786±0.041	---	-0.197±0.022	-0.034±0.257	-0.654±0.026
24	-0.92±0.017	-0.261±0.011	-0.728±0.044	-0.74±0.041	---	-0.32±0.022	-0.119±0.257	-0.469±0.026
25	-0.827±0.021	-0.247±0.009	-0.712±0.03	-0.743±0.025	---	-0.013±0.02	-0.092±0.023	-0.441±0.037
26	0.000517±	0.000192±	0.000548±	0.000185±	0.001049±	0.000708±	0.001245±	0.001091±
27	2.001±0.007	2.044±0.014	1.983±0.025	2.075±0.042	2.021±0.023	2.107±0.127	2.048±0.018	2.075±0.007
28	1.012±0.019	1.071±0.022	0.992±0.009	0.812±0.016	0.983±0.092	1.073±0.008	1.07±0.003	0.981±0.005
29	1.944±0.27	1.422±0.10	1.759±0.056	1.864±0.352	0.778±0.099	0.671±0.128	0.801±0.225	0.753±0.208
30	0.84±0.003	0.85±0.022	0.87±0.02	0.88±0.01	0.84±0.057	0.82±0.126	0.830 ±034	0.92±0.014

APPENDIX K: Intracellular flux distribution from model (II)

#	Flux Rate*
Gluconeogenesis Pathway, PPP, Glycogen storage	
v_{u1}, v_{u2}, v_{u3}	0.48
v_{u4}, v_{u5}	3.05
v_{u6}	7.20
v_{u38}	0.14
v_{u43}	0.40
TCA cycle	
v_{u7}, v_{u8}	26.33
v_{u9}	26.33
v_{u10}	27.09
v_{u11}, v_{u12}	29.20
Urea Cycle	
v_{u13}, v_{u14}	2.90
Amino Acid Catabolism	
v_{u15}	0.12
v_{u16}	1.50
v_{u17}	0.16
v_{u18}	0.62
v_{u19}	1.18
v_{u20}	0.73
v_{u24}	-0.40
v_{u25}	0.38
v_{u26}	2.15
v_{u27}	0.06
v_{u29}	0.42
v_{u30}	0.18
v_{u31}	-1.43
v_{u32}	0.13
v_{u40}	-0.09
v_{u41}	-0.47
v_{u47}	0.44
v_{u48}	0.73

Fatty Acid, Lipid and Glycerol Metabolism	
v_{u33}	2.78
v_{u34}	1.31
v_{u35}	2.04
v_{u42}	0.13
v_{u44}	2.09
v_{u45}	0.56
Oxygen Uptake , Electron Transport System	
v_{u36}	58.65
v_{u37}	23.09
v_{u46}	82.34

* μmol/million cell/day

BIBLIOGRAPHY

Adams LA, Angulo P. 2006. Treatment of non-alcoholic fatty liver disease. Postgrad Med J 82(967):315-22.

Allen JW, Bhatia SN. 2002. Engineering liver therapies for the future. Tissue Eng 8:725-37.

Allen JW, Hassanein T, Bhatia SN. 2001. Advances in bioartificial liver devices. Hepatology 34(3):447-455.

Arai K, Lee K, Berthiaume F, Tompkins RG, Yarmush ML. 2001. Intrahepatic amino acid and glucose metabolism in a D-galactosamine-induced rat liver failure model. Hepatology 34(2):360-71.

Arnaud A, Fontana L, Angulo AJ, Gil A, Lopez-Pedrosa JM. 2003. Exogenous nucleosides alter the intracellular nucleotide pool in hepatic cell cultures. Implications in cell proliferation and function. Clin Nutr 22(4):391-9.

Bailey JE. 1998. Mathematical modeling and analysis in biochemical engineering: past accomplishments and future opportunities. Biotechnol Prog 14(1):8-20.

Bartlett DW, Davis ME. 2006. Insights into the kinetics of siRNA-mediated gene silencing from live-cell and live-animal bioluminescent imaging. Nucleic Acids Res 34(1):322-33.

Beard DA, Babson E, Curtis E, Qian H. 2004. Thermodynamic constraints for biochemical networks. J Theor Biol 228(3):327-33.

Beard DA, Liang SD, Qian H. 2002. Energy balance for analysis of complex metabolic networks. Biophys J 83(1):79-86.

Beard DA, Qian H. 2005. Thermodynamic-based computational profiling of cellular regulatory control in hepatocyte metabolism. Am J Physiol Endocrinol Metab 288(3):E633-44.

Behre J, Wilhelm T, von Kamp A, Ruppin E, Schuster S. 2008. Structural robustness of metabolic networks with respect to multiple knockouts. J Theor Biol 252(3):433-41.

Bell SL, Palsson BO. 2005. Expa: a program for calculating extreme pathways in biochemical reaction networks. Bioinformatics 21(8):1739-40.

Berman HK, Newgard CB. 1998. Fundamental metabolic differences between hepatocytes and islet beta-cells revealed by glucokinase overexpression. Biochemistry 37(13):4543-52.

Bhatia SN, Yarmush ML, Toner M. 1997. Controlling cell interactions by micropatterning in co-cultures: Hepatocytes and 3T3 fibroblasts. Journal of Biomedical Materials Research 34(2):189-199.

Bonarius HPJ, Schmid G, Tramper J. 1997. Flux analysis of underdetermined metabolic networks: The quest for the missing constraints. Trends in Biotechnology 15(8):308-314.

Boon L, Meijer AJ. 1991. Oxygen tension does not affect urea synthesis in perifused rat hepatocytes. Eur J Biochem 195(2):455-7.

Brass EP, Tahiliani AG, Allen RH, Stabler SP. 1990. Coenzyme A metabolism in vitamin B-12-deficient rats. J Nutr 120(3):290-7.

Burelle Y, Fillipi C, Peronnet F, Leverve X. 2000. Mechanisms of increased gluconeogenesis from alanine in rat isolated hepatocytes after endurance training.

Am J Physiol Endocrinol Metab 278(1):E35-42.
Burgard AP, Maranas CD. 2003. Optimization-based framework for inferring and testing hypothesized metabolic objective functions. Biotechnol Bioeng 82(6):670-7.
Burgard AP, Pharkya P, Maranas CD. 2003. Optknock: a bilevel programming framework for identifying gene knockout strategies for microbial strain optimization. Biotechnol Bioeng 84(6):647-57.
Burghardt TP, Lyke JE, Ajtai K. 1996. Fluorescence emission and anisotropy from rhodamine dimers. Biophys Chem 59(1-2):119-31.
Chalhoub E, Hanson RW, Belovich JM. 2007. A computer model of gluconeogenesis and lipid metabolism in the perfused liver. Am J Physiol Endocrinol Metab 293(6):E1676-86.
Chan C, Berthiaume F, Lee K, Yarmush ML. 2003a. Metabolic flux analysis of cultured hepatocytes exposed to plasma. Biotechnol Bioeng 81(1):33-49.
Chan C, Berthiaume F, Lee K, Yarmush ML. 2003b. Metabolic flux analysis of hepatocyte function in hormone- and amino acid-supplemented plasma. Metab Eng 5(1):1-15.
Chan C, Berthiaume F, Nath BD, Tilles AW, Toner M, Yarmush ML. 2004. Hepatic tissue engineering for adjunct and temporary liver support: critical technologies. Liver Transpl 10(11):1331-42.
Chan C, Berthiaume F, Washizu J, Toner M, Yarmush ML. 2002. Metabolic pre-conditioning of cultured cells in physiological levels of insulin: generating resistance to the lipid-accumulating effects of plasma in hepatocytes. Biotechnol Bioeng 78(7):753-60.
Chan C, Hwang D, Stephanopoulos GN, Yarmush ML, Stephanopoulos G. 2003c. Application of multivariate analysis to optimize function of cultured hepatocytes. Biotechnol Prog 19(2):580-98.
Christensen HN, Oxender DL, Liang M, Vatz KA. 1965. The use of N-methylation to direct route of mediated transport of amino acids. J Biol Chem 240(9):3609-16.
Chvatal V. 1983. Linear Programming Freeman Press, New York
Covert MW, Famili I, Palsson BO. 2003. Identifying constraints that govern cell behavior: a key to converting conceptual to computational models in biology? Biotechnol Bioeng 84(7):763-72.
Darmaun D. 2000. Role of glutamine depletion in severe illness. Diabetes Nutr Metab 13(1):25-30.
De Maria C, Grassini D, Vozzi F, Vinci B, Landi A, Ahluwalia A, Vozzi G. 2008. HEMET: mathematical model of biochemical pathways for simulation and prediction of HEpatocyte METabolism. Comput Methods Programs Biomed 92(1):121-34.
Demetriou AA, Brown RS, Jr., Busuttil RW, Fair J, McGuire BM, Rosenthal P, Am Esch JS, 2nd, Lerut J, Nyberg SL, Salizzoni M and others. 2004. Prospective, randomized, multicenter, controlled trial of a bioartificial liver in treating acute liver failure. Ann Surg 239(5):660-7; discussion 667-70.
Dufour S, Rousse N, Canioni P, Diolez P. 1996. Top-down control analysis of temperature effect on oxidative phosphorylation. Biochem J 314 (Pt 3):743-51.
Dunn JC, Tompkins RG, Yarmush ML. 1991. Long-term in vitro function of adult hepatocytes in a collagen sandwich configuration. Biotechnol Prog 7(3):237-45.
Dunn JC, Tompkins RG, Yarmush ML. 1992. Hepatocytes in collagen sandwich:

evidence for transcriptional and translational regulation. J Cell Biol 116(4):1043-53.

Dunn JC, Yarmush ML, Koebe HG, Tompkins RG. 1989. Hepatocyte function and extracellular matrix geometry: long-term culture in a sandwich configuration. Faseb J 3(2):174-7.

Dykxhoorn DM, Novina CD, Sharp PA. 2003. Killing the messenger: short RNAs that silence gene expression. Nat Rev Mol Cell Biol 4(6):457-67.

Edwards JS, Covert M, Palsson B. 2002. Metabolic modelling of microbes: the flux-balance approach. Environ Microbiol 4(3):133-40.

Edwards JS, Ibarra RU, Palsson BO. 2001. In silico predictions of Escherichia coli metabolic capabilities are consistent with experimental data. Nat Biotechnol 19(2):125-30.

Edwards JS, Palsson BO. 2000. The Escherichia coli MG1655 in silico metabolic genotype: its definition, characteristics, and capabilities. Proc Natl Acad Sci U S A 97(10):5528-33.

Ehlde M, Zacchi G. 1997. A general formalism for metabolic control analysis. Chemical Engineering Science 52(15):2599-2606.

Fafournoux P, Remesy C, Demigne C. 1983. Control of alanine metabolism in rat liver by transport processes or cellular metabolism. Biochem J 210(3):645-52.

Farrell GC, Larter CZ. 2006. Nonalcoholic fatty liver disease: from steatosis to cirrhosis. Hepatology 43(2 Suppl 1):S99-S112.

Fell DA. 1992. Metabolic control analysis: a survey of its theoretical and experimental development. Biochem J 286 (Pt 2):313-30.

Flendrig LM, Maas MA, Daalhuisen J, Ladiges NC, La Soe JW, Te Velde AA, Chamuleau RA. 1998. Does the extend of the culture time of primary hepatocytes in a bioreactor affect the treatment efficacy of a bioartificial liver? Int J Artif Organs 21(9):542-7.

Fraenkel DG. 1992. Genetics and intermediary metabolism. Annu Rev Genet 26:159-77.

Garcia-Rocha M, Roca A, De La Iglesia N, Baba O, Fernandez-Novell JM, Ferrer JC, Guinovart JJ. 2001. Intracellular distribution of glycogen synthase and glycogen in primary cultured rat hepatocytes. Biochem J 357(Pt 1):17-24.

Garcia M, Rager J, Wang Q, Strab R, Hidalgo IJ, Owen A, Li J. 2003. Cryopreserved human hepatocytes as alternative in vitro model for cytochrome p450 induction studies. In Vitro Cell Dev Biol Anim 39(7):283-7.

Gebhardt R, Hengstler JG, Muller D, Glockner R, Buenning P, Laube B, Schmelzer E, Ullrich M, Utesch D, Hewitt N and others. 2003. New hepatocyte in vitro systems for drug metabolism: metabolic capacity and recommendations for application in basic research and drug development, standard operation procedures. Drug Metab Rev 35(2-3):145-213.

Gebhardt R, Kleemann E. 1987. Hormonal regulation of amino acid transport system N in primary cultures of rat hepatocytes. Eur J Biochem 166(2):339-44.

Gerlach JC. 1997. Long-term liver cell cultures in bioreactors and possible application for liver support. Cell Biol Toxicol 13(4-5):349-55.

Gianchandani EP, Oberhardt MA, Burgard AP, Maranas CD, Papin JA. 2008. Predicting biological system objectives de novo from internal state measurements. BMC Bioinformatics 9:43.

Gines P, Li X, Brown SE, Nakamura T, Guzelian PS, Heasley LE, Schrier RW, Nemenoff RA. 1996. Inhibitory actions of cyclic adenosine monophosphate and pertussis toxin define two distinct epidermal growth factor-regulated pathways leading to activation of mitogen-activated protein kinase in rat hepatocytes. Hepatology 23(5):1167-73.

Gombert AK, Nielsen J. 2000. Mathematical modelling of metabolism. Curr Opin Biotechnol 11(2):180-6.

Gu S, Roderick HL, Camacho P, Jiang JX. 2000. Identification and characterization of an amino acid transporter expressed differentially in liver. Proc Natl Acad Sci U S A 97(7):3230-5.

Gu S, Villegas CJ, Jiang JX. 2005. Differential regulation of amino acid transporter SNAT3 by insulin in hepatocytes. J Biol Chem 280(28):26055-62.

Guynn RW, Veloso D, Lawson JW, Veech RL. 1974. The concentration and control of cytoplasmic free inorganic pyrophosphate in rat liver in vivo. Biochem J 140(3):369-75.

Guyomard C, Rialland L, Fremond B, Chesne C, Guillouzo A. 1996. Influence of alginate gel entrapment and cryopreservation on survival and xenobiotic metabolism capacity of rat hepatocytes. Toxicol Appl Pharmacol 141(2):349-56.

Haimes YY, Lasdon U, Wismer DA. 1971. On a bicriterion formulation of the problems of integrated system identification and system optimization. IEEE Transactions on Systems, Man, and Cybernetics 1:296-297.

Hall SK, Chakraborty J., J. RR. 1997. Chemical exposure and toxic response: CRC Press, Inc.

Hatzimanikatis V, Bailey JE. 1997. Effects of spatiotemporal variations on metabolic control: Approximate analysis using (log)linear kinetic models. Biotechnol Bioeng 54(2):91-104.

Haussinger D, Soboll S, Meijer AJ, Gerok W, Tager JM, Sies H. 1985. Role of plasma membrane transport in hepatic glutamine metabolism. Eur J Biochem 152(3):597-603.

Heinrich R, Rapoport TA. 1974. A linear steady-state treatment of enzymatic chains. General properties, control and effector strength. Eur J Biochem 42(1):89-95.

Higuchi A, Satoh M, Kobayashi K, Cho CS, Akaike T, Tak TM, Egashira S, Matsuoka Y, Natori SH. 2006. Albumin and urea production by hepatocytes cultured on polyurethane foaming membranes coated with extracellular matrix. Journal of Membrane Science 280(1-2):983-989.

Hosagrahara VP, Hansen LK, Beilman GJ, Remmel RP. 2000. Evaluation of the effect of culture matrices on induction of CYP3A isoforms in cultured porcine hepatocytes. Chem Biol Interact 127(1):91-106.

Hulek P, Dresslerova I. 2009. [Metabolic syndrome and the liver (NAFLD/NASH)]. Vnitr Lek 55(7-8):646-9.

Hutvagner G, Zamore PD. 2002. A microRNA in a multiple-turnover RNAi enzyme complex. Science 297(5589):2056-60.

Hyde R, Taylor PM, Hundal HS. 2003. Amino acid transporters: roles in amino acid sensing and signalling in animal cells. Biochemical Journal 373:1-18.

Ibarra RU, Edwards JS, Palsson BO. 2002. Escherichia coli K-12 undergoes adaptive evolution to achieve in silico predicted optimal growth. Nature 420(6912):186-9.

Iles RA, Cohen RD, Rist AH, Baron PG. 1977. The mechanism of inhibition by acidosis of gluconeogenesis from lactate in rat liver. Biochem J 164(1):185-91.

Jalan R, Williams R. 2002. Acute-on-chronic liver failure: pathophysiological basis of therapeutic options. Blood Purif 20(3):252-61.

Jones DP, Mason HS. 1978. Gradients of O2 concentration in hepatocytes. J Biol Chem 253(14):4874-80.

Joseph SK, Bradford NM, McGivan JD. 1978. Characteristics of the transport of alanine, serine and glutamine across the plasma membrane of isolated rat liver cells. Biochem J 176(3):827-36.

Kane BJ, Zinner MJ, Yarmush ML, Toner M. 2006. Liver-specific functional studies in a microfluidic array of primary mammalian hepatocytes. Analytical Chemistry 78(13):4291-4298.

Kanehisa M, Goto S. 2000. KEGG: kyoto encyclopedia of genes and genomes. Nucleic Acids Res 28(1):27-30.

Kauffman KJ, Prakash P, Edwards JS. 2003. Advances in flux balance analysis. Curr Opin Biotechnol 14(5):491-6.

Kern A, Bader A, Pichlmayr R, Sewing KF. 1997. Drug metabolism in hepatocyte sandwich cultures of rats and humans. Biochem Pharmacol 54(7):761-72.

Khannapho C, Zhao H, Bonde BK, Kierzek AM, Avignone-Rossa CA, Bushell ME. 2008. Selection of objective function in genome scale flux balance analysis for process feed development in antibiotic production. Metab Eng 10(5):227-33.

Kitiyakara C, Chabrashvili T, Jose P, Welch WJ, Wilcox CS. 2001. Effects of dietary salt intake on plasma arginine. Am J Physiol Regul Integr Comp Physiol 280(4):R1069-75.

Klamt S, Stelling J. 2002. Combinatorial complexity of pathway analysis in metabolic networks. Mol Biol Rep 29(1-2):233-6.

Klamt S, Stelling J. 2003. Two approaches for metabolic pathway analysis? Trends Biotechnol 21(2):64-9.

Klamt S, Stelling J, Ginkel M, Gilles ED. 2003. FluxAnalyzer: exploring structure, pathways, and flux distributions in metabolic networks on interactive flux maps. Bioinformatics 19(2):261-9.

Knorr AL, Jain R, Srivastava R. 2007. Bayesian-based selection of metabolic objective functions. Bioinformatics 23(3):351-7.

Krause P, Saghatolislam F, Koenig S, Unthan-Fechner K, Probst I. 2009. Maintaining hepatocyte differentiation in vitro through co-culture with hepatic stellate cells. In Vitro Cell Dev Biol Anim 45(5-6):205-12.

Kummel A, Panke S, Heinemann M. 2006. Putative regulatory sites unraveled by network-embedded thermodynamic analysis of metabolome data. Mol Syst Biol 2:2006 0034.

Lee JM, Gianchandani EP, Papin JA. 2006. Flux balance analysis in the era of metabolomics. Brief Bioinform 7(2):140-50.

Lee K, Berthiaume F, Stephanopoulos GN, Yarmush DM, Yarmush ML. 2000a. Metabolic flux analysis of postburn hepatic hypermetabolism. Metab Eng 2(4):312-27.

Lee K, Berthiaume F, Stephanopoulos GN, Yarmush ML. 1999. Metabolic flux analysis: a powerful tool for monitoring tissue function. Tissue Eng 5(4):347-68.

Lee K, Berthiaume F, Stephanopoulos GN, Yarmush ML. 2003. Profiling of dynamic changes in hypermetabolic livers. Biotechnol Bioeng 83(4):400-15.

Lee S, Phalakornkule C, Domach MM, Grossmann IE. 2000b. Recursive MILP model for finding all the alternate optima in LP models for metabolic networks. Computers & Chemical Engineering 24(2-7):711-716.

Lee WM. 2008. Etiologies of acute liver failure. Semin Liver Dis 28(2):142-52.

Lee WM, Hynan LS, Rossaro L, Fontana RJ, Stravitz RT, Larson AM, Davern TJ, 2nd, Murray NG, McCashland T, Reisch JS and others. 2009. Intravenous N-acetylcysteine improves transplant-free survival in early stage non-acetaminophen acute liver failure. Gastroenterology 137(3):856-64, 864 e1.

Li AP, Jurima-Romet M. 1997. Applications of primary human hepatocytes in the evaluation of pharmacokinetic drug-drug interactions: evaluation of model drugs terfenadine and rifampin. Cell Biol Toxicol 13(4-5):365-74.

Li Z, Yarmush ML, Chan C. 2004. Insulin concentration during preconditioning mediates the regulation of urea synthesis during exposure to amino acid-supplemented plasma. Tissue Eng 10(11-12):1737-46.

Liou IW, Larson AM. 2008. Role of liver transplantation in acute liver failure. Semin Liver Dis 28(2):201-9.

Lipscomb JC, Poet TS. 2008. In vitro measurements of metabolism for application in pharmacokinetic modeling. Pharmacol Ther 118(1):82-103.

Llaneras F, Pico J. 2008. Stoichiometric modelling of cell metabolism. J Biosci Bioeng 105(1):1-11.

Lloyd TD, Orr S, Skett P, Berry DP, Dennison AR. 2003. Cryopreservation of hepatocytes: a review of current methods for banking. Cell Tissue Bank 4(1):3-15.

Longmore WJ, Niethe CM, McDaniel ML. 1969. Effect of CO2 concentration on intracellular pH and on glycogen synthesis from glycerol and glucose in isolated perfused rat liver. J Biol Chem 244(23):6451-7.

Mahadevan R, Edwards JS, Doyle FJ, 3rd. 2002. Dynamic flux balance analysis of diauxic growth in Escherichia coli. Biophys J 83(3):1331-40.

Malandro MS, Kilberg MS. 1996. Molecular biology of mammalian amino acid transporters. Annual Review of Biochemistry 65:305-336.

Marchesini G, Marzocchi R, Noia M, Bianchi G. 2005. Branched-chain amino acid supplementation in patients with liver diseases. Journal of Nutrition 135(6):1596S-1601S.

Marin S, Lee WN, Bassilian S, Lim S, Boros LG, Centelles JJ, FernAndez-Novell JM, Guinovart JJ, Cascante M. 2004. Dynamic profiling of the glucose metabolic network in fasted rat hepatocytes using [1,2-13C2]glucose. Biochem J 381(Pt 1):287-94.

Matthew HW, Sternberg J, Stefanovich P, Morgan JR, Toner M, Tompkins RG, Yarmush ML. 1996a. Effects of plasma exposure on cultured hepatocytes: Implications for bioartificial liver support. Biotechnol Bioeng 51(1):100-11.

Matthew HWT, Sternberg J, Stefanovich P, Morgan JR, Toner M, Tompkins RG, Yarmush ML. 1996b. Effects of plasma exposure on cultured hepatocytes: Implications for bioartificial liver support. Biotechnology and Bioengineering 51(1):100-111.

Mavrovouniotis ML. 1991. Estimation of standard Gibbs energy changes of biotransformations. J Biol Chem 266(22):14440-5.

Mavrovouniotis ML. 1993. Identification of localized and distributed bottlenecks in metabolic pathways. Proc Int Conf Intell Syst Mol Biol 1:275-83.

McGinnity DF, Soars MG, Urbanowicz RA, Riley RJ. 2004. Evaluation of fresh and cryopreserved hepatocytes as in vitro drug metabolism tools for the prediction of metabolic clearance. Drug Metab Dispos 32(11):1247-53.

Moreno-Sanchez R, Saavedra E, Rodriguez-Enriquez S, Olin-Sandoval V. 2008. Metabolic control analysis: a tool for designing strategies to manipulate metabolic pathways. J Biomed Biotechnol 2008:597913.

Mundt A, Puhl G, Muller A, Sauer I, Muller C, Richard R, Fotopoulou C, Doll R, Gabelein G, Hohn W and others. 2002. A method to assess biochemical activity of liver cells during clinical application of extracorporeal hybrid liver support. Int J Artif Organs 25(6):542-8.

Nagrath D, Avila-Elchiver M, Berthiaume F, Tilles AW, Messac A, Yarmush ML. 2007. Integrated energy and flux balance based multiobjective framework for large-scale metabolic networks. Ann Biomed Eng 35(6):863-85.

Neff GW, Bonham A, Tzakis AG, Ragni M, Jayaweera D, Schiff ER, Shakil O, Fung JJ. 2003. Orthotopic liver transplantation in patients with human immunodeficiency virus and end-stage liver disease. Liver Transpl 9(3):239-47.

Nielsen J. 2003. It is all about metabolic fluxes. J Bacteriol 185(24):7031-5.

Nolan RP, Fenley AP, Lee K. 2006. Identification of distributed metabolic objectives in the hypermetabolic liver by flux and energy balance analysis. Metab Eng 8(1):30-45.

Nussler AK, Wang A, Neuhaus P, Fischer J, Yuan J, Liu L, Zeilinger K, Gerlach J, Arnold PJ, Albrecht W. 2001. The suitability of hepatocyte culture models to study various aspects of drug metabolism. Altex 18(2):91-101.

Page JL, Johnson MC, Olsavsky KM, Strom SC, Zarbl H, Omiecinski CJ. 2007. Gene expression profiling of extracellular matrix as an effector of human hepatocyte phenotype in primary cell culture. Toxicol Sci 97(2):384-97.

Palacin M, Estevez R, Bertran J, Zorzano A. 1998. Molecular biology of mammalian plasma membrane amino acid transporters. Physiological Reviews 78(4):969-1054.

Papin JA, Stelling J, Price ND, Klamt S, Schuster S, Palsson BO. 2004. Comparison of network-based pathway analysis methods. Trends Biotechnol 22(8):400-5.

Park JK, Lee DH. 2005. Bioartificial liver systems: current status and future perspective. J Biosci Bioeng 99(4):311-9.

Parkin DM, Bray F, Ferlay J, Pisani P. 2001. Estimating the world cancer burden: Globocan 2000. Int J Cancer 94(2):153-6.

Pfeiffer T, Sanchez-Valdenebro I, Nuno JC, Montero F, Schuster S. 1999. METATOOL: for studying metabolic networks. Bioinformatics 15(3):251-7.

Phalakornkule C, Lee S, Zhu T, Koepsel R, Ataai MM, Grossmann IE, Domach MM. 2001. A MILP-based flux alternative generation and NMR experimental design strategy for metabolic engineering. Metabolic Engineering 3(2):124-137.

Pharkya P, Burgard AP, Maranas CD. 2003. Exploring the overproduction of amino acids using the bilevel optimization framework OptKnock. Biotechnol Bioeng 84(7):887-99.

Poolman MG, Venkatesh KV, Pidcock MK, Fell DA. 2004. A method for the

determination of flux in elementary modes, and its application to Lactobacillus rhamnosus. Biotechnol Bioeng 88(5):601-12.

Price ND, Reed JL, Palsson BO. 2004. Genome-scale models of microbial cells: evaluating the consequences of constraints. Nat Rev Microbiol 2(11):886-97.

Quant PA, Tubbs PK, Brand MD. 1989. Treatment of rats with glucagon or mannoheptulose increases mitochondrial 3-hydroxy-3-methylglutaryl-CoA synthase activity and decreases succinyl-CoA content in liver. Biochem J 262(1):159-64.

Raghunathan AU, Biegler LT. 2003. Mathematical programs with equilibrium constraints (MPECs) in process engineering. Computers & Chemical Engineering 27(10):1381-1392.

Raghunathan AU, Perez-Correa JR, Bieger LT. 2003. Data reconciliation and parameter estimation in flux-balance analysis. Biotechnol Bioeng 84(6):700-9.

Ramakrishna R, Edwards JS, McCulloch A, Palsson BO. 2001. Flux-balance analysis of mitochondrial energy metabolism: consequences of systemic stoichiometric constraints. Am J Physiol Regul Integr Comp Physiol 280(3):R695-704.

Raman K, Chandra N. 2009. Flux balance analysis of biological systems: applications and challenges. Brief Bioinform 10(4):435-49.

Ravasz E, Somera AL, Mongru DA, Oltvai ZN, Barabasi AL. 2002. Hierarchical organization of modularity in metabolic networks. Science 297(5586):1551-5.

Reder C. 1988. Metabolic control theory: a structural approach. J Theor Biol 135(2):175-201.

Riascos CAM, Gombert AK, Pinto JM. 2005. A global optimization approach for metabolic flux analysis based on labeling balances. Computers & Chemical Engineering 29(3):447-458.

Riordan S, Williams R. 1997. Bioartificial liver support: developments in hepatocyte culture and bioreactor design. Br Med Bull 53(4):730-44.

Rozga J. 2006. Liver support technology--an update. Xenotransplantation 13(5):380-9.

Sand TE, Christoffersen T. 1988. A simple medium for the study of hepatocyte growth in culture under defined conditions. In Vitro Cell Dev Biol 24(10):981-4.

Sauer U, Heinemann M, Zamboni N. 2007. Genetics. Getting closer to the whole picture. Science 316(5824):550-1.

Schilling CH, Covert MW, Famili I, Church GM, Edwards JS, Palsson BO. 2002. Genome-scale metabolic model of Helicobacter pylori 26695. J Bacteriol 184(16):4582-93.

Schilling CH, Letscher D, Palsson BO. 2000. Theory for the systemic definition of metabolic pathways and their use in interpreting metabolic function from a pathway-oriented perspective. J Theor Biol 203(3):229-48.

Schuetz R, Kuepfer L, Sauer U. 2007. Systematic evaluation of objective functions for predicting intracellular fluxes in Escherichia coli. Mol Syst Biol 3:119.

Schuster S, Dandekar T, Fell DA. 1999. Detection of elementary flux modes in biochemical networks: a promising tool for pathway analysis and metabolic engineering. Trends Biotechnol 17(2):53-60.

Schuster S, Fell DA, Dandekar T. 2000. A general definition of metabolic pathways useful for systematic organization and analysis of complex metabolic networks. Nat Biotechnol 18(3):326-32.

Schuster S, Hilgetag C, Woods JH, Fell DA. 2002a. Reaction routes in biochemical reaction systems: algebraic properties, validated calculation procedure and example from nucleotide metabolism. J Math Biol 45(2):153-81.

Schuster S, Pfeiffer T, Moldenhauer F, Koch I, Dandekar T. 2002b. Exploring the pathway structure of metabolism: decomposition into subnetworks and application to Mycoplasma pneumoniae. Bioinformatics 18(2):351-61.

Schwartz JM, Kanehisa M. 2005. A quadratic programming approach for decomposing steady-state metabolic flux distributions onto elementary modes. Bioinformatics 21 Suppl 2:ii204-5.

Schwarz R, Musch P, von Kamp A, Engels B, Schirmer H, Schuster S, Dandekar T. 2005. YANA - a software tool for analyzing flux modes, gene-expression and enzyme activities. BMC Bioinformatics 6:135.

Seglen PO. 1976. Preparation of isolated rat liver cells. Methods Cell Biol 13:29-83.

Segre D, Vitkup D, Church GM. 2002. Analysis of optimality in natural and perturbed metabolic networks. Proc Natl Acad Sci U S A 99(23):15112-7.

Sharma NS, Ierapetritou MG, Yarmush ML. 2005. Novel quantitative tools for engineering analysis of hepatocyte cultures in bioartificial liver systems. Biotechnol Bioeng 92(3):321-35.

Shawcross D, Wendon J. 2009. Acute-On-Chronic Liver Failure in Cirrhosis: Defining and Managing Organ Dysfunction. Yearbook of Intensive Care and Emergency Medicine: Springer Berlin Heidelberg. p 658-670.

Shi CG, Lu J, Zhang GQ. 2005. An extended Kuhn-Tucker approach for linear bilevel programming. Applied Mathematics and Computation 162(1):51-63.

Shlomi T, Berkman O, Ruppin E. 2005. Regulatory on/off minimization of metabolic flux changes after genetic perturbations. Proc Natl Acad Sci U S A 102(21):7695-700.

Siess EA, Brocks DG, Wieland OH. 1978. Distribution of metabolites between the cytosolic and mitochondrial compartments of hepatocytes isolated from fed rats. Hoppe Seylers Z Physiol Chem 359(7):785-98.

Siess EA, Kientsch-Engel RI, Wieland OH. 1982. Role of free oxaloacetate in ketogenesis. Derivation from the direct measurement of mitochondrial [3-hydroxybutyrate]/[acetoacetate] ratio in hepatocytes. Eur J Biochem 121(3):493-9.

Siess EA, Kientsch-Engel RI, Wieland OH. 1984. Concentration of free oxaloacetate in the mitochondrial compartment of isolated liver cells. Biochem J 218(1):171-6.

Smilkstein MJ, Knapp GL, Kulig KW, Rumack BH. 1988. Efficacy of oral N-acetylcysteine in the treatment of acetaminophen overdose. Analysis of the national multicenter study (1976 to 1985). N Engl J Med 319(24):1557-62.

Soboll S, Scholz R, Heldt HW. 1978. Subcellular metabolite concentrations. Dependence of mitochondrial and cytosolic ATP systems on the metabolic state of perfused rat liver. Eur J Biochem 87(2):377-90.

Song EW, Lee SK, Wang J, Ince N, Ouyang N, Min J, Chen JS, Shankar P, Lieberman J. 2003. RNA interference targeting Fas protects mice from fulminant hepatitis. Nature Medicine 9(3):347-351.

Spurway TD, Sherratt HA, Pogson CI, Agius L. 1997. The flux control coefficient of carnitine palmitoyltransferase I on palmitate beta-oxidation in rat hepatocyte cultures. Biochem J 323 (Pt 1):119-22.

Stefanovich P, Matthew HW, Toner M, Tompkins RG, Yarmush ML. 1996. Extracorporeal plasma perfusion of cultured hepatocytes: effect of intermittent perfusion on hepatocyte function and morphology. J Surg Res 66(1):57-63.

Stelling J, Klamt S, Bettenbrock K, Schuster S, Gilles ED. 2002. Metabolic network structure determines key aspects of functionality and regulation. Nature 420(6912):190-3.

Stephanopoulos GN, Aristidou AA, Nielsen J. 1998. Metabolic Engineering: Principles and Methodologies. San Diego,CA: Academic Press.

Strain AJ, Neuberger JM. 2002. A bioartificial liver--state of the art. Science 295(5557):1005-9.

Szyperski T. 1998. 13C-NMR, MS and metabolic flux balancing in biotechnology research. Q Rev Biophys 31(1):41-106.

Tilles AW, Berthiaume F, Yarmush ML, Toner M. 2002. Critical issues in bioartificial liver development. Technol Health Care 10(3-4):177-86.

Torres NV, Voit EO. 2002. Pathway Analysis and Optimization in Metabolic Engineering Cambrige, UK: Cambridge University Press.

Trinh CT, Wlaschin A, Srienc F. 2009. Elementary mode analysis: a useful metabolic pathway analysis tool for characterizing cellular metabolism. Appl Microbiol Biotechnol 81(5):813-26.

Tuschl G, Lauer B, Mueller SO. 2008. Primary hepatocytes as a model to analyze species-specific toxicity and drug metabolism. Expert Opin Drug Metab Toxicol 4(7):855-70.

Uygun K, Matthew HW, Huang Y. 2007. Investigation of metabolic objectives in cultured hepatocytes. Biotechnol Bioeng 97(3):622-37.

Vallino JJ, Stephanopoulos G. 1994. Carbon Flux Distributions at the Pyruvate Branch Point in Corynebacterium-Glutamicum during Lysine Overproduction. Biotechnology Progress 10(3):320-326.

Van Schaftingen E, Hue L, Hers HG. 1980. Control of the fructose-6-phosphate/fructose 1,6-bisphosphate cycle in isolated hepatocytes by glucose and glucagon. Role of a low-molecular-weight stimulator of phosphofructokinase. Biochem J 192(3):887-95.

Varma A, Palsson BO. 1994a. Metabolic Flux Balancing - Basic Concepts, Scientific and Practical Use. Bio-Technology 12(10):994-998.

Varma A, Palsson BO. 1994b. Stoichiometric flux balance models quantitatively predict growth and metabolic by-product secretion in wild-type Escherichia coli W3110. Appl Environ Microbiol 60(10):3724-31.

Verma P, Verma V, Ray P, Ray AR. 2007. Formation and characterization of three dimensional human hepatocyte cell line spheroids on chitosan matrix for in vitro tissue engineering applications. In Vitro Cell Dev Biol Anim 43(10):328-37.

Wagner C, Urbanczik R. 2005. The geometry of the flux cone of a metabolic network. Biophys J 89(6):3837-45.

Wang NS, Stephanopoulos G. 1983. Application of macroscopic balances to the identification of gross measurement errors. Biotechnol Bioeng 25(9):2177-208.

Wang Q, Yang Y, Ma H, Zhao X. 2007. Metabolic network properties help assign weights to elementary modes to understand physiological flux distributions. Bioinformatics 23(9):1049-52.

Washizu J, Berthiaume F, Chan C, Tompkins RG, Toner M, Yarmush ML. 2000a. Optimization of rat hepatocyte culture in citrated human plasma. Journal of Surgical Research 93(2):237-246.

Washizu J, Berthiaume F, Mokuno Y, Tompkins RG, Toner M, Yarmush ML. 2001. Long-term maintenance of cytochrome P450 activities by rat hepatocyte/3T3 cell co-cultures in heparinized human plasma. Tissue Engineering 7(6):691-703.

Washizu J, Chan C, Berthiaume F, Tompkins RG, Toner M, Yarmush ML. 2000b. Amino acid supplementation improves cell-specific functions of the rat hepatocytes exposed to human plasma. Tissue Engineering 6(5):497-504.

Watanabe FD, Mullon CJ, Hewitt WR, Arkadopoulos N, Kahaku E, Eguchi S, Khalili T, Arnaout W, Shackleton CR, Rozga J and others. 1997. Clinical experience with a bioartificial liver in the treatment of severe liver failure. A phase I clinical trial. Ann Surg 225(5):484-91; discussion 491-4.

Weibel ER, Staubli W, Gnagi HR, Hess FA. 1969. Correlated morphometric and biochemical studies on the liver cell. I. Morphometric model, stereologic methods, and normal morphometric data for rat liver. J Cell Biol 42(1):68-91.

Wiback SJ, Mahadevan R, Palsson BO. 2003. Reconstructing metabolic flux vectors from extreme pathways: defining the alpha-spectrum. J Theor Biol 224(3):313-24.

Wiback SJ, Palsson BO. 2002. Extreme pathway analysis of human red blood cell metabolism. Biophys J 83(2):808-18.

Wiechert W. 2001. 13C metabolic flux analysis. Metab Eng 3(3):195-206.

Williamson DH, Bates MW, Krebs HA. 1968. Activity and intracellular distribution of enzymes of ketone-body metabolism in rat liver. Biochem J 108(3):353-61.

Williamson DH, Lund P, Krebs HA. 1967. The redox state of free nicotinamide-adenine dinucleotide in the cytoplasm and mitochondria of rat liver. Biochem J 103(2):514-27.

Wurm M, Lubei V, Caronna M, Hermann M, Buttiglieri S, Bodamer O, Muehl A, Tetta C, Margreiter R, Hengster P. 2009. Introduction of a novel prototype bioartificial liver support system utilizing small human hepatocytes in rotary culture. Tissue Eng Part A 15(5):1063-73.

Yang F, Beard DA. 2006. Thermodynamically based profiling of drug metabolism and drug-drug metabolic interactions: a case study of acetaminophen and ethanol toxic interaction. Biophys Chem 120(2):121-34.

Yang H, Roth CM, Ierapetritou MG. 2009. A rational design approach for amino acid supplementation in hepatocyte culture. Biotechnol Bioeng 103(6):1176-91.

Yoon J, Lee K. 2007. Metabolic flux profiling of reaction modules in liver drug transformation. Pac Symp Biocomput:193-204.

Zamboni N, Kummel A, Heinemann M. 2008. anNET: a tool for network-embedded thermodynamic analysis of quantitative metabolome data. BMC Bioinformatics 9:199.

Zupke C, Stephanopoulos G. 1995. Intracellular flux analysis in hybridomas using mass balances and in vitro (13)C nmr. Biotechnol Bioeng 45(4):292-303.

Zupke CA, Stefanovich P, Berthiaume F, Yarmush ML. 1998. Metabolic effects of stress mediators on cultured hepatocytes. Biotechnol Bioeng 58(2-3):222-30.

CURRICULUM VITAE

HONG YANG

EDUCATION

2005-2010 **Ph.D., Chemical and Biochemical Engineering**
Rutgers, the State University of New Jersey, New Brunswick, NJ
Thesis: Design and Analysis of Amino Acid Supplementation in Hepatocyte Culture Using *in vitro* Experiment and Mathematical Modeling

2004-2008 **M.S., Chemical and Biochemical Engineering**
Rutgers, the State University of New Jersey, New Brunswick, NJ

1999-2002 **M.E., Chemical Engineering**
Dalian University of Technology, Dalian, China
Thesis: Operational Flexibility Analysis of Chemical Plants

1995-1999 **B.E. School of Chemical Engineering**
Dalian University of Technology, Dalian, China
Thesis: Improvement of Chemical and Mechanical Properties of HPVC/SBR Mixture

OTHER EXPERIENCE

09/2009-12/2009 Wired Bio-1 Graduate Mentor, Douglass Project for Rutgers Women

2004-2009 Graduate/Teaching Assistant, Chemical and Biochemical Engineering, Rutgers, the State University of New Jersey

2002-2004 Technology Advisor, Dalian Polymer New Material Co., Ltd, China

PUBLICATIONS

- **H. Yang,** M.G. Ierapetritou, C.M. Roth, Effects of Amino Acid Transport Limitations on Cultured Hepatocytes, *manuscript in preparation*
- V. Iyer, **H. Yang**, M.G. Ierapetritou, C.M. Roth, Effects of Glucose and Insulin Level on HepG2 cell Metabolism, *manuscript in preparation*
- **H. Yang**, C.M. Roth, M.G. Ierapetritou, Analysis of Amino Acid Supplementation Effects on Hepatocyte Cultures Using Flux Balance Analysis, submitted, *PLoS ONE*
- **H. Yang**, C.M. Roth, M.G. Ierapetritou, A Rational Design Approach for Amino Acid Supplementation in Hepatocyte Culture, *Biotech & Bioeng,* 2009, 103(6), 1176-1191
- **H. Yang**, S.W. Zhang, Flexibility Analysis of Chemical Plant Using Matlab, *Computers and Applied Chemistry,* 2003, 20, 163-167
- **H. Yang**, D. Wu, S.W. Zhang, C.Y. Wang, Y.G. Yu, CO_2 Recovery from Hydrogen Production Exhaust Gas, *Large Scale Nitrogenous Fertilizer Industry,* 2002, 25, 277-280
- **H. Yang**, S.W. Zhang, X.S. Wang, Flexibility Analysis of a Methanol Rectification Tower in Rectisol Process, *Computers and Applied Chemistry*, 2001 (Suppl), 18(10), 120-123